Continuum Diffusion Modeling Using the SMOL Package

Finite Element Method Application

Yuhui Cheng
ycheng@mccammon.ucsd.edu

NBCR Summer Institute

Aug. 6, 2009

http://mccammon.ucsd.edu/smol/doc/lectures/nbcr080609.pdf

Outline

- To introduce diffusion-controlled diffusion reactions.
- To introduce the biological applications of the finite element tool kit (FEtk).
- To introduce the basic math background in solving diffusion problems.
- Examples to solve steady-state and time-dependent diffusion equations and preliminary visualization.

➢ Analytical tests

➢ mAChE case

➢ Neuromuscular Junction

- Finite element Poisson-Nernst-Planck solvers and future possible projects.

Enzyme catalysis: mathematics

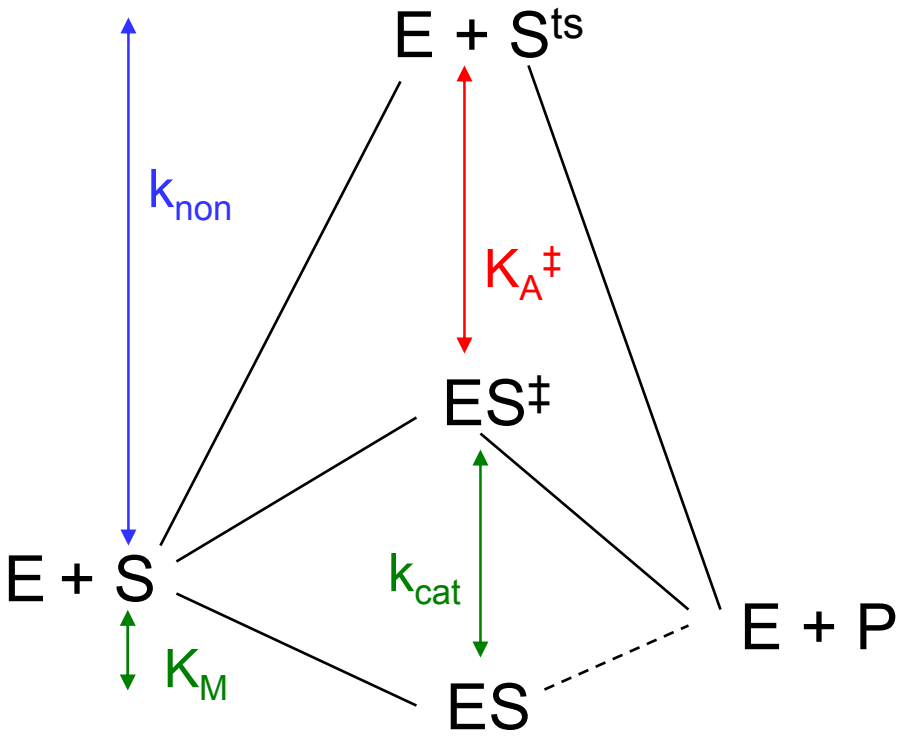

$$E + S \underset{}{\overset{k_{non}}{\rightleftharpoons}} E + S^{ts}$$

$$k_{cat}/K_M = k_{non} * K_A^{\ddagger}$$

Enzymes exert remarkable control over k_{cat}/K_M relative to the variation of k_{non}

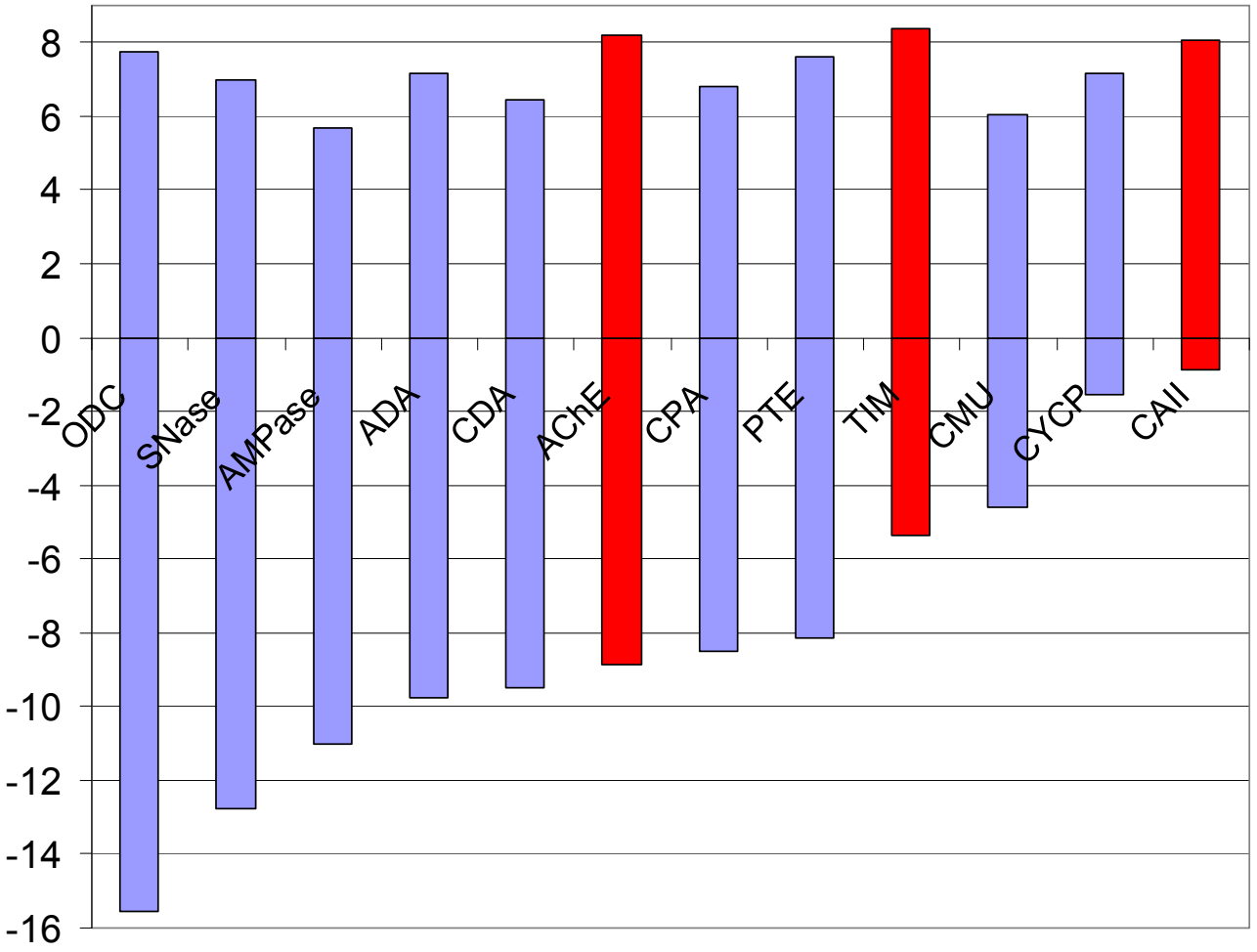

k_{cat}/K_M: $10^{2.5}$ variation

k_{non}: 10^{14} variation

Radzicka, A. and Wolfenden, G. (1995). *Science* **267** (5194), 90-93.

Diffusion-controlled enzymes

Molecular encounter limits k_{cat}/K_M if k_2 is high

$$E + S \xleftrightarrow{k_1/k_{-1}} ES \xrightarrow{k_2} E + P$$

What is the limit of the molecular encounter rate?

1) According to Smolouchowski equation, E-S collision rate is limited to ~10^9 $M^{-1}S^{-1}$

2) Orientational constraints limit the reactive encounter rate to ~10^6 $M^{-1}S^{-1}$

3) Electrostatic attraction or guidance of S to E can raise the diffusion limit to 10^8-10^9 $M^{-1}S^{-1}$

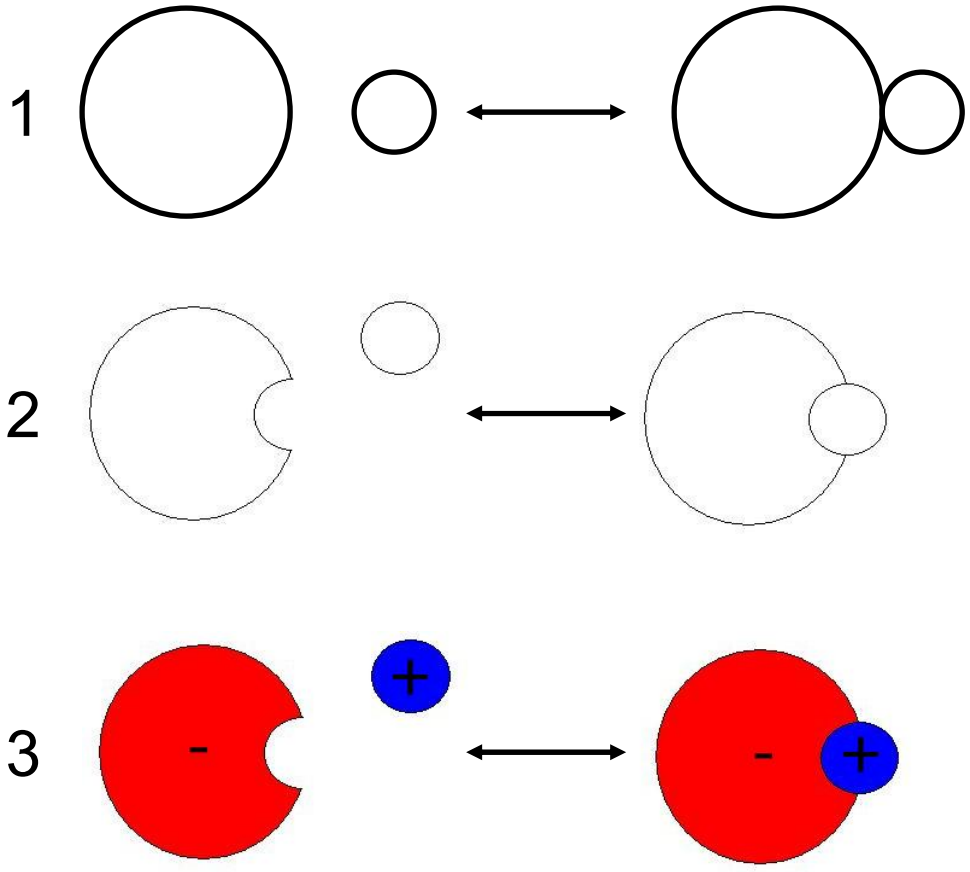

Alberty, R.A. and Hammes, G.G. (1958). *J. Phys Chem* **62**, 154-59

Electrostatics causes large differences in barnase-barstar association rates

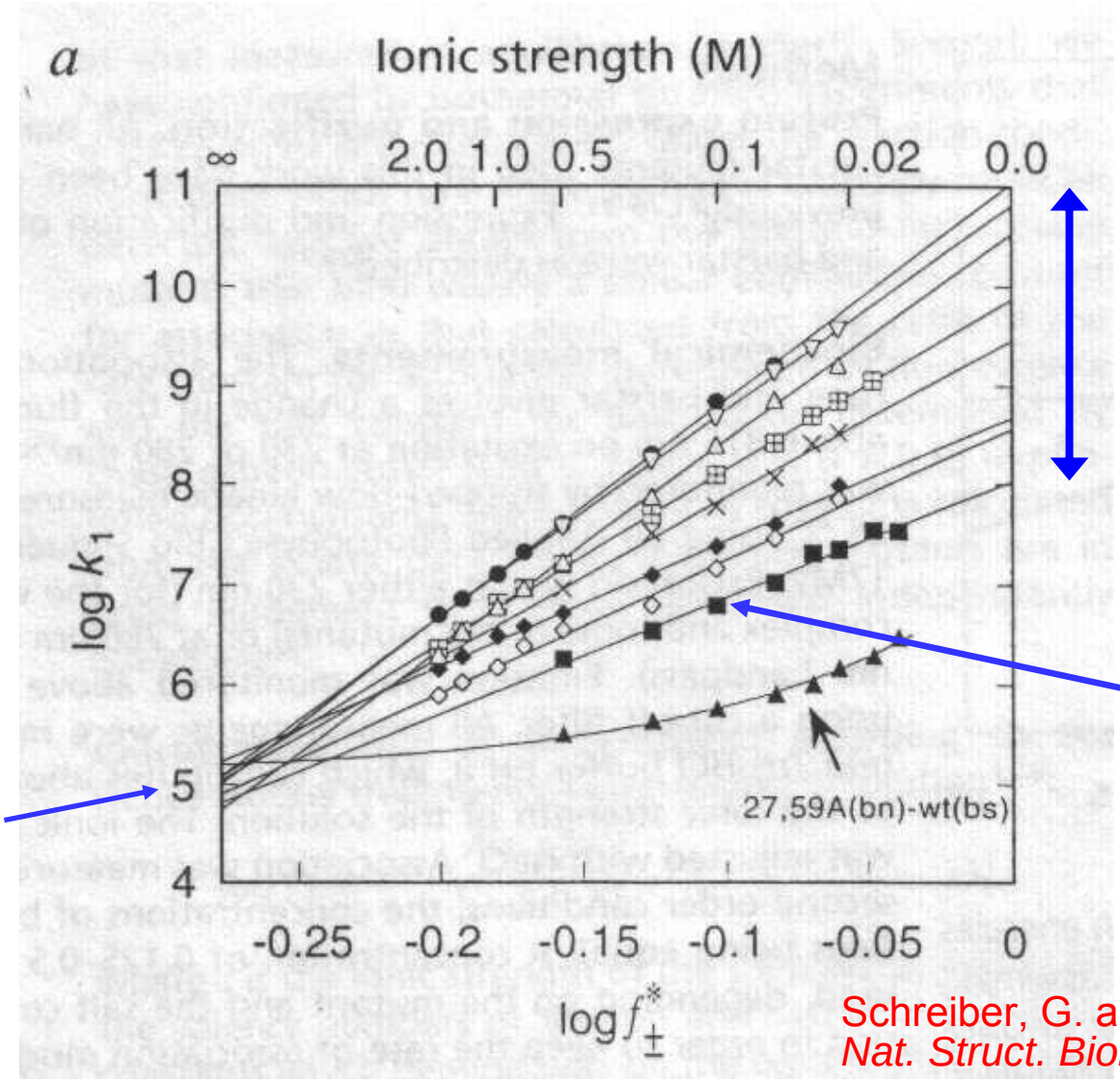

Wild type (top) and barnase mutants

~1000x variation in k_1 at 0.1M ionic strength

Basal k_1 ~ 10^5 $M^{-1}s^{-1}$

Schreiber, G. and Fersht, A.R. (1996). *Nat. Struct. Biol.* **3** (5), 427-431.

Summary: enzymes overcome two physical problems

- Chemical efficiency
  - Geometry (entropic problem)
  - High-energy intermediates (enthalpic problem)
  - Enzyme rate does not appear to be limited by k_{non}
- Molecular encounter
  - Coulomb's law (enthalpic effect)
  - Steering (entropic effect)

Introduction to FEtk

- http://www.fetk.org/
- The primary FETK ANSI-C software libraries are:

  (1) *MALOC* is a Minimal Abstraction Layer for Object-oriented C/C++ programs.

  (2) *PUNC* is Portable Understructure for Numerical Computing (requires MALOC).

  (3) *GAMER* is a Geometry-preserving Adaptive MeshER (requires MALOC).

  (4) *SG* is a Socket Graphics tool for displaying polygons (requires MALOC).

  (5) *MC* is a 2D/3D AFEM code for nonlinear geometric PDE (requires MALOC; optionally uses PUNC+GAMER+SG).

Smoluchowski Equation

Describes the over-damped diffusion dynamics of non-interacting particles in a potential field.

$$\frac{\partial p(\vec{r},t\,|\,\vec{r}_0,t_0)}{\partial t} = \nabla \cdot D\left[\nabla - \beta\vec{F}(\vec{r})\right]p(\vec{r},t\,|\,\vec{r}_0,t_0)$$

Or for $\vec{F}(\vec{r}) = -\nabla U(\vec{r})$

$$\frac{\partial p(\vec{r},t\,|\,\vec{r}_0,t_0)}{\partial t} = \nabla \cdot De^{-\beta U(\vec{r})}\nabla e^{\beta U(\vec{r})}\,p(\vec{r},t\,|\,\vec{r}_0,t_0)$$

Steady-state Formation

$$\frac{\partial p(\vec{r},t)}{\partial t} = 0$$

$$\Rightarrow \quad \nabla \cdot D(\vec{r})[\nabla p(\vec{r}) + \beta p(\vec{r}) \nabla U(\vec{r})] = 0$$

Or in flux operator J:

$$\nabla \cdot \vec{J} p(\vec{r}) = 0$$

where

$$\vec{J} p(\vec{r}) = D(\vec{r})[\nabla p(\vec{r}) + \beta p(\vec{r}) \nabla U(\vec{r})]$$

Poisson-Boltzmann Equation

$$-\nabla\cdot\varepsilon(x)\nabla U(x) \quad +\bar{\kappa}^2(x)\sinh U(x) = \frac{4\pi e_c^2}{kT}\sum_i z_i\delta(x-x_i)$$

$$-\nabla\cdot\varepsilon(x)\nabla u(x)+\bar{\kappa}^2(x)\sinh[u(x)+G]=\nabla\cdot((\varepsilon-\varepsilon_m)\nabla G$$

$$-\nabla\cdot\varepsilon(x)\nabla G_i = q_i\delta_i$$

$$G_i = \frac{q_i}{\varepsilon_m}\frac{1}{|x-x_i|}$$

$$U(x) = u(x)+\sum_{i=1}^{N_m} G_i$$

Boundary conditions for SSSE

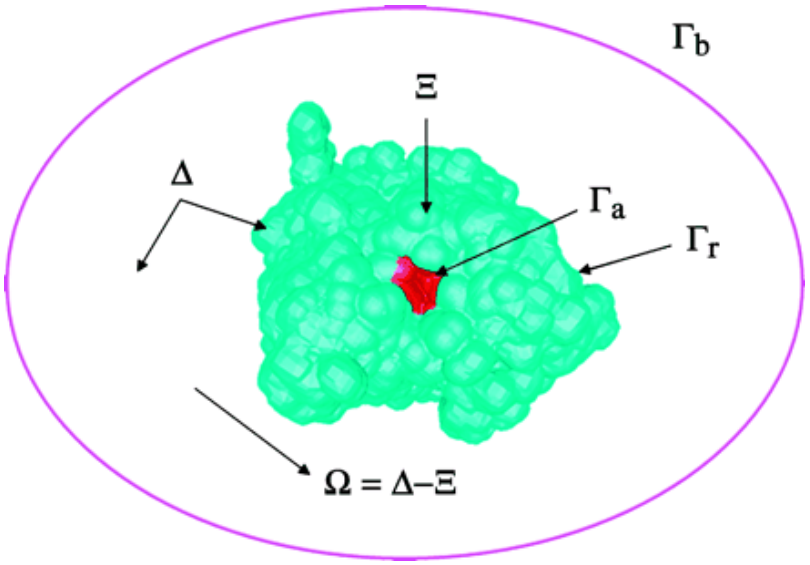

- Δ -- whole domain
- Ξ -- biomolecular domain
- Ω -- free space in Δ
- Γ_a – reactive region
- Γ_r – reflective region
- Γ_b – boundary for Δ

(1) $p(\vec{r}) = p_{bulk}$ for $\vec{r} \in \Gamma_b$

(2) $p(\vec{r}) = 0$ (Dirichlet BC) for $\vec{r} \in \Gamma_a$

or $\vec{n} \cdot \vec{J}p(\vec{r}) = \alpha(\vec{r})\, p(\vec{r})$ (Robin BC)

(3) $\vec{n} \cdot \vec{J}p(\vec{r}) = 0$ for $x \in \Gamma_r$

Diffusion rate:

$$k = \frac{\int_{\Gamma_a} \vec{n} \cdot \vec{J}p(\vec{r})\, dS}{p_{bulk}}$$

Finite element discretization of SSSE

1. Define a function space $V_h=\{v_i\}$ (v_i : piece-wise linear FE basis functions defined over each tetrahedral vertex), and assume the solution to SSSE has the form of

$$p_h(\vec{r}) = \sum_i a_i v_i(\vec{r}), \;\; p_h \in \bar{p}_h + V_h$$

2. The second derivatives of V_h are not well defined, thus need reformulation of SSSE by integrating it with a test function v:

$$\int_\Omega v(\vec{r}) \nabla \cdot \vec{J}p(\vec{r}) d\vec{r}^3 = 0$$

Weak form of SSSE

$$\Rightarrow \quad \int_\Omega \nabla v(\vec{r}) \cdot \vec{J}p(\vec{r}) d\vec{r}^3 - \int_{\Gamma_a} v(s)\alpha(s)p(s)ds - \int_{\Gamma_b} v(s)\vec{J}\bar{p}(s) \cdot \vec{n}(s)ds = 0$$

$$\text{or} \quad \int_\Omega \nabla v(\vec{r}) \cdot \vec{J}p(\vec{r}) d\vec{r}^3 - \int_{\Gamma_a \cup \Gamma_b} v(s)\vec{J}\bar{p}(s) \cdot \vec{n}(s)ds = 0$$

http://www3.interscience.wiley.com/cgi-bin/fulltext/73503240/PDFSTART

Weak formation of SSSE

$$\nabla \cdot [v \nabla u] = \nabla u \cdot \nabla v + v \nabla \cdot \nabla u$$

Find $p_h \in \bar{p}_h + V_h$ such as $< F(p_h), v_i >= 0$ for all $v_i \in V_h$

$$< F(p_h), v_i >= \int_{\Omega} \nabla v(x) \cdot Jp(x) dx - \int_{\Gamma_a} v(s) \alpha(s) p(s) ds - \int_{\Gamma_b} v(s) J\bar{p}(s) \cdot n(s) ds$$

$$< F(p_h), v_i >= \int_{\Omega} \nabla v(x) \cdot Jp(x) dx - \int_{\Gamma_a \cup \Gamma_b} v(s) J\bar{p}(s) \cdot n(s) ds$$

Note that the boundary integral on Γ_b vanishes due to the test function vanishes on the non-reactive boundaries.

Bilinear linearization form of SSSE

To apply a Newton iteration, we need to linearize $< F(u), v >$

$$\langle DF(u)w, v\rangle = \frac{d}{dt}\langle F(u+tw), v\rangle = \int_\Omega D\nabla w \cdot \nabla v dx$$

Algorithm 3.2. *(Damped-inexact-Newton)*

- *Given an initial* u
- *While* $(|\langle F(u), v\rangle| > TOL$ for some $v)$ *do:*
  (1) *Find* δ *such that* $\langle DF(u)\delta, v\rangle = -\langle F(u), v\rangle + r, \ \forall v$
  (2) *Set* $u = u + \lambda\delta$
- *end while*

Posteriori ERROR ESTIMATOR

$$\eta_s^2 = h_s^2 \| \nabla \cdot J_h \|_{L^2(s)}^2 + \frac{1}{2} \sum_{f \in I(s)} h_f^2 \| [n_f \cdot (D \nabla p(r))] \|_{L^2(f)}^2$$

h_s represent the size of the element.

$J_h(p;x)$ is the current estimate of the flux.

$f \in S$ denotes a face of simplex

h_s is the size of the face f

$[n \cdot J_h]$ denotes to the ``jump'' term across faces interior to the simplex.

$$err = \sqrt{\sum_s \eta_s^2}$$

Mesh Marking and Refinement

Algorithm 3.1. *(Adaptive multilevel finite element approximation)*

- *While* $(\|u - u_h\|_X > \epsilon)$ *do:*
  - (1) *Find* $u_h \in \bar{u}_h + V_h \subset H_0^1(\Omega)$ *such that* $\langle F(u_h), v_h \rangle = 0, \ \forall\ v_h \in V_h \subset H_0^1(\Omega)$.
  - (2) *Estimate* $\|u - u_h\|_X$ *over each element.*
  - (3) *Initialize two temporary simplex lists as empty:* $Q1 = Q2 = \emptyset$.
  - (4) *Place simplices with large error on the "refinement" list* $Q1$.
  - (5) *Bisect all simplices in* $Q1$ *(removing them from* $Q1$*), and place any nonconforming simplices created on the list* $Q2$.
  - (6) $Q1$ *is now empty; set* $Q1 = Q2$, $Q2 = \emptyset$.
  - (7) *If* $Q1$ *is not empty, goto (5).*
- *End While.*

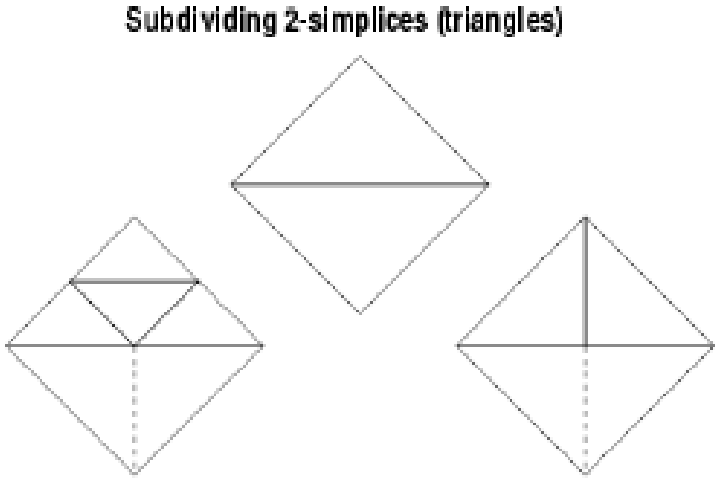

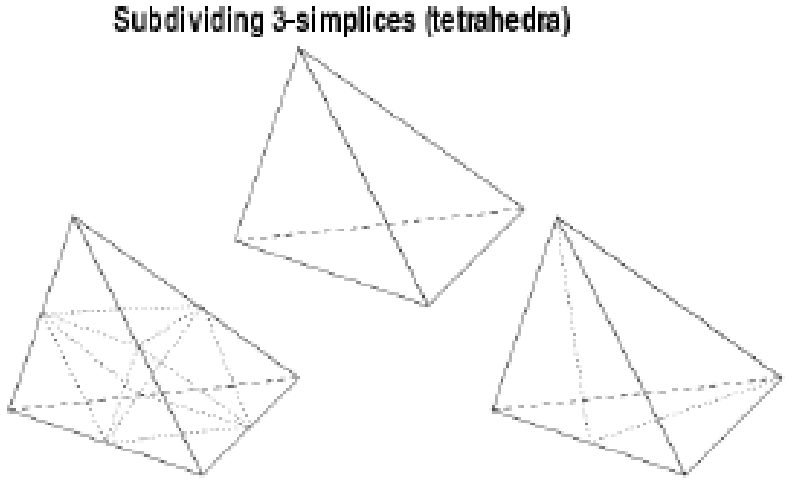

Potential gradient mapping

Currently, we have three ways to obtain potential gradient $\nabla U(r)$:

- Boundary element method:

  Pro: it can easily calculate the $\nabla U(r)$ at any spatial position.

  Con: $\nabla U(r)$ near the protein surface is hard to calculate accurately.

- Finite difference method:

  APBS: $\nabla U(r_j) = \dfrac{U(r_{j+1}) - U(r_{j-1})}{2h}$

- Finite element method:

  Treat the cubic grid as the FE cubic mesh

  Use basis functions to calculate the force on the tetrahedral FE node position.

Potential gradient mapping

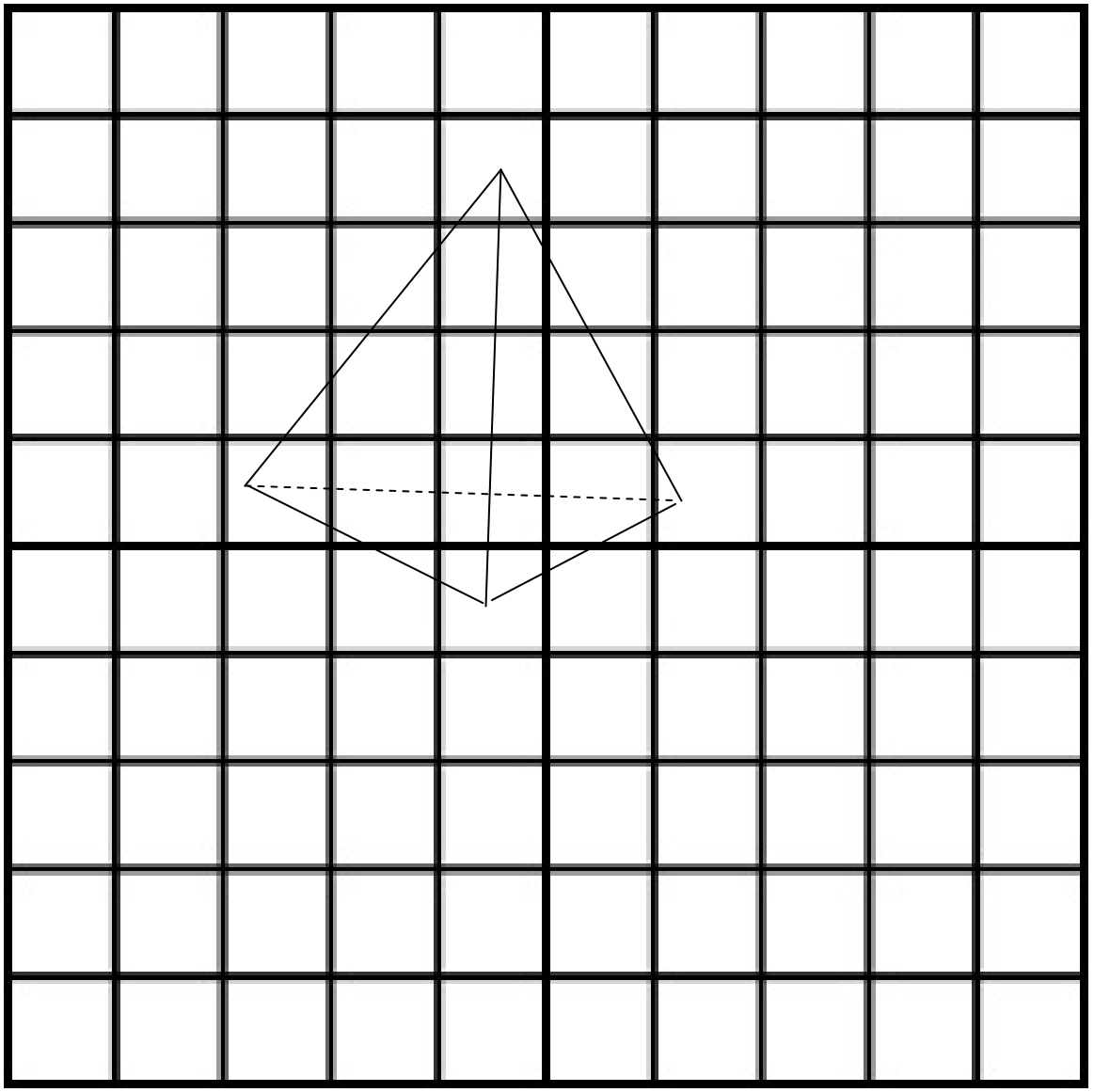

Solving Electrostatics and Diffusion by FEtk

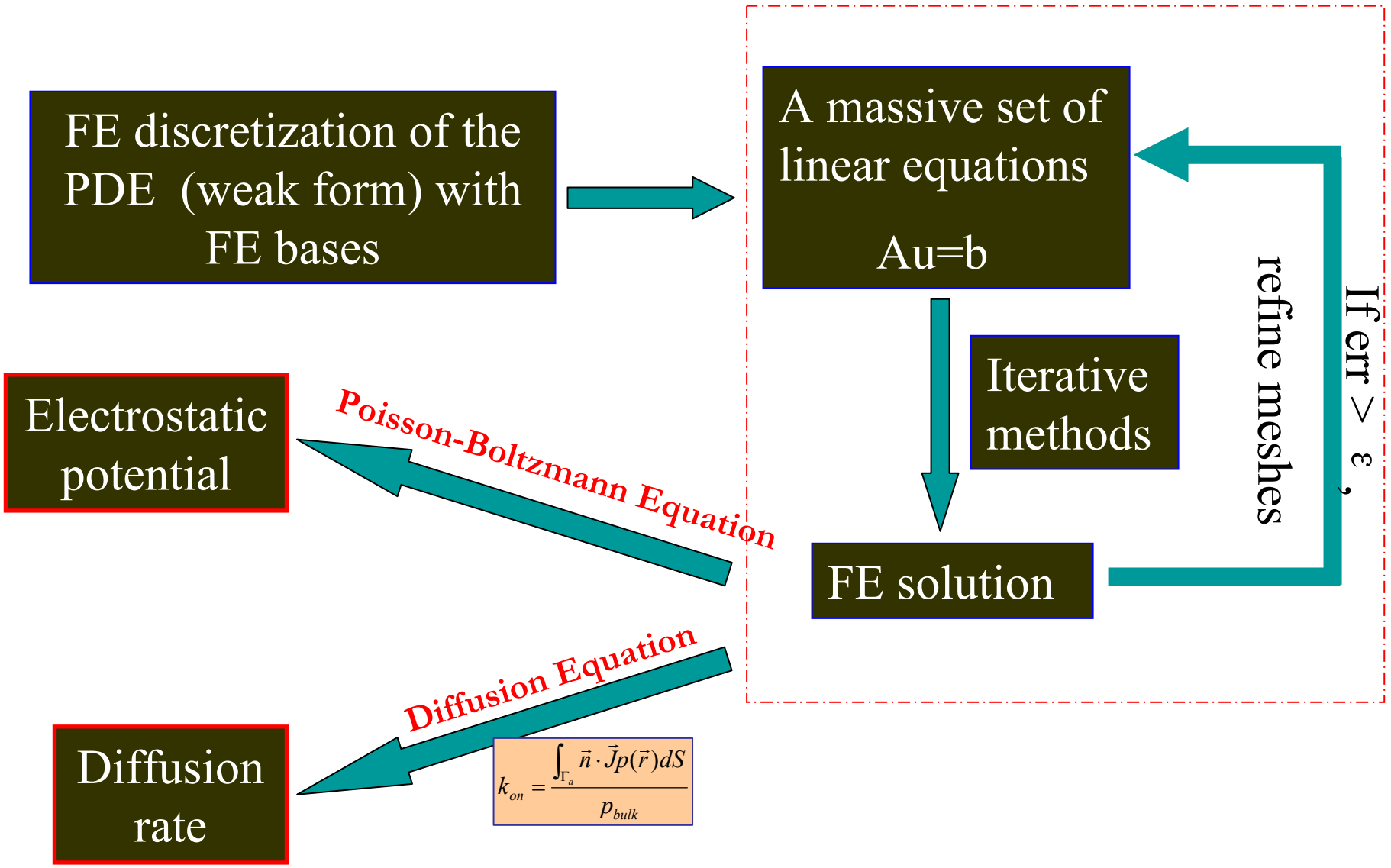

Sample input files

- NOTE:
- # model parameters
- charge 0.0 /* ligand charge */
- conc 1.0 /* initial ligand concentration at the outer boundary */
- diff 78000.0 /* diffusion coeficient, unit: $Å^2/\mu s$ */
- temp 300.0 /* temperature, unit: Kelvin */
- # potential gradient methods
- METHtype BEM /* you can choose BEM or FEM */
- # mapping method
- map NONE /* you can choose NONE/DIRECT/FEM */
- # steady-state or time-dependent
- tmkey TDSE /* you can choose SSSE or TDSE */
- # input paths
- mol ../../pqr/ion_yuhui.pqr
- mesh ../../mesh/sphere_4.m
- mgrid ../../potential/pot-0.dx /* for APBS input */
- dPMF ../../force/evosphere_4.dat /* for BEM input */
- end 0

Manage your input parameters

- NOTE:

${solver}

- the default input file: smol.in

${solver} -ifnam filename

- the default iteration method: CG(lkey=2).

BCG (lkey=4 or 5), BCGSTAB(lkey=6)

${solver} -lkey 2

- default maximal number of iterative steps: 5000

${solver} –lmax 8000

Manage your input parameters (cont.)

- NOTE:
- the default timestep: $5.0*10^{-6}\mu s$

${solver} -dt $5.0*10^{-5}$

- the default number of time steps:500

${solver} –nstep 1000

- the default concentration output frequency: 50

${solver} –cfreq 100

- the default reactive integral output frequency: 1

${solver} –efreq 5

- the default restart file writing frequency: 1000

${solver} –pfreq 5000

Tetrahedral mesh generation: GAMer

PBE solver

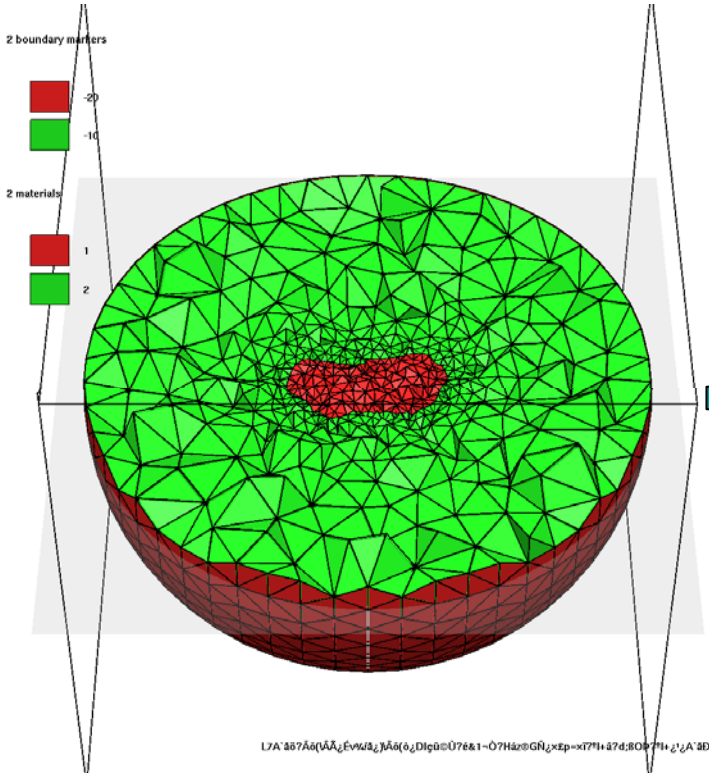

SMOL solver

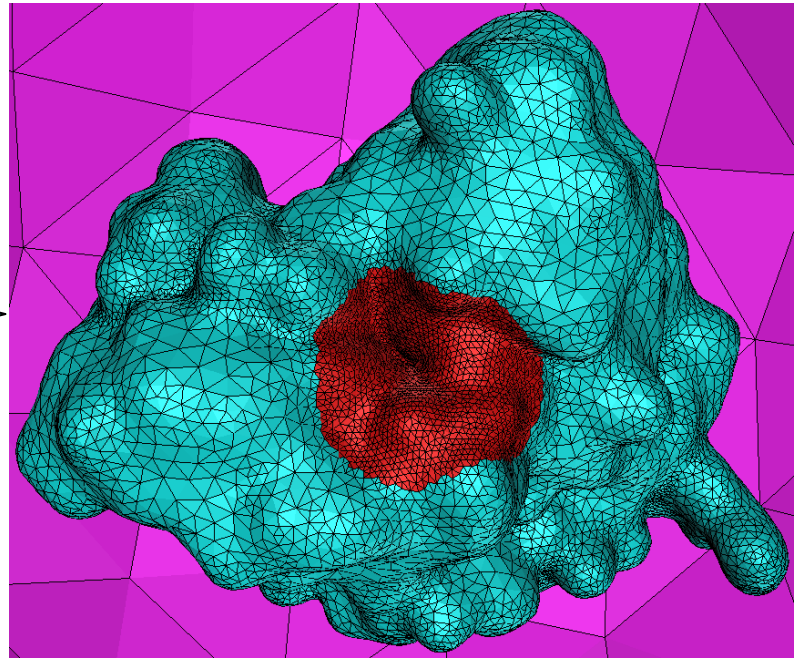

http://www.fetk.org/codes/gamer/

Example 1: Analytical test

The finite element problem domain is the space between two concentric spheres. The boundary Γ_b is Dirichlet, and Γ_a is reactive Robin.

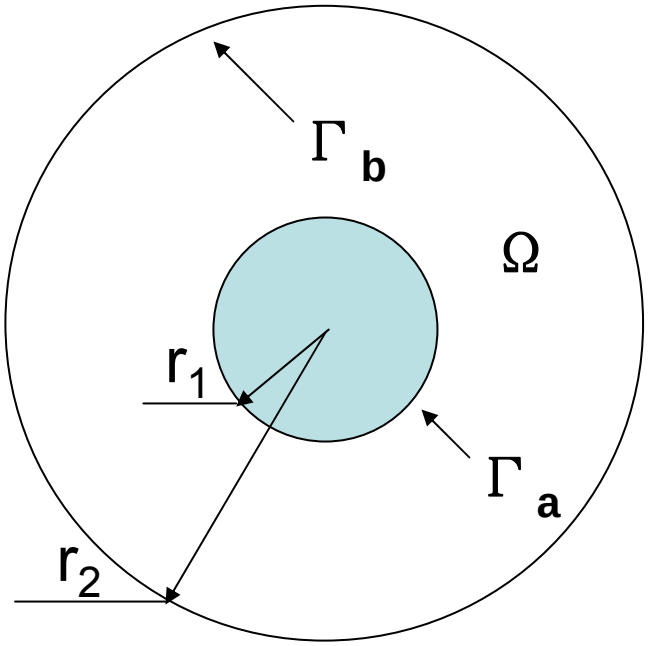

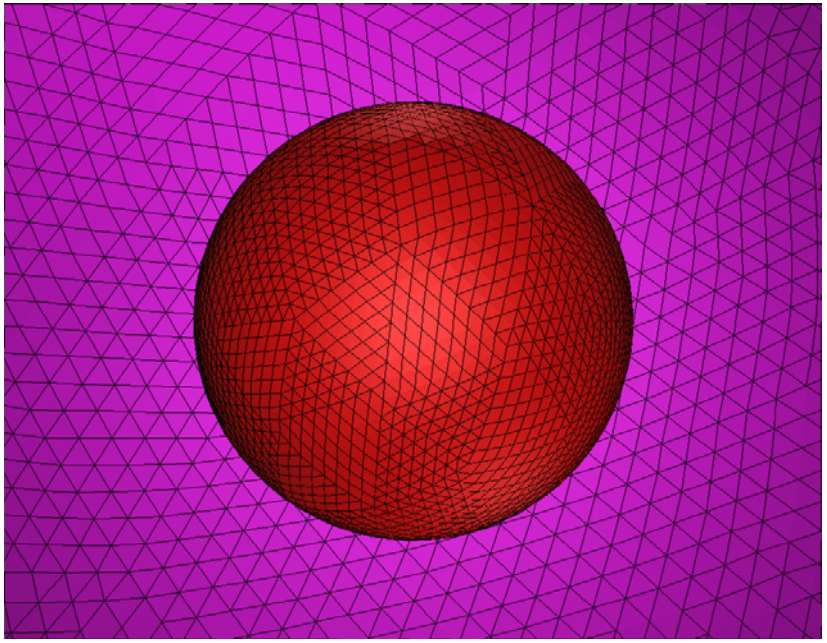

Example 1: Analytical test

For a spherically symmetric system with a Coulombic form of the PMF, W(r) = q/(4 π ε r), the SSSE can be written as

$$\frac{1}{r^2}\frac{\partial}{\partial r}(r^2 Jp) = \frac{1}{r^2}\frac{\partial}{\partial r}(r^2 D(\frac{\partial p}{\partial r} - \beta p \frac{qq_l}{4\pi\varepsilon r^2})) = 0$$

Suppose $Q = \frac{\beta q q_l}{4\pi\varepsilon}$, $p(r_1) = 0; p(r_2) = p_{bulk}$

Then, $k_{on} = \frac{4\pi Q D r_1^2}{e^{-\frac{Q}{r_2}} - e^{-\frac{Q}{r_1}}}$ If Q = 0, $k_{on} = \frac{4\pi D r_1^2}{\frac{1}{r_1} - \frac{1}{r_2}}$

Example 1: Analytical test

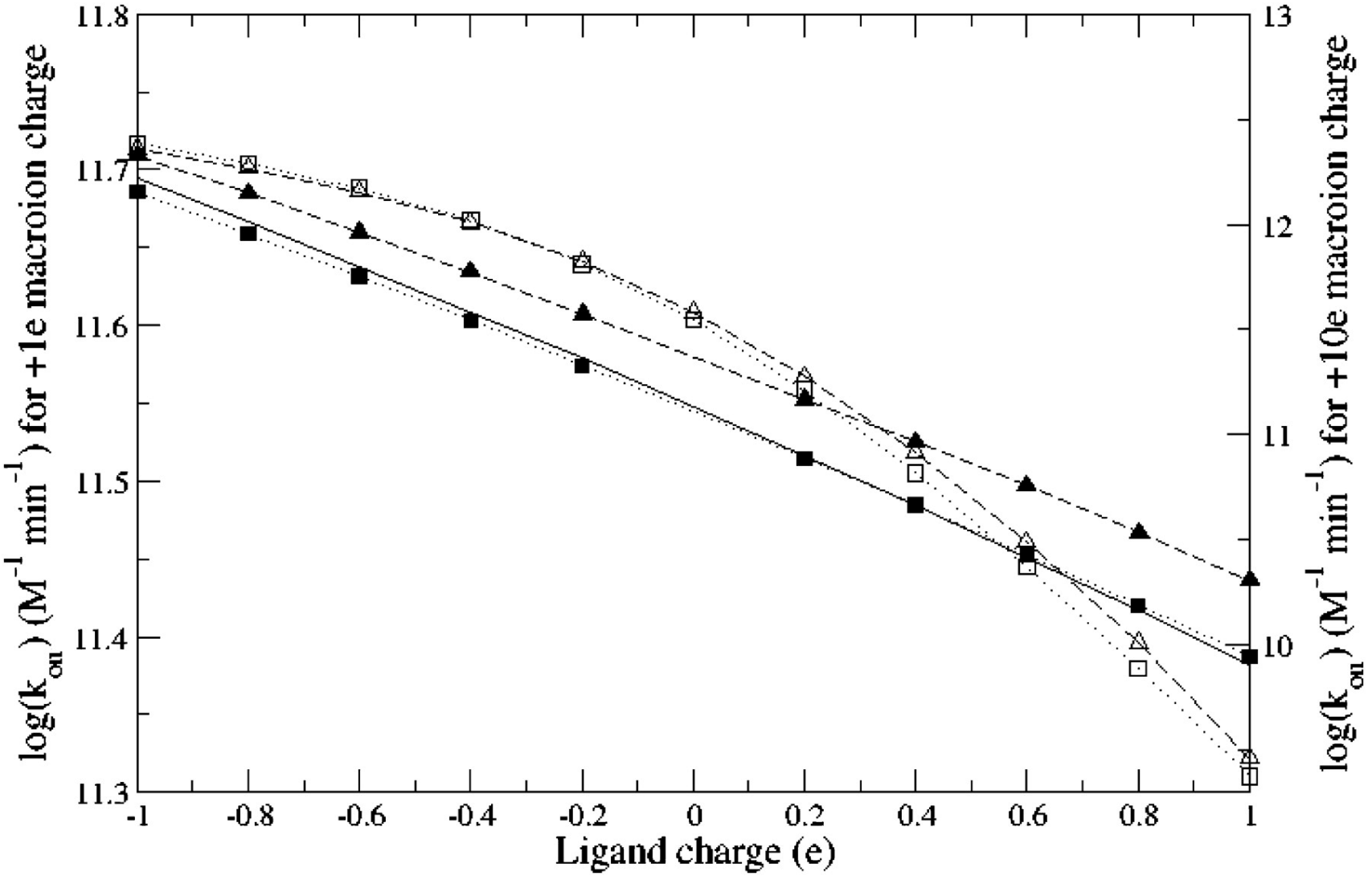

Example 1: Analytical test (q = 1.0)

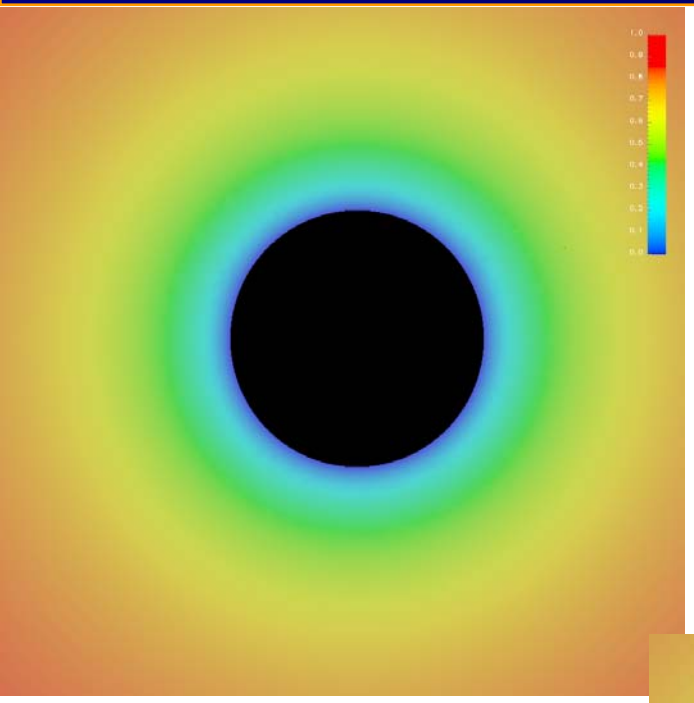

$q_l = -1.0e$

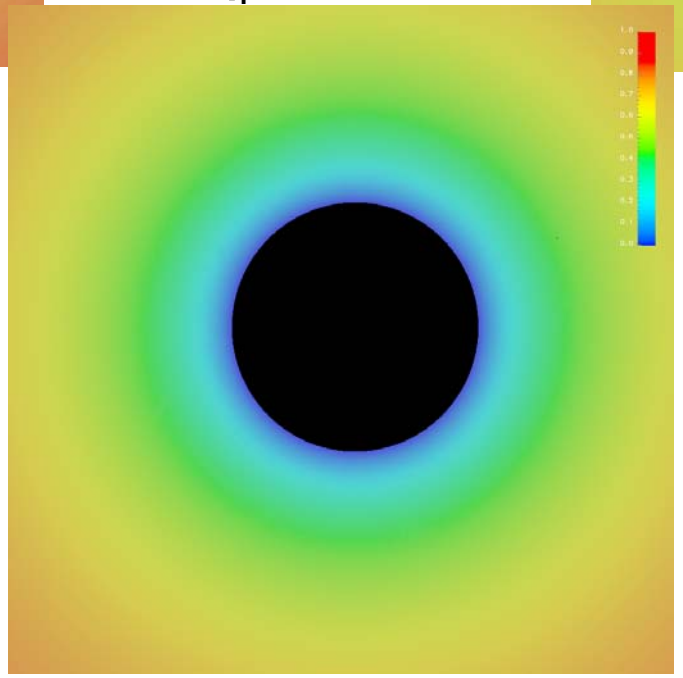

$q_l = 0.0e$

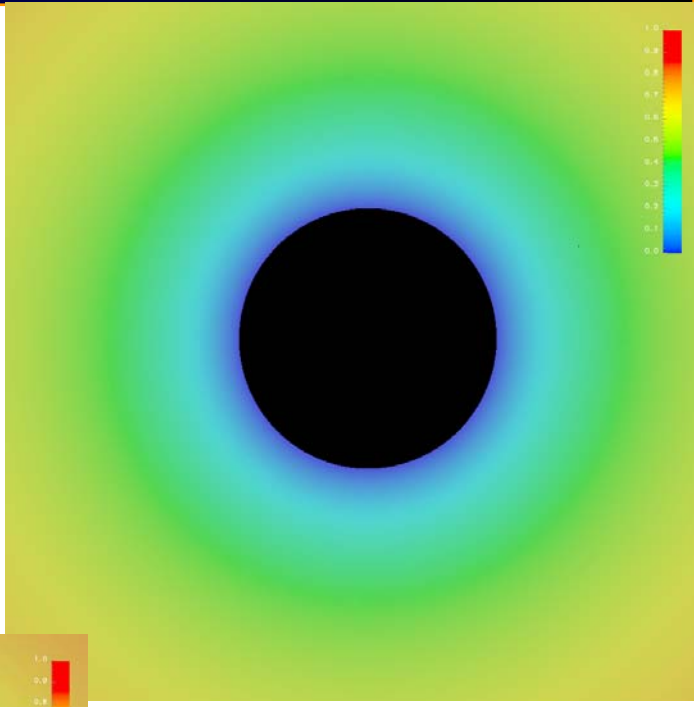

$q_l = 1.0e$

Example 1: Analytical test ($qq_l = 1.0$)

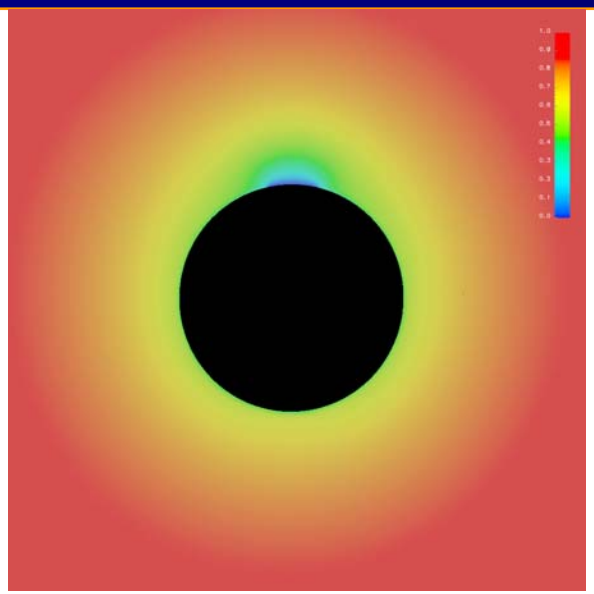

0.000M

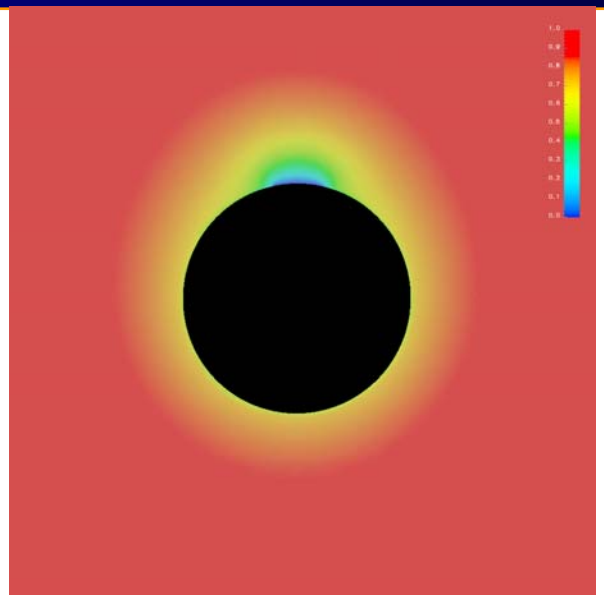

0.075M

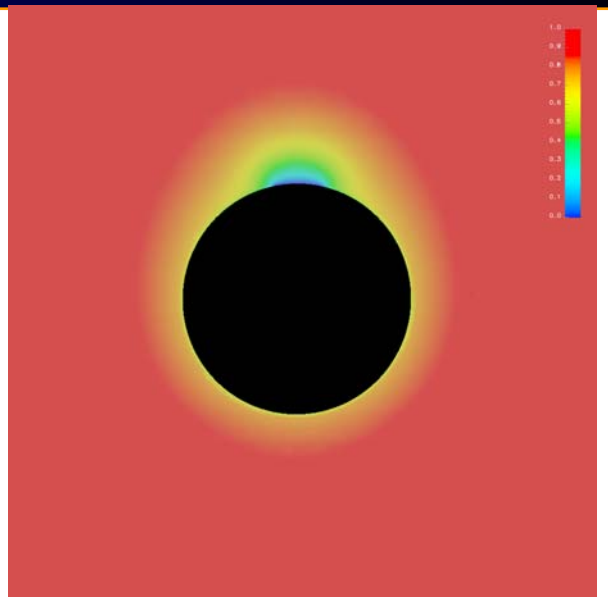

0.150M

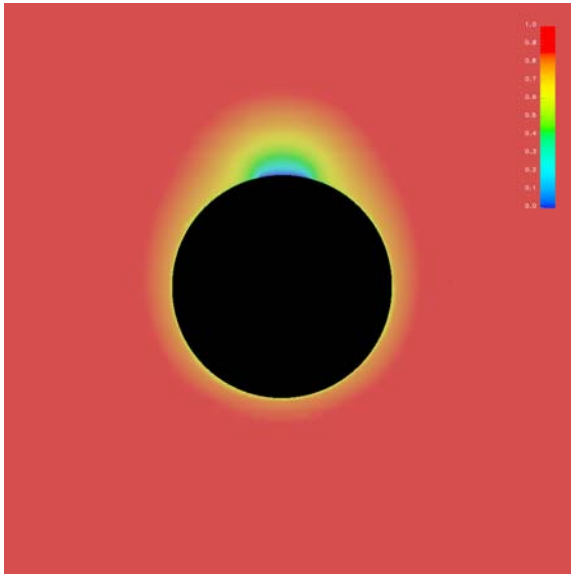

0.300M

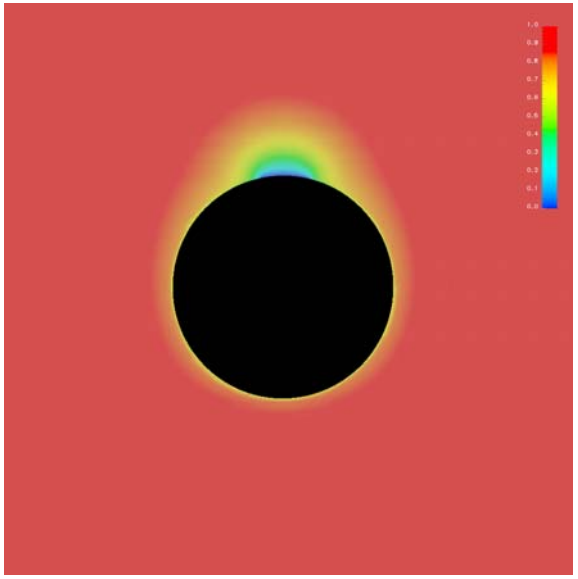

0.450M

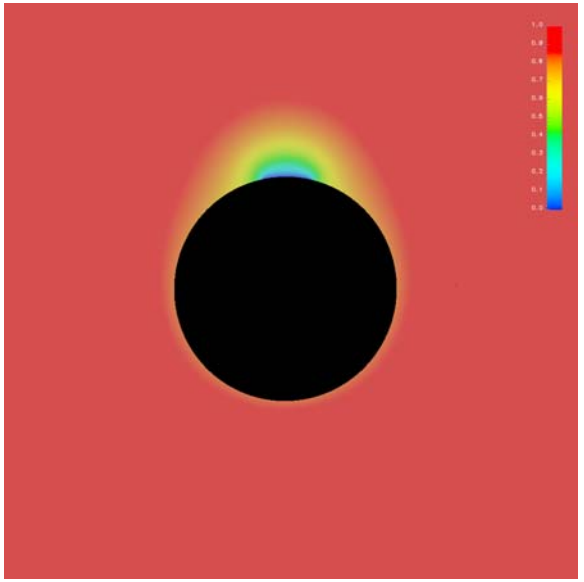

0.670M

Example 1: Analytical test ($qq_l = 0.0$)

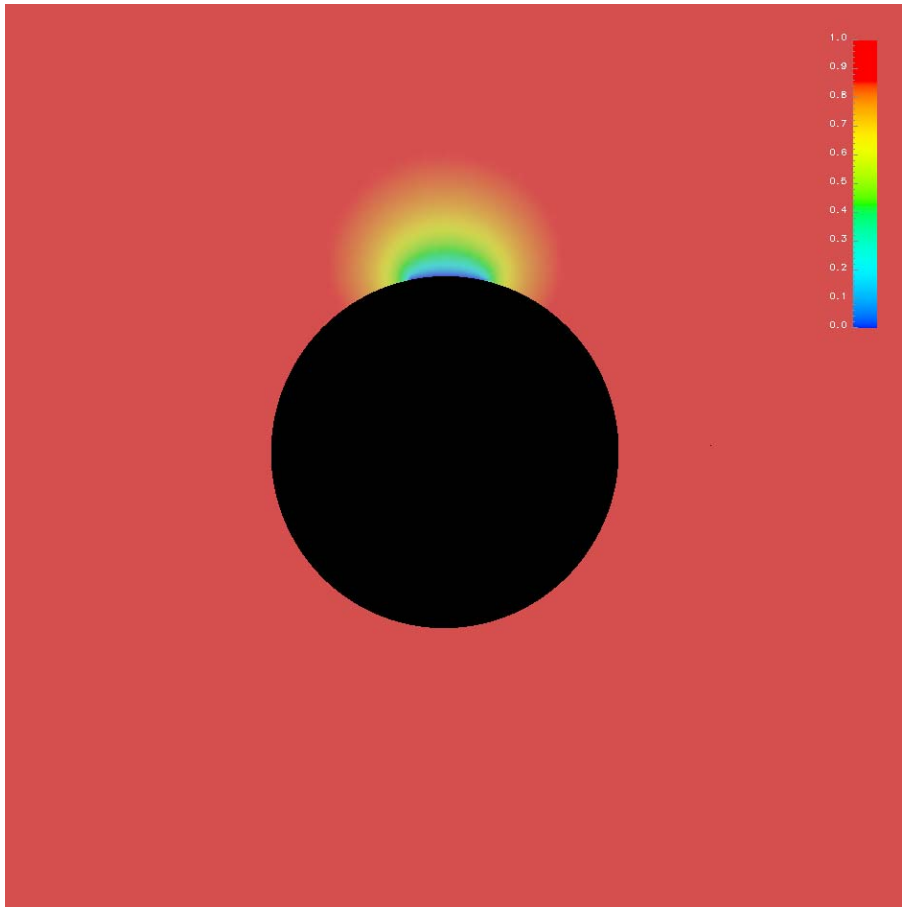

0.000M

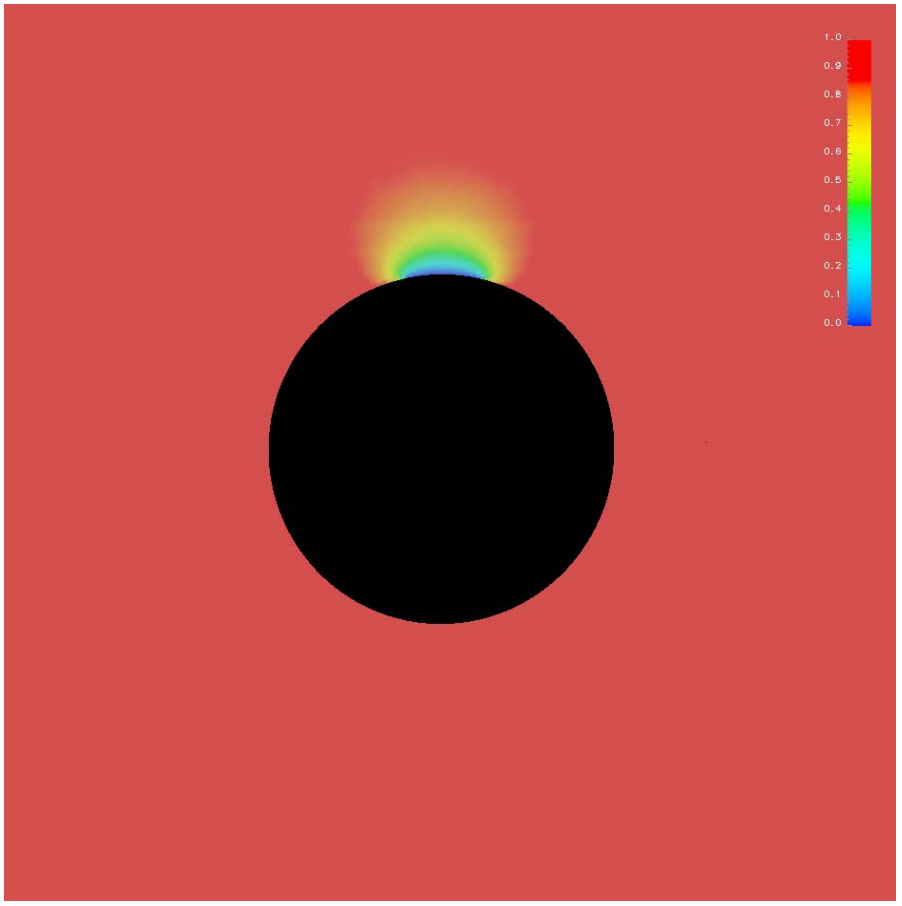

0.600M

Certainly, there is no difference at any ionic strength.

Example 1: Analytical test ($qq_l = -1.0$)

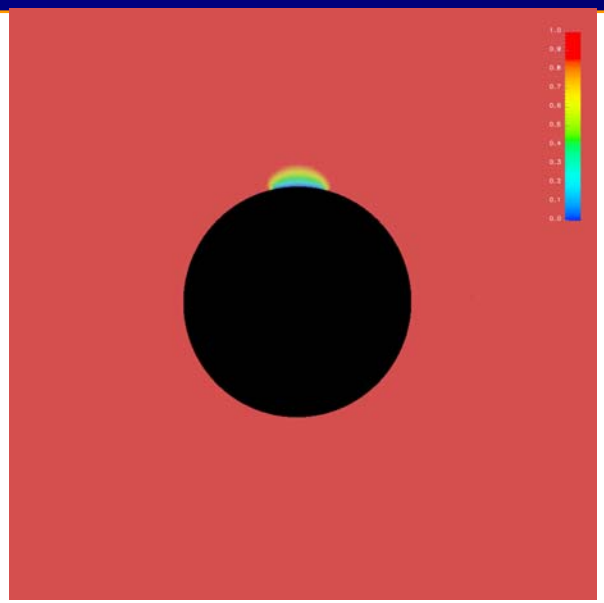

0.000M

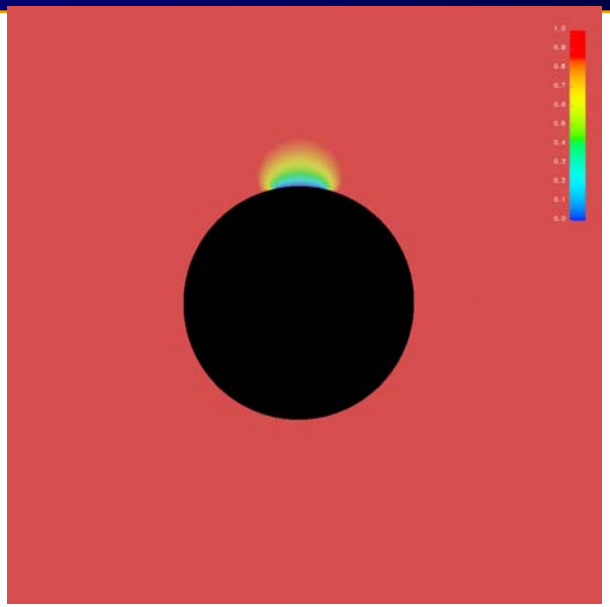

0.075M

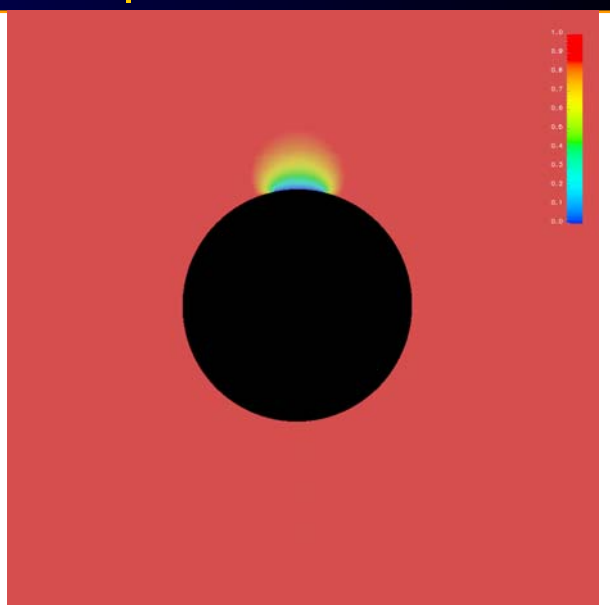

0.150M

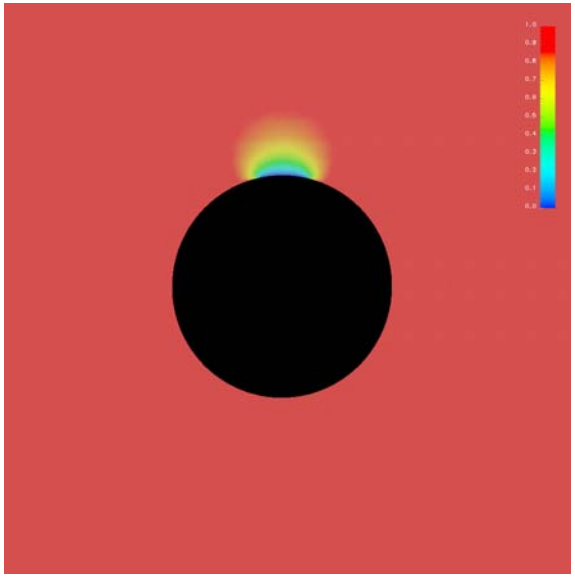

0.300M

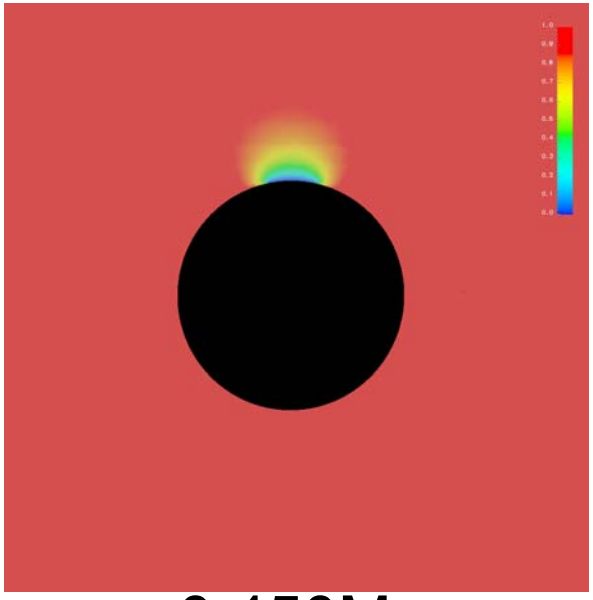

0.450M

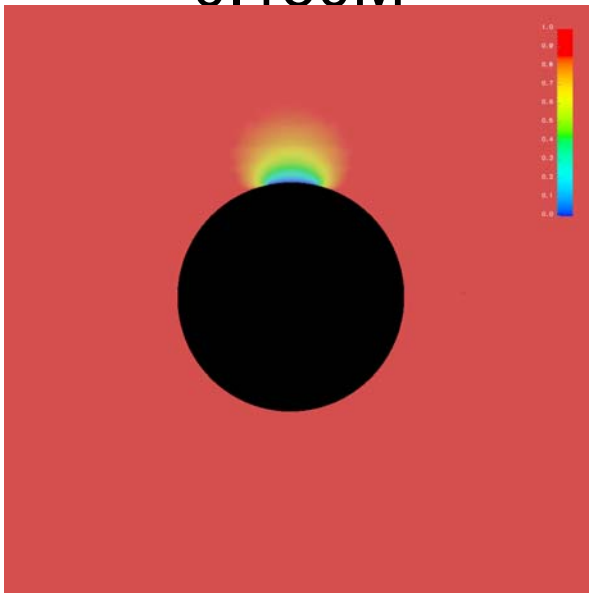

0.600M

Why Study AChE?

- AChE breaks down ACh at the post-synapse in the neuromuscular junction, terminating the neural signal
- Because of its critical function, AChE is a target for medical agents, insecticides, chemical warfare agents
- The reaction is extremely fast, approaching diffusion limit. Thus a good target to study diffusion both experimentally and computationally
- Part of efforts toward synapse simulation at cellular level

Sub-types of AChE

Three different types of AChE subunits from the same gene, but with alternative splicing of the C-terminal:

- Type R ('readthrough') produce soluble monomers; they are expressed during development and induced by stress in the mouse brain.
- Type H ('hydrophobic') produce GPI-anchored dimers, but also secreted molecules; they are mostly expressed in red blood cells, where their function is unknown.
- Type T ('tailed') represent the forms expressed in brain and muscle. This is the dominate form of AChE, and also exists for butyrylcholinesterase (BChE).

From Gene to protein

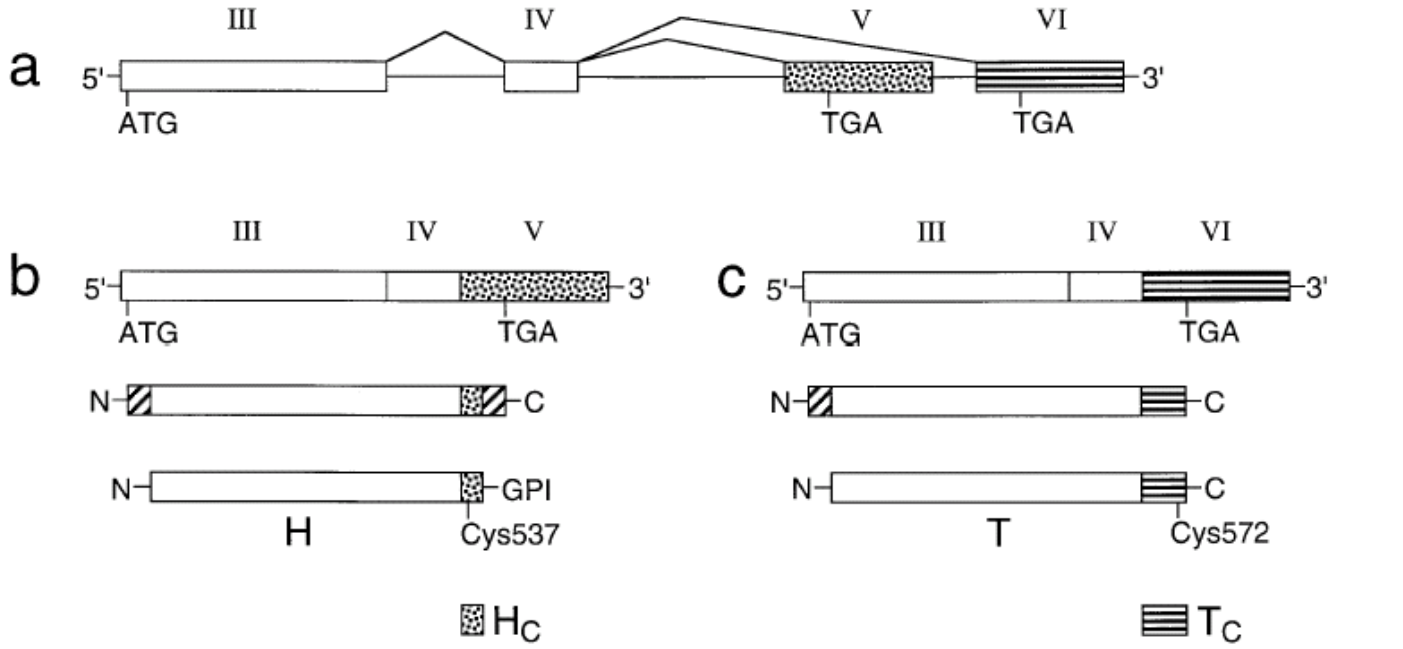

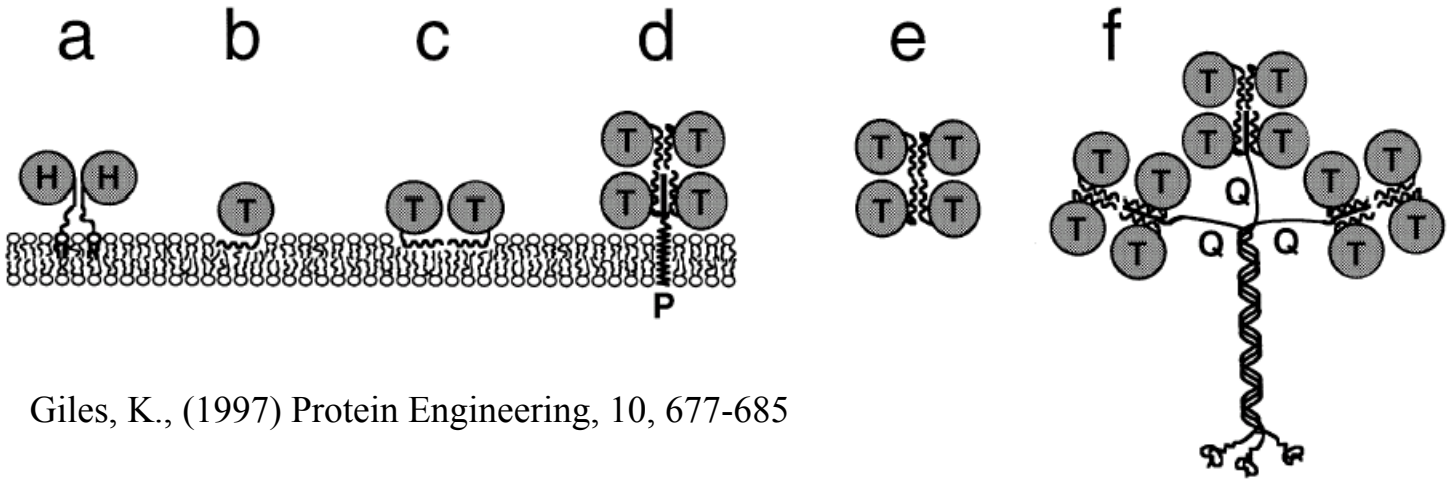

Giles, K., (1997) Protein Engineering, 10, 677-685

Catalytic Mechanism in AChE

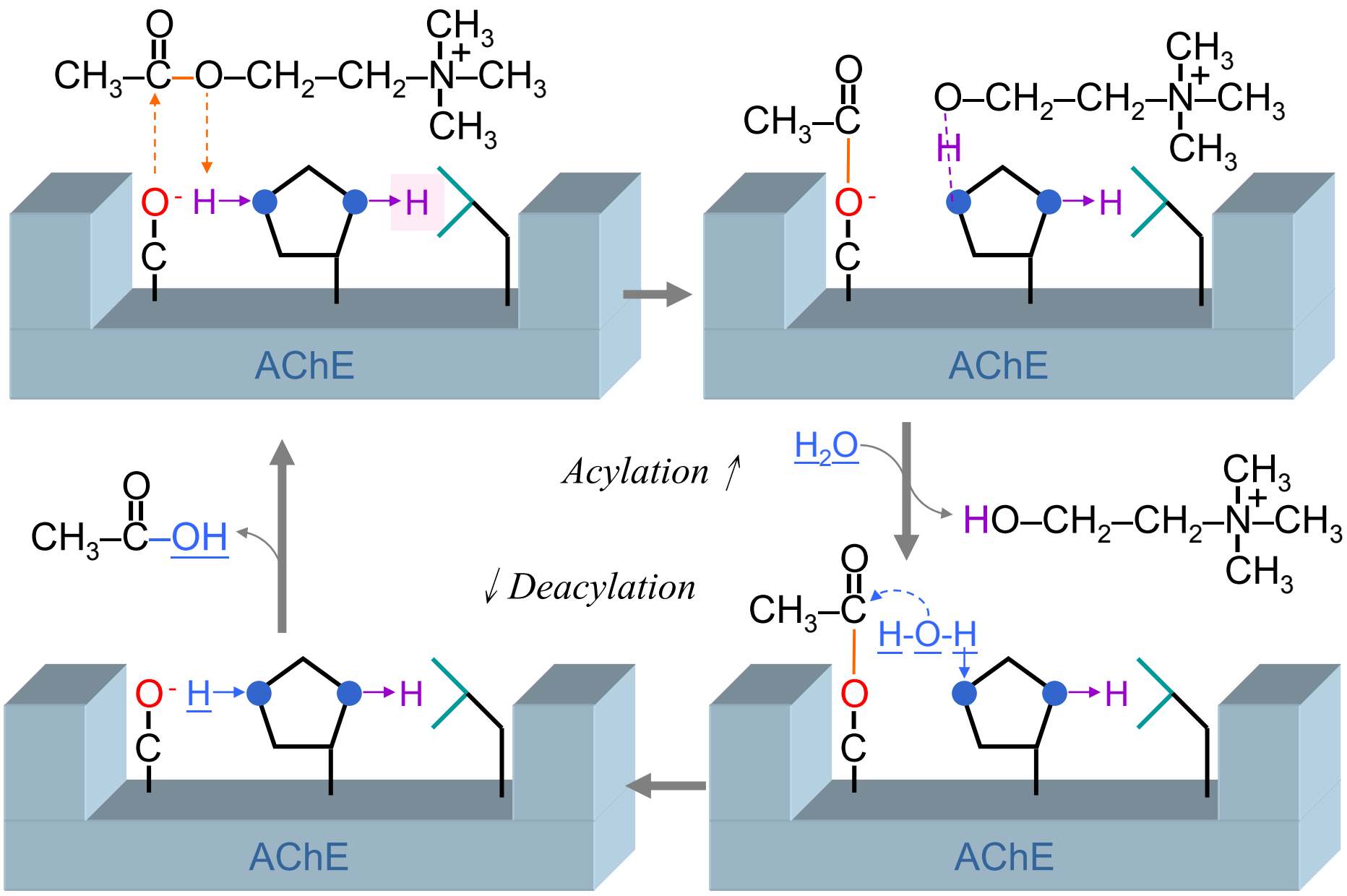

Adapted from Dressler & Potter (1991) Discovering Enzymes, p.243

AChE Catalytic Center

AChE has a '*deep gorge*' leading to its active site

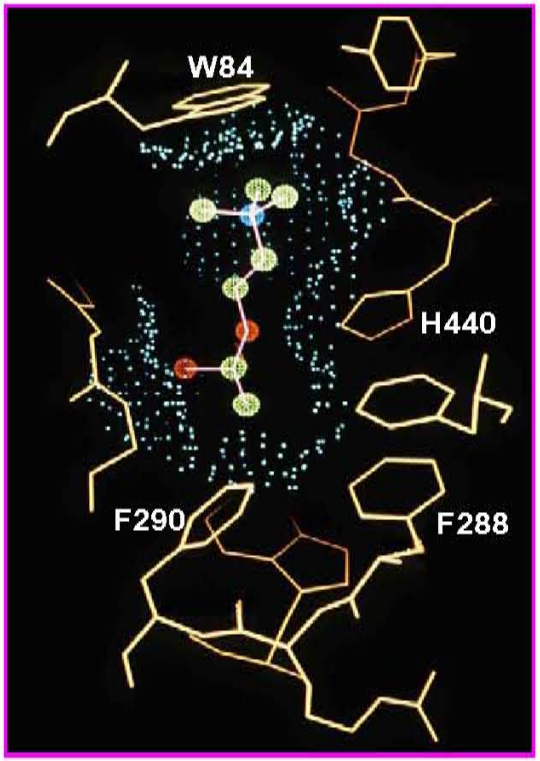

ACh bound in AChE active site

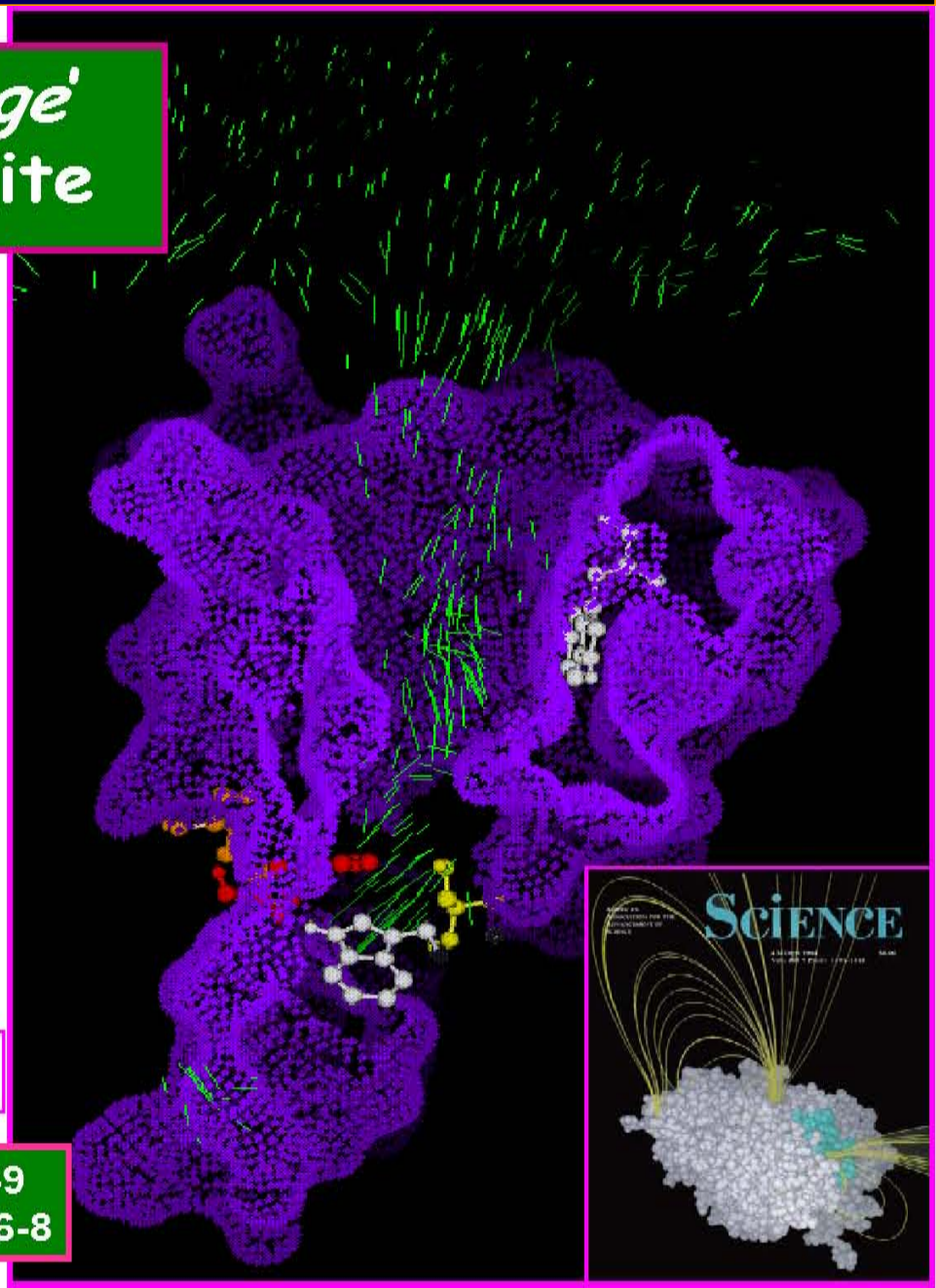

Sussman *et al* SIlman (1991) *Science* 253, 872-9
GIlson *et al* Sussman (1994) *Science* 263, 1276-8

Finite element mesh generation

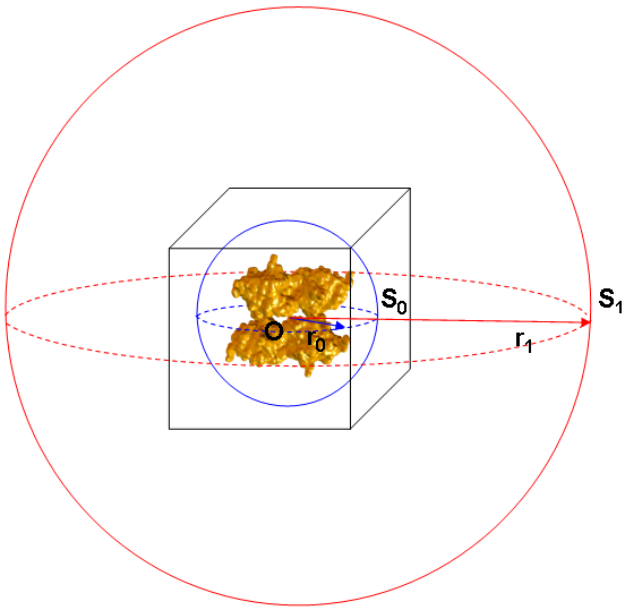

- GAMer (Holst Group @ UCSD):

(http://www.fetk.org/codes/gamer/)

- $r_1 \sim 40r_0$ (r: biomolecule size)
- Adaptive tetrahedral mesh generation by contouring a grid-based inflated vdW accessibility map for region S_0
- Extend mesh to region S_1 spatial adaptively

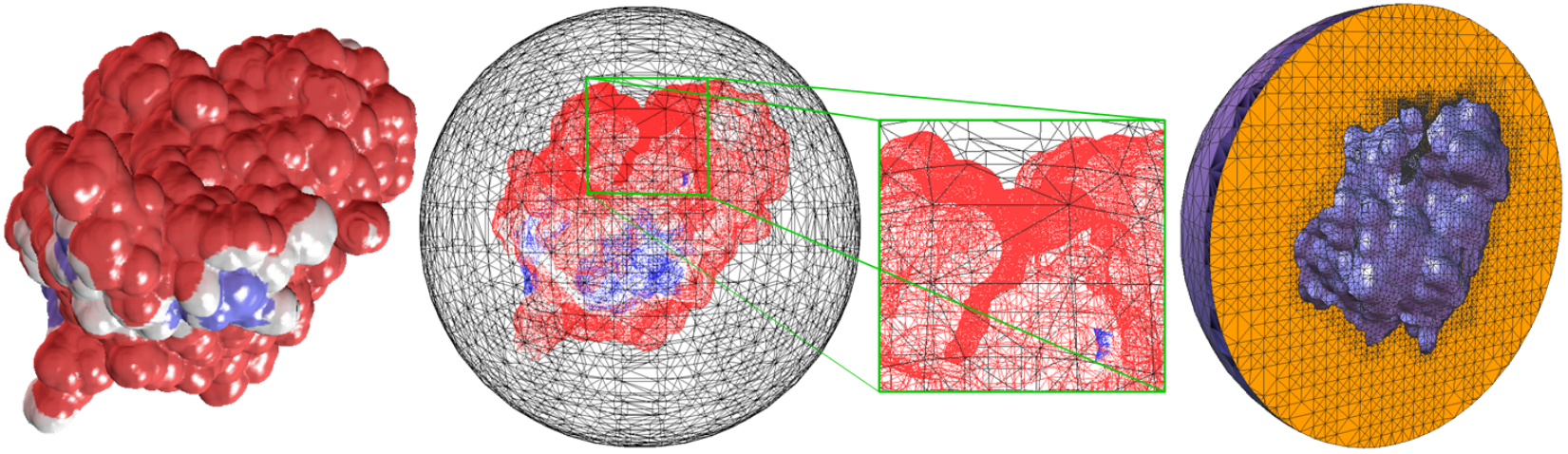

Reactive boundary assignment

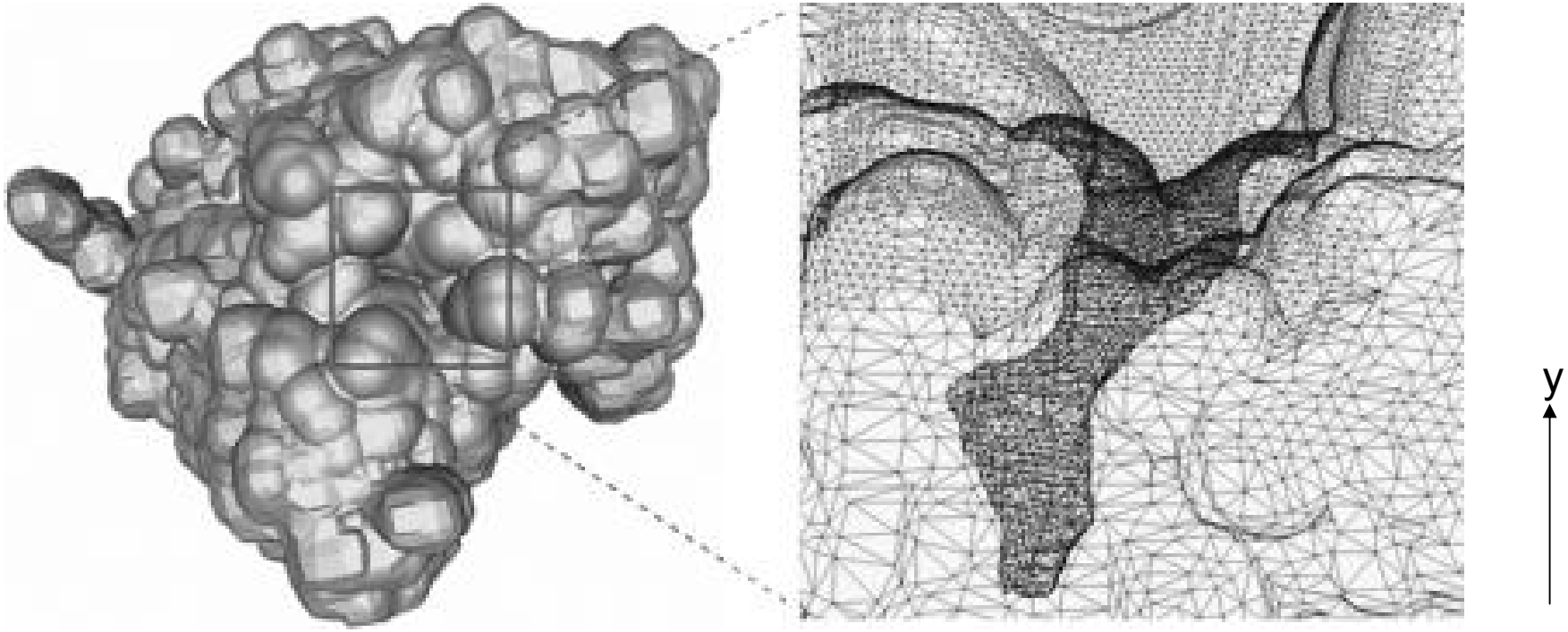

The origin: carbonyl carbon of Ser203

Sphere 1: (0.0, 16.6, 0.0) r = 12Å

Sphere 2: (0.0, 13.6, 0.0) r = 6Å

Sphere 3: (0.0, 10.6, 0.0) r = 6Å

Sphere 4: (0.0, 7.6, 0.0) r = 6Å

Sphere 5: (0.0, 4.6, 0.0) r = 6Å

Sphere 6: (0.0, 1.6, 0.0) r = 6Å

Reactive boundary assignment

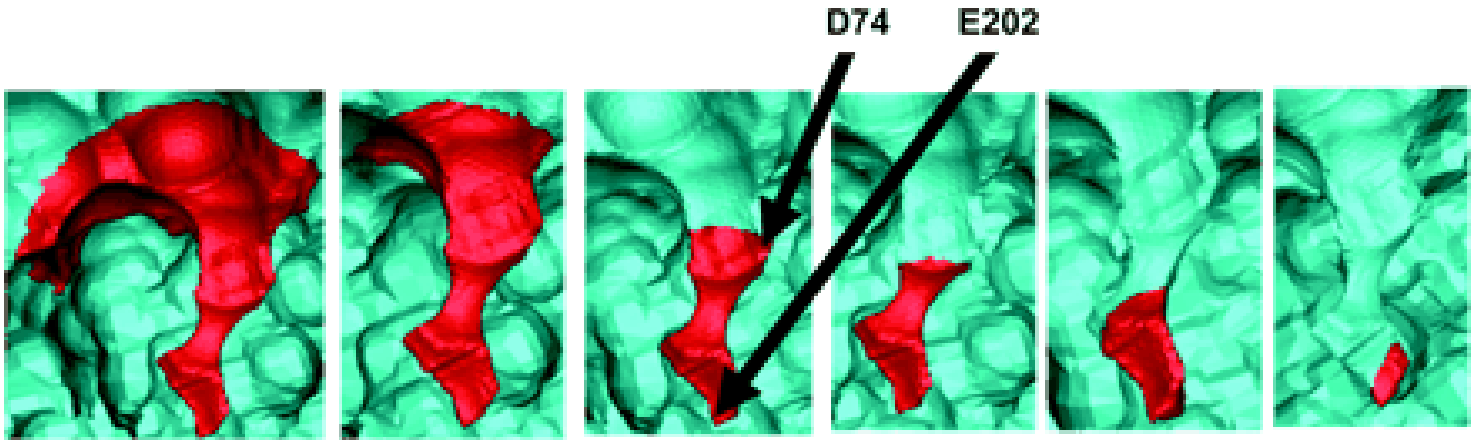

(a)

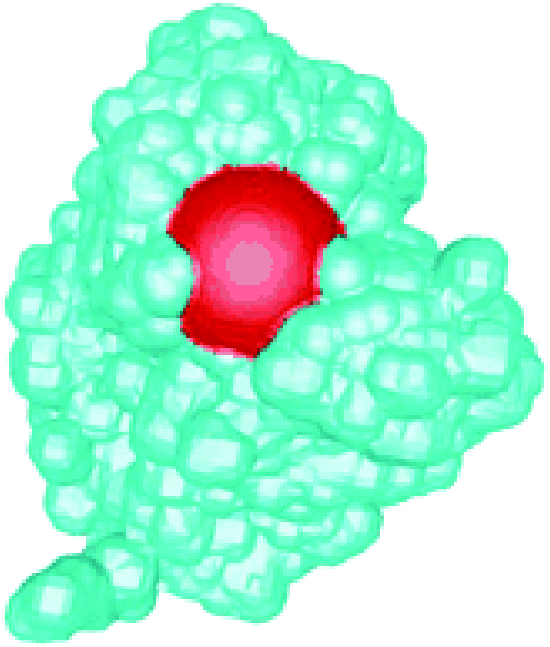

(b)

mAChE wild-type ligand binding rate

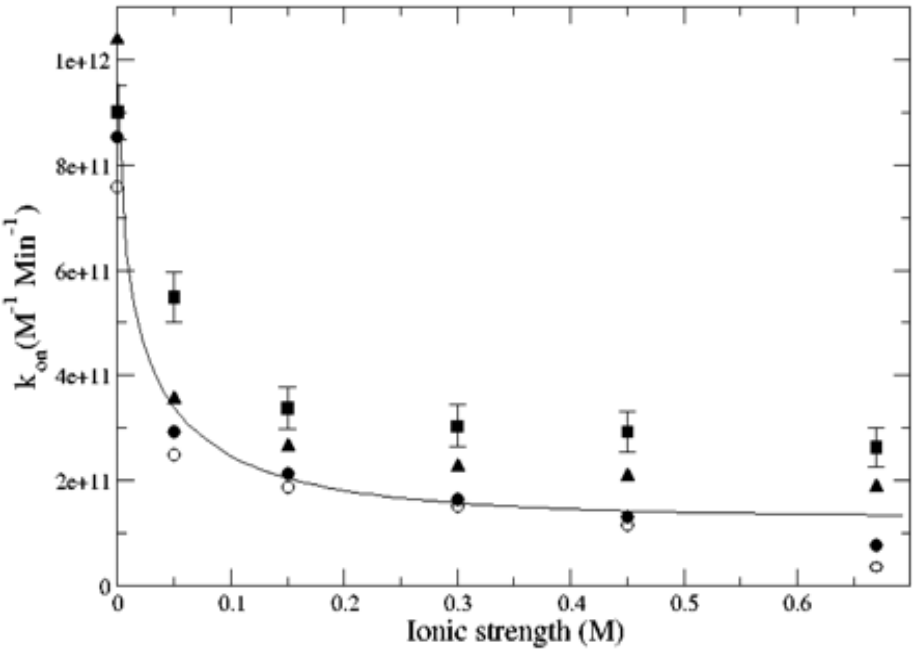

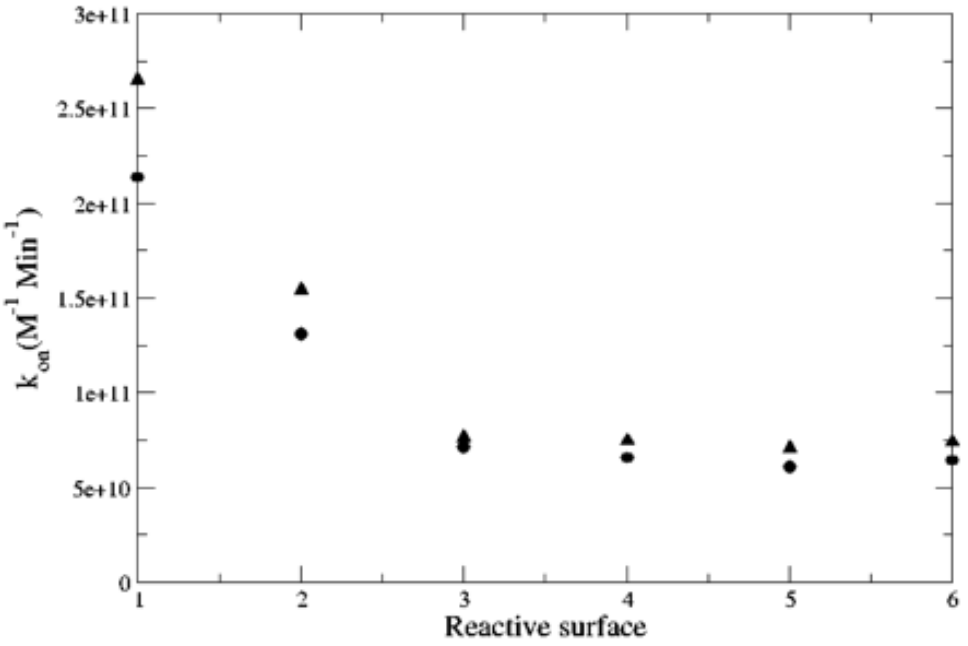

Debye-Huckel limiting law:

$$k_{on} = (k_{on}^{0} - k_{on}^{H})10^{-1.18|z_E z_I|\sqrt{I}} + k_{on}^{H}$$

Mesh quality and refinement

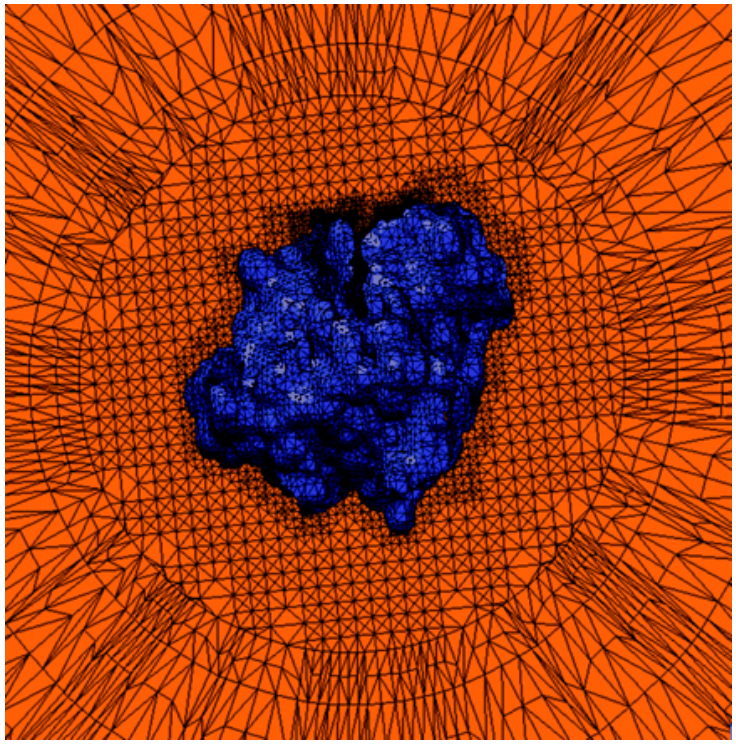

$\varepsilon < 5.0 \times 10^5$

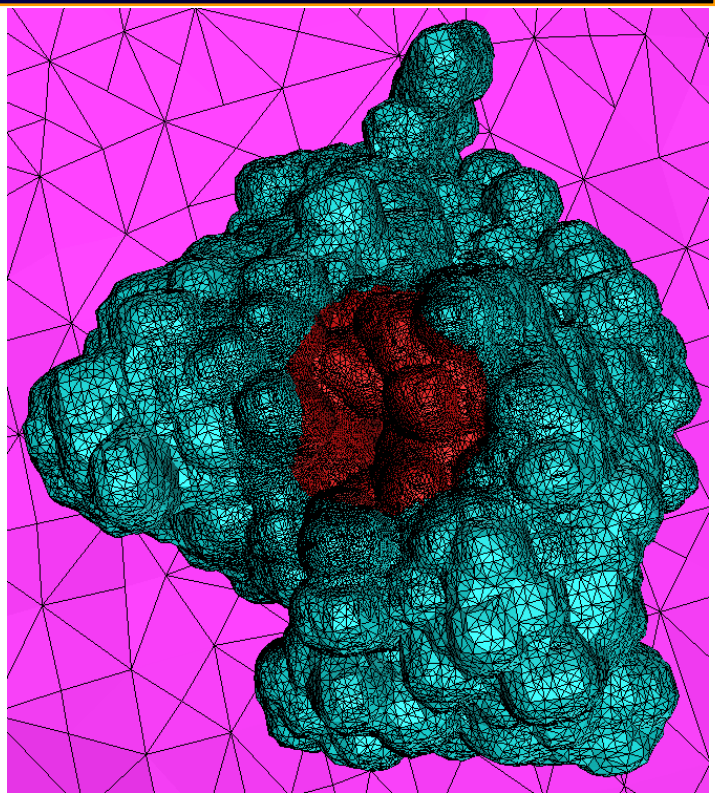

original: 121,670 node,
656,823 simplexes.

final: 1,144,585 node,
6,094,440 simplexes.

Why do we need to refine the mesh?

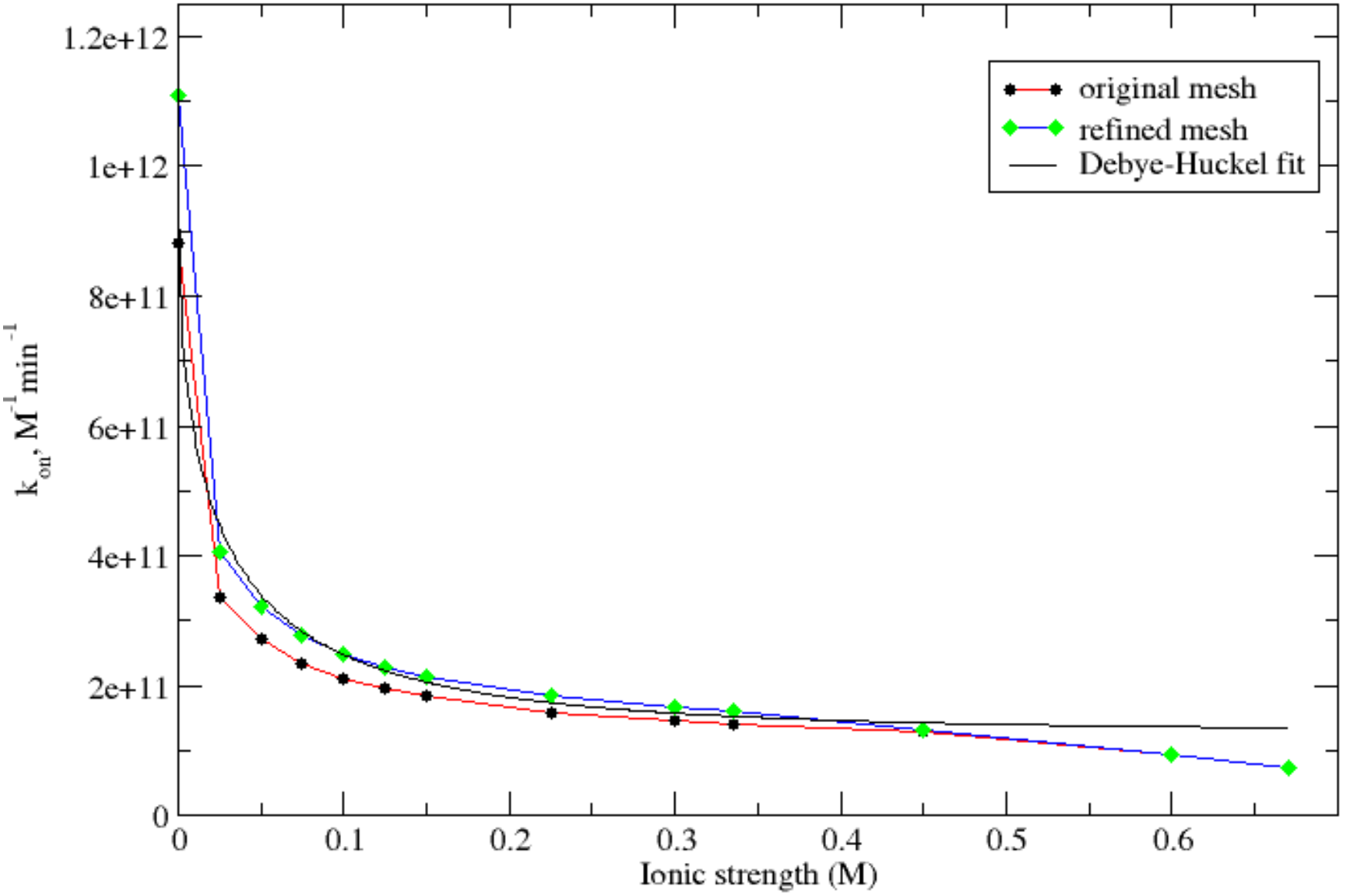

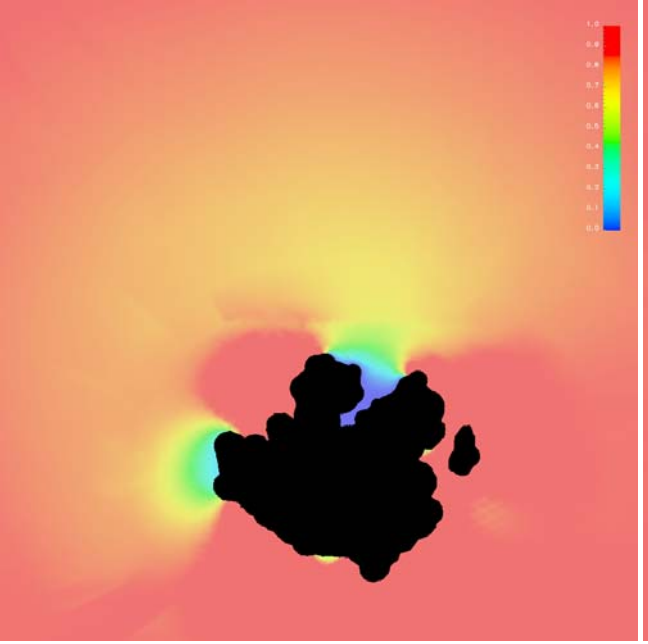

0.025 M

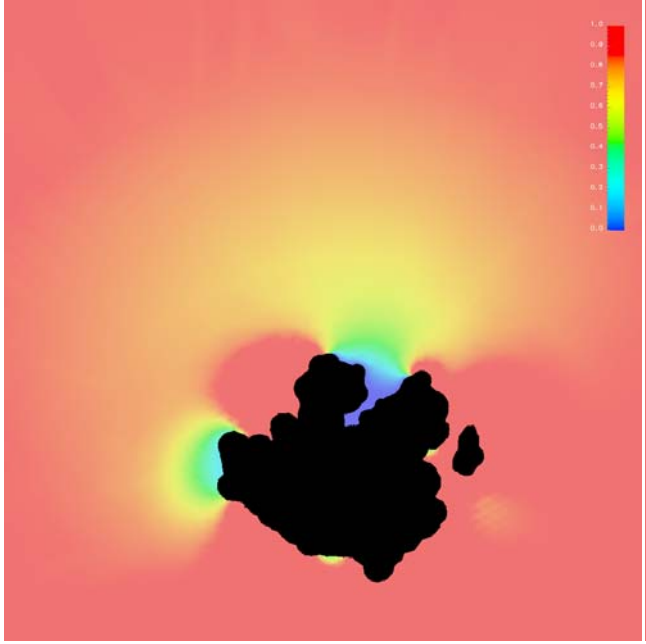

0.050 M

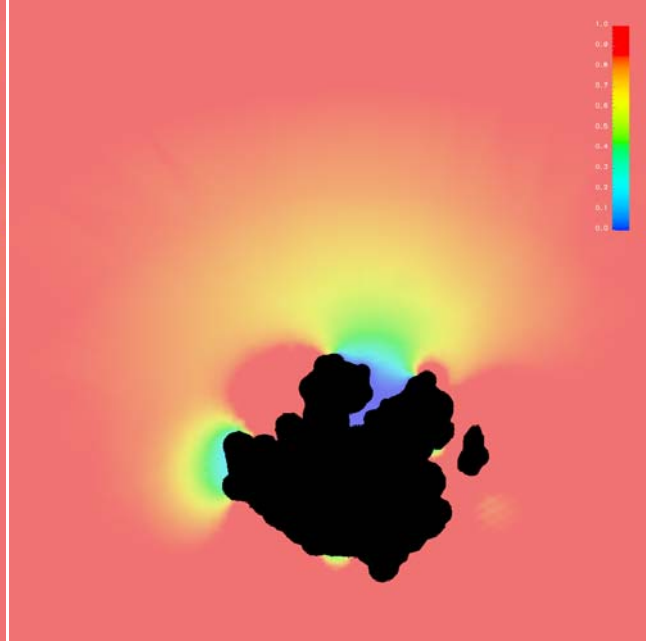

0.100 M

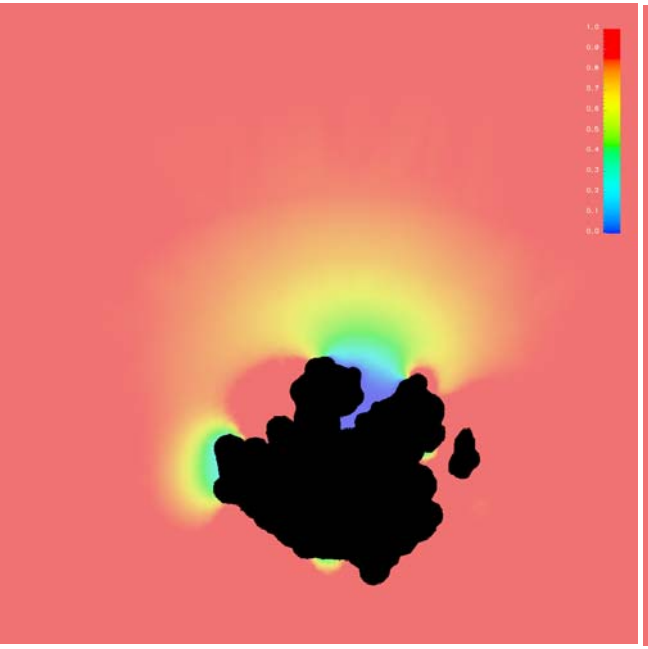

0.225 M

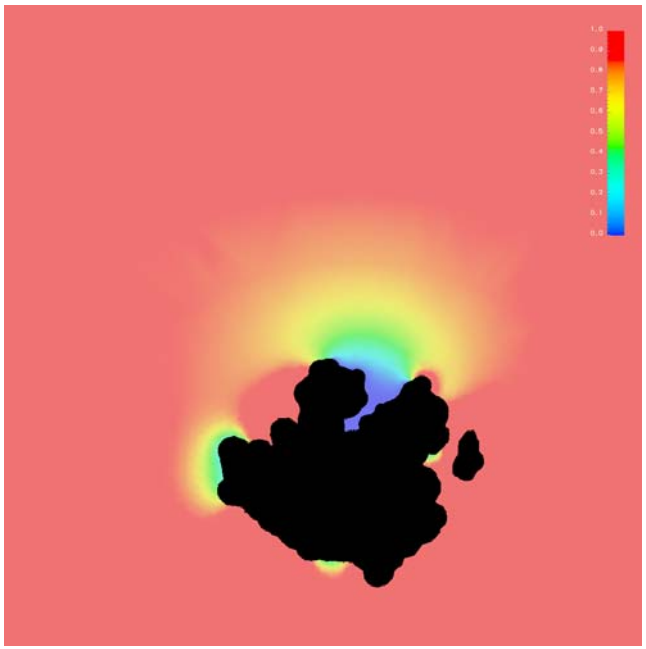

0.450 M

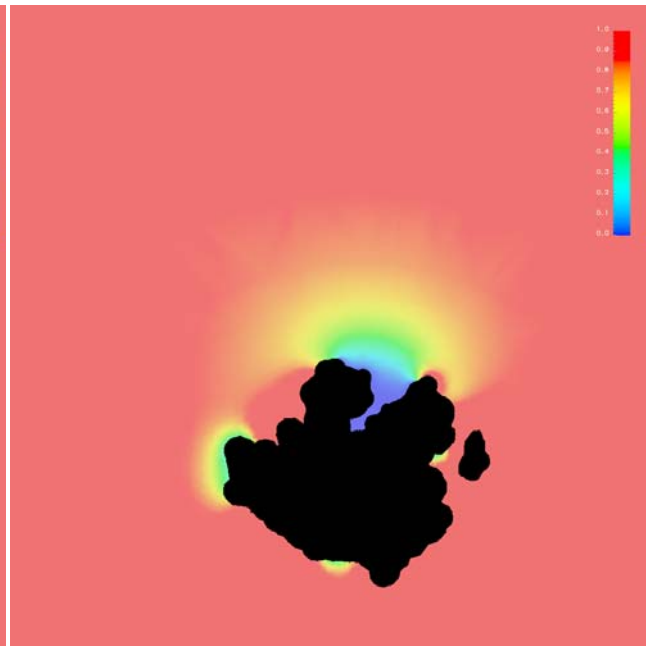

0.670 M

What can we learn from last several cases?

- The concentration distribution is affected by the ionic strength substantially.

- k_{on} exhibits an ionic strength dependence strongly indicative of electrostatic acceleration. The high ionic strength environment lessens the electrostatic interactions between the active site and the ligand, (cf. J. Mol. Biol. 1999, 291, 149-162)

The Quaternary Association of AChE

• In mammalian CNS, AChE exists as an amphiphilic tetramer anchored to the membrane by a hydrophobic non-catalytic subunit (PRiMA)

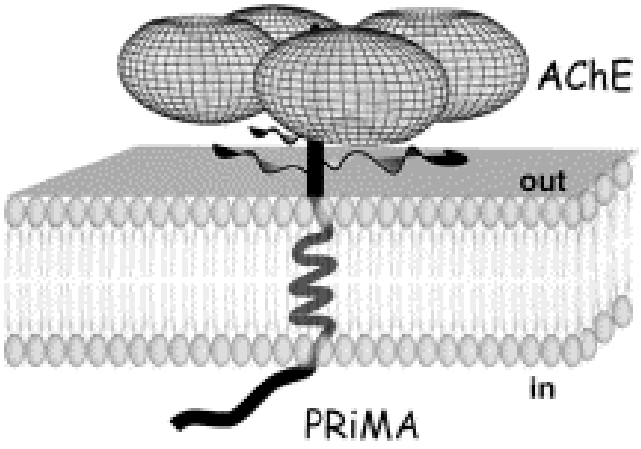

• In NMJ, AChE is an asymmetric form containing 1-3 tetramer associated with the basal lamina by a collagen-like structural subunit ColQ

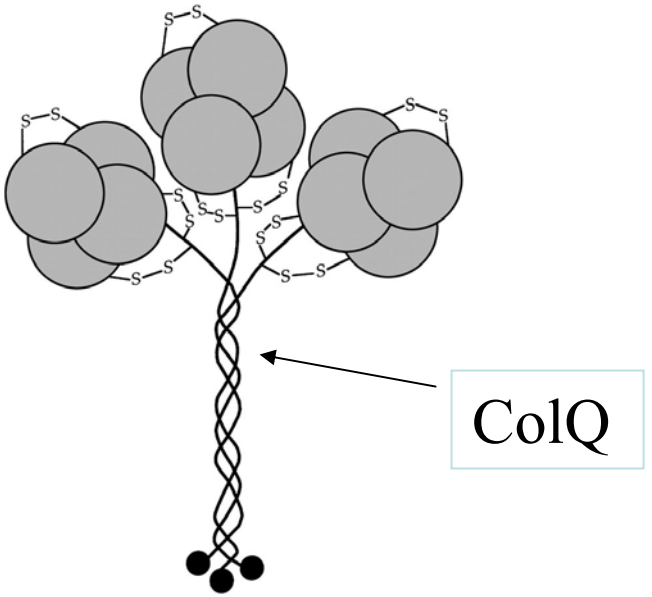

Tetramer: Dimer of Dimers

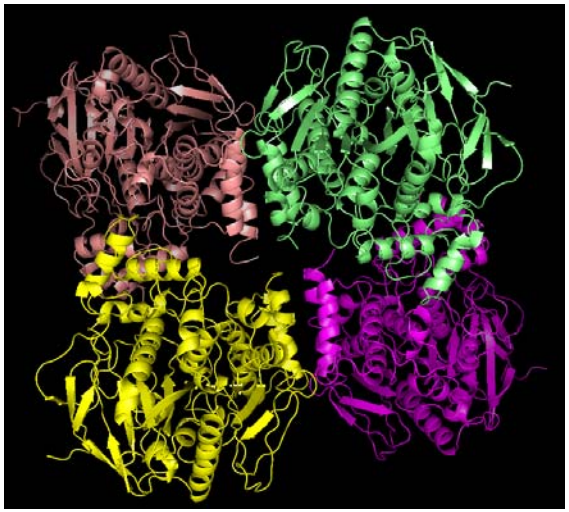

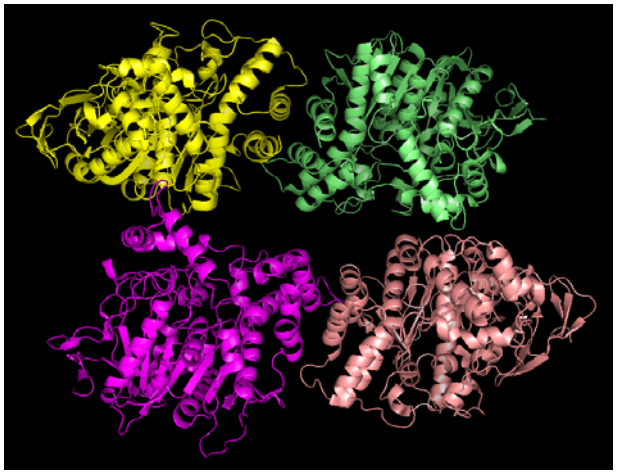

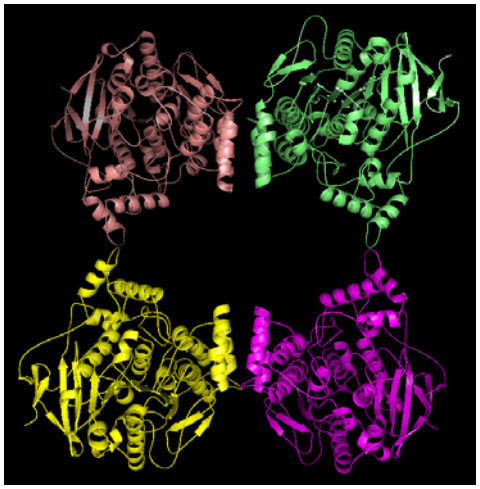

- PDB: 1MAA
- Residues 549-583 deleted
- Only forms monomer or dimer in solution
- Dimer-dimer interaction similar to Fas2-AChE (omega loop = loop II), resulting in two occluded gorges

PDB: 1C2O	1C2B(1EAA)
Trypsin released form of AChE from E. *electrocus*	
Crystal grown at pH8 4°C	pH6 20°C
Compact, square nonplanar	Loose, pseudo-square planar;
four-helix boundle parallel	anti-parallel
two gorges partially blocked	all gorges open

- additional density for C-terminal t peptide observed, but not resolved.

Heteromeric Association with PRAD

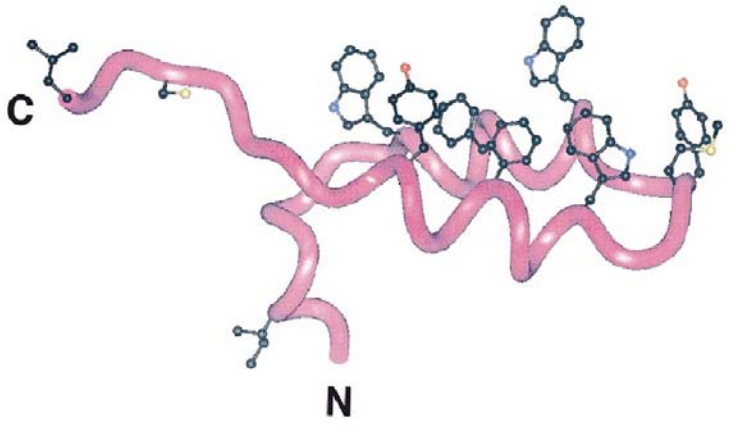

Giles, K. (1997) Protein Engineering, 6, 677-685

- t peptide sequence (40 or 41 res) highly conserved
- PRAD = Proline Rich Attachment Domain
- PRAD is required to form tetramer in solution

Bon,S. Coussen, F., Massoulie, J. (1997) JBC, 272, 3016-3021

Bon, S. et al. (2003) Eur. J. Biochem, 271, 33-47

ColQ_ Mouse

LPGLDQKKRG SHKACCLLMP PPPPLFPPPF FRGSRSPLLS PDMKNLLELE ASPSPCIQGS
LGSPGPPGQG PPGLPGKTGP KGEKGDLGRP GRKGRPGPPG VPGMPGPVGW PGPEGPRGEK
GDLGMMGLPG SRGPMGSKGF PGSRGEKGSR GERGDLGPKG EKGFPGFPGM LGQKGEMGPK
GESGLAGHRG PTGRPGKRGK QGQKGDSGIM GPHGKPGPSG QPGRQGPPGA PGPPSA

PRMA_ Mouse

MLLRDLVPRH GCCWPSLLLH CALHPLWGLV QVTHAEPQKS CSKVTDSCQH ICQCRPPPPL
PPPPPPPPPP RLLSAPAPNS TSCPAEDSWW SGLVIIVAVV CASLVFLTVL VIICYKAIKR
KPLRKDENGT SVAEYPMSSS QSHKGVDVNA AVV

A flexible Tetramer?

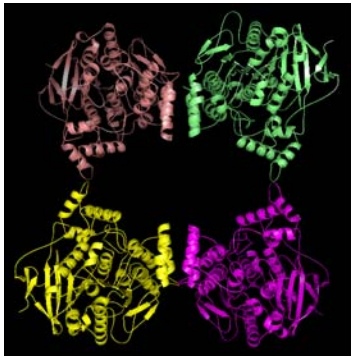

1C2B
Flat square
Quasi-planar

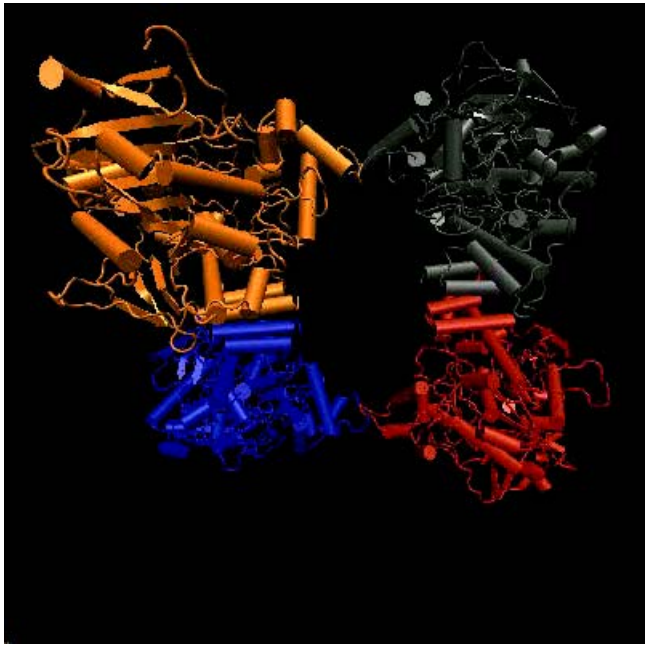

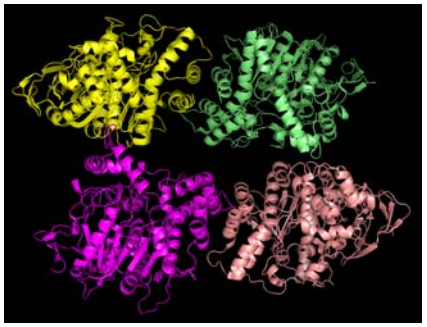

1C2O

Compact

Tetrahedral Mesh for mAChE Tetramer

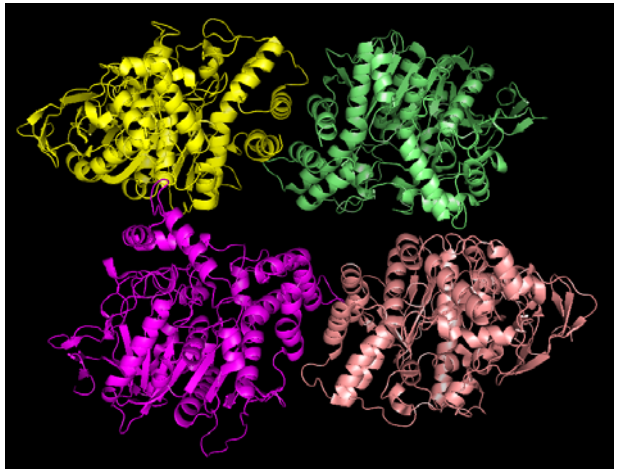

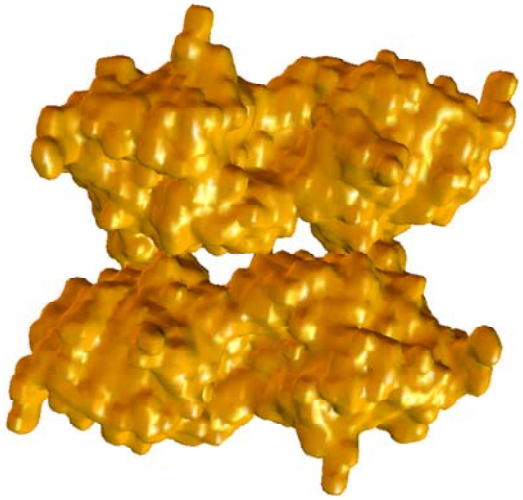

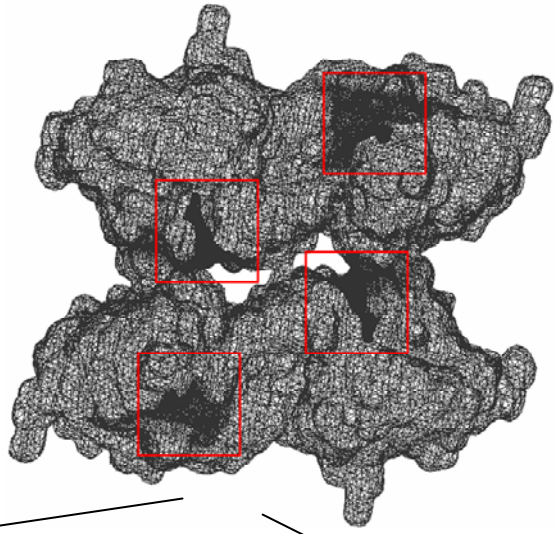

Reactive surface is assigned according to previous studies on monomeric mAChE

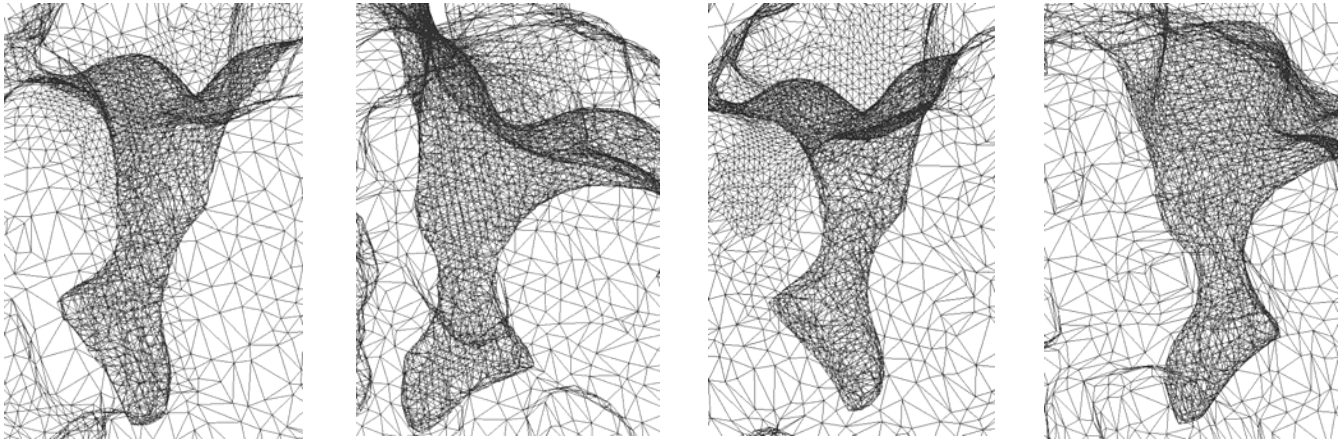

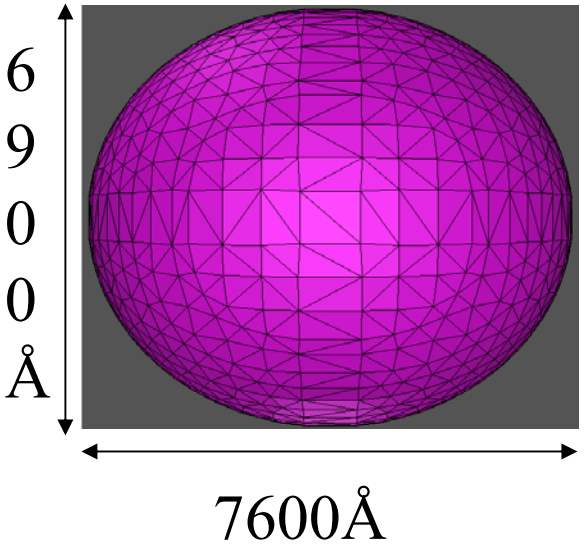

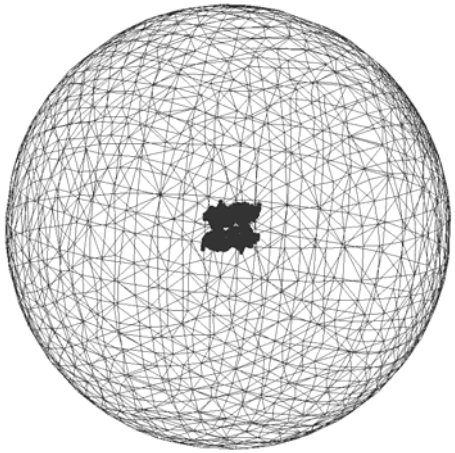

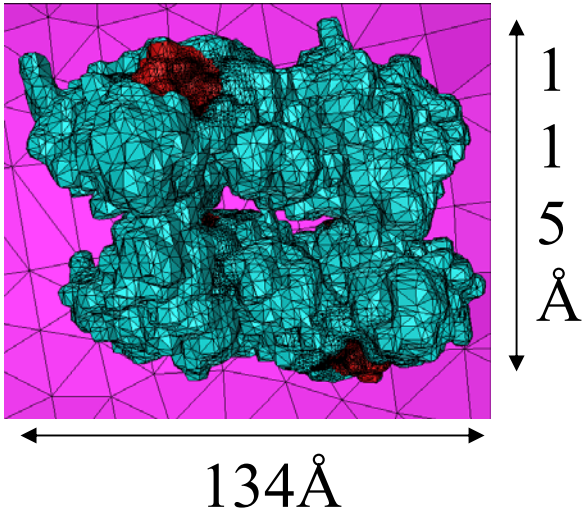

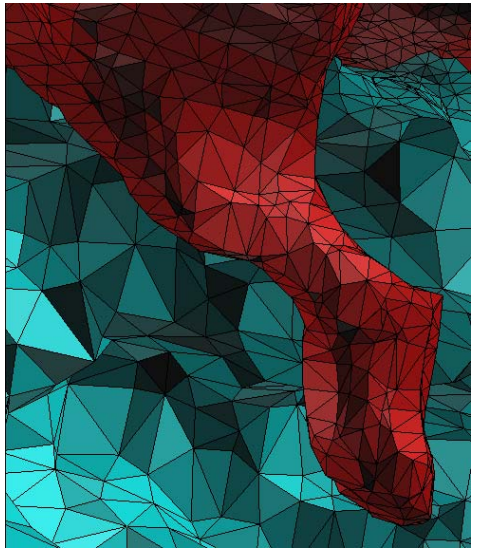

Typical Mesh quality:

726186 simplices, 142643 vertices

Joe-Liu: 0.999(best),0.0154(worst)

Edge-Ratio: 1.03(best), 8.48(worst)

Volume: 1.73e-4(S), 9.35e8(L)

Short Edge: 0.039(S), 363 (L)

Long Edge: 0.148 (S), 861 (L)

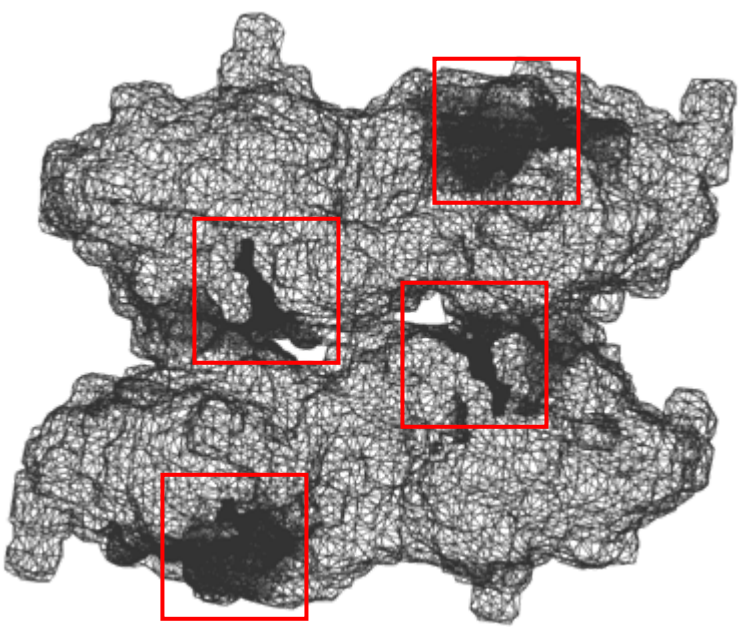

1C2O

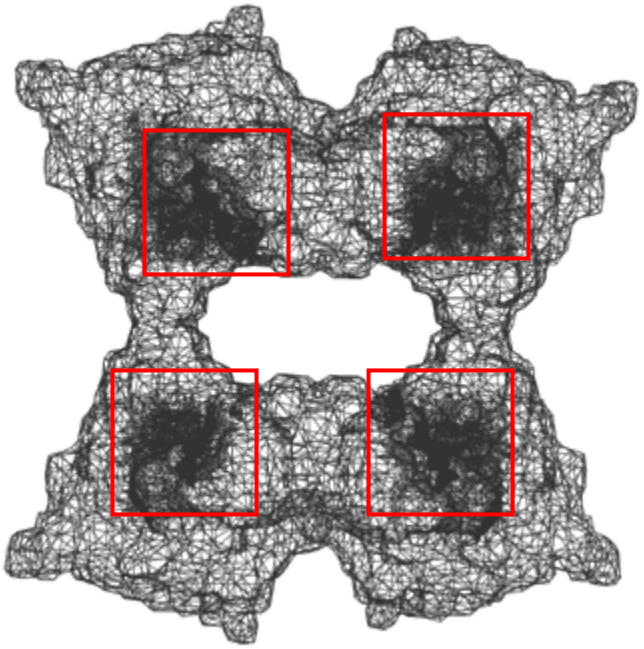

1C2B

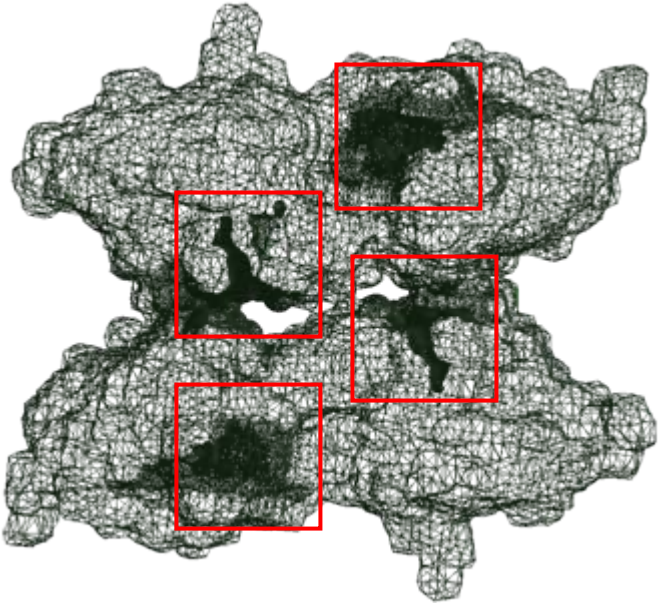

Int4

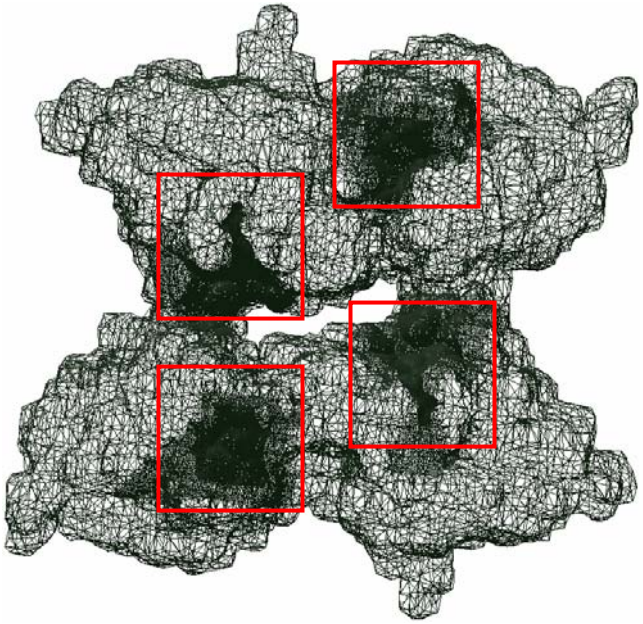

Int3

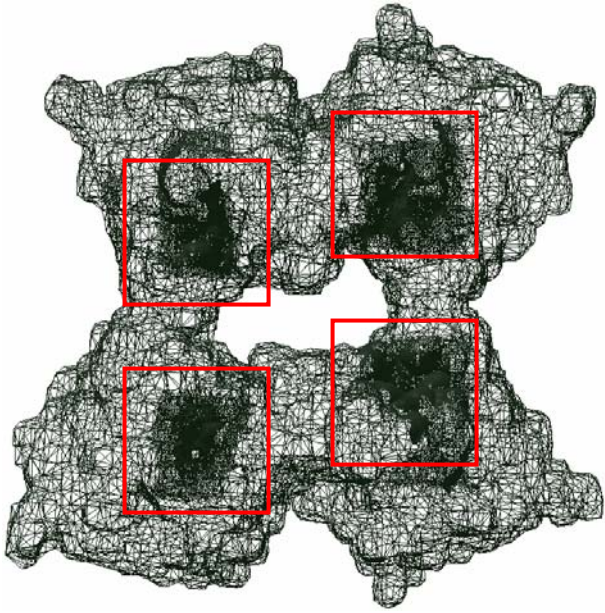

Int2

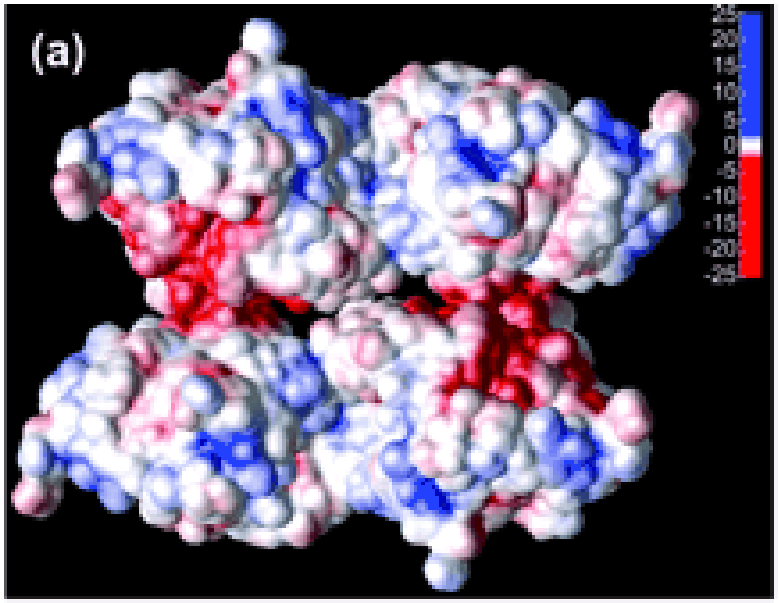
(a)
25
20
15
10
5
0
-5
-10
-15
-20
-25

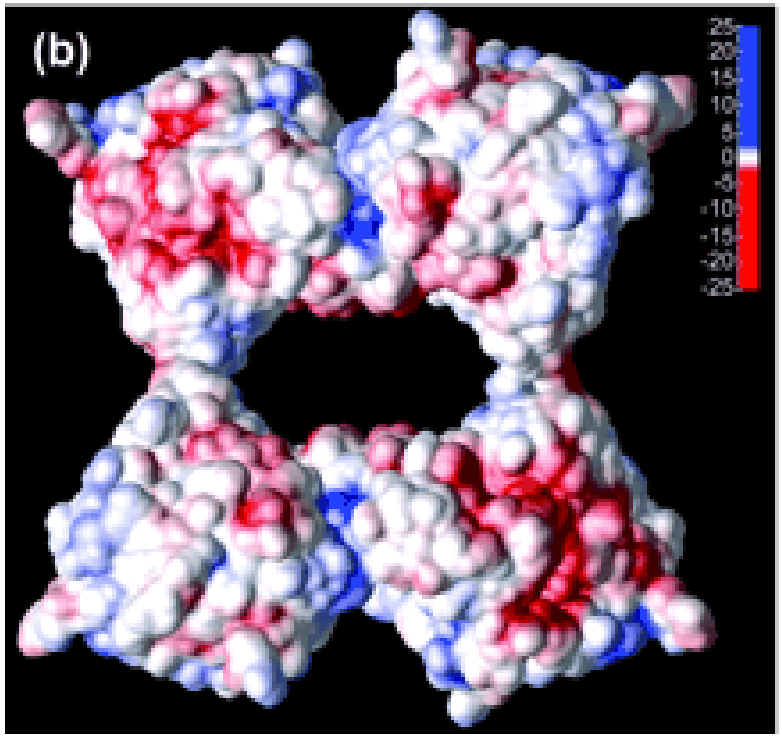
(b)
25
20
15
10
5
0
-5
-10
-15
-20
-25

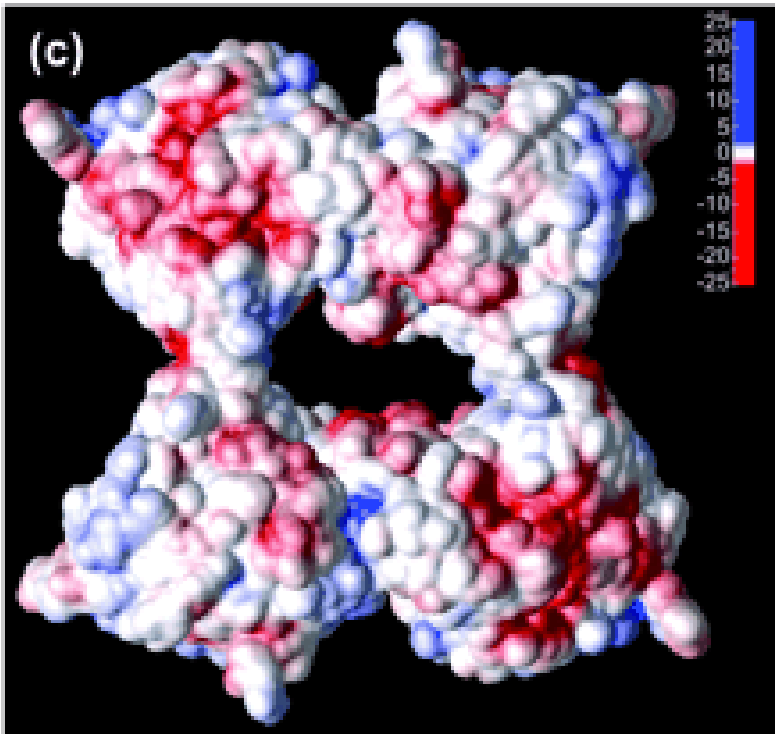
(c)
25
20
15
10
5
0
-5
-10
-15
-20
-25

PMF Calculation

- APBS 0.5.1 (http://agave.wustl.edu/)
- Grid hierarchy (0-10)
- Apolar forces and dielectric boundary omitted
- No coupling b/w PMF and diffusing particle (Poisson-Nerst-Plank Eqn)
- No correlation b/w diffusing species

Grid#	dx(Å)	dy(Å)	dz(Å)	*x	*y	*z
0	0.44	0.38	0.38	-	-	-
1	0.89	0.78	0.80	2.0	2.0	2.0
2	1.33	1.16	1.20	1.5	1.5	1.5
3	2.00	1.73	1.80	1.5	1.5	1.5
4	3.00	2.60	2.71	1.5	1.5	1.5
5	4.49	3.91	4.07	1.5	1.5	1.5
6	6.73	5.87	6.11	1.5	1.5	1.5
7	10.11	8.80	9.16	1.5	1.5	1.5
8	15.16	13.20	13.73	1.5	1.5	1.5
9	22.73	19.80	20.60	1.5	1.5	1.5
10	34.09	29.71	30.89	1.5	1.5	1.5

SSSE Solver Details

- Smol is developed by Baker's group at WUSTL (http://agave.wustl.edu/)
- Based on Mike Holst's Fetk (http://www.fetk.org)
- Diffusing particle (based on TFK+): q = +1e, R=2.0 Å, D = 78000 $Å^2/\mu s$
- Ionic strengths: 0.00, 0.01, 0.05, 0.10, 0.20, 0.300, 0.450, and 0.670 M.
- Reactive surface is assigned with zero Dirichlet boundary condition (perfectly absorbing)
- p_{bulk} = 1.0 M

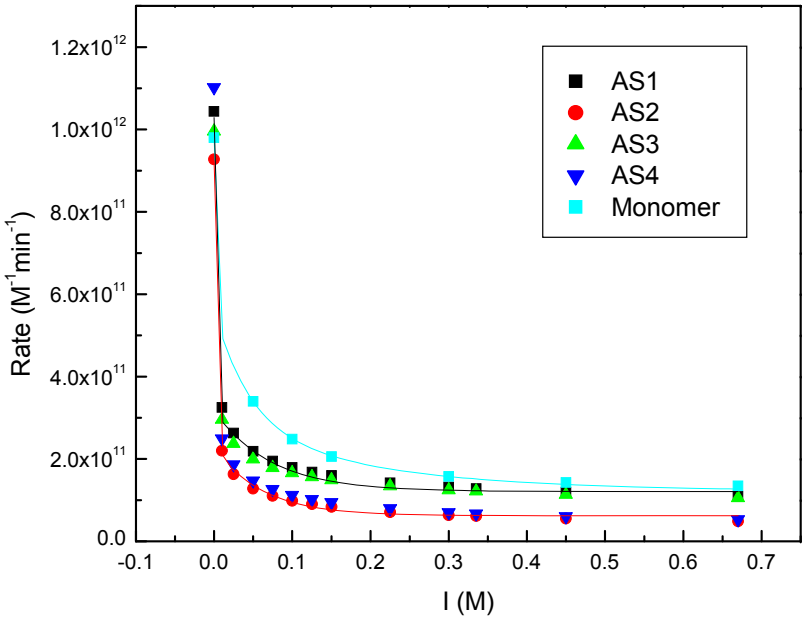

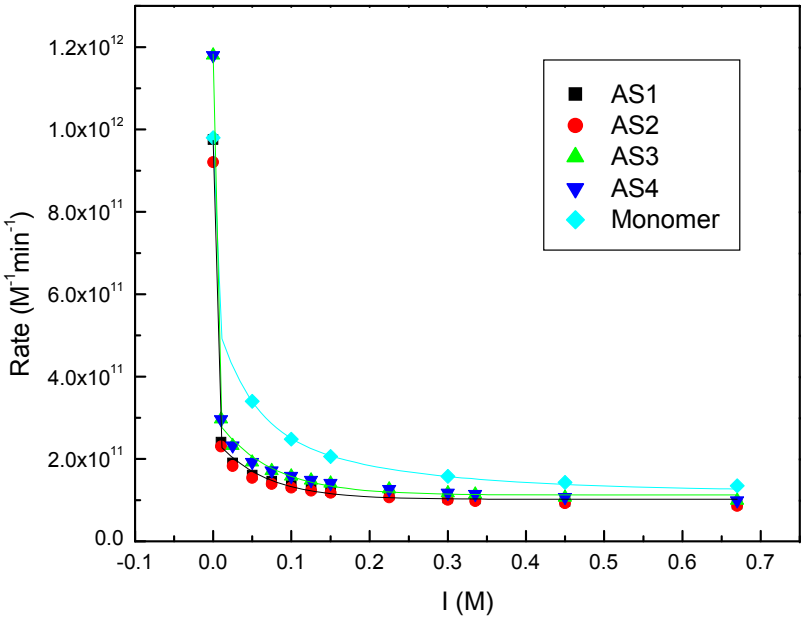

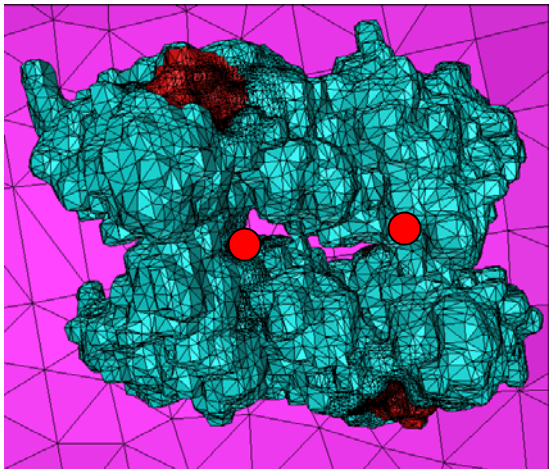

1C2O (compact)

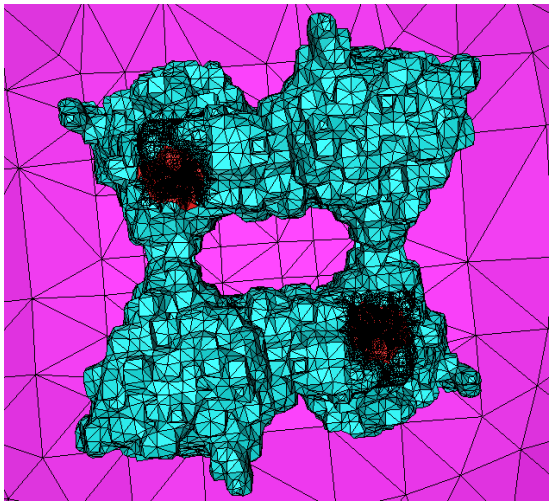

1C2B (loose)

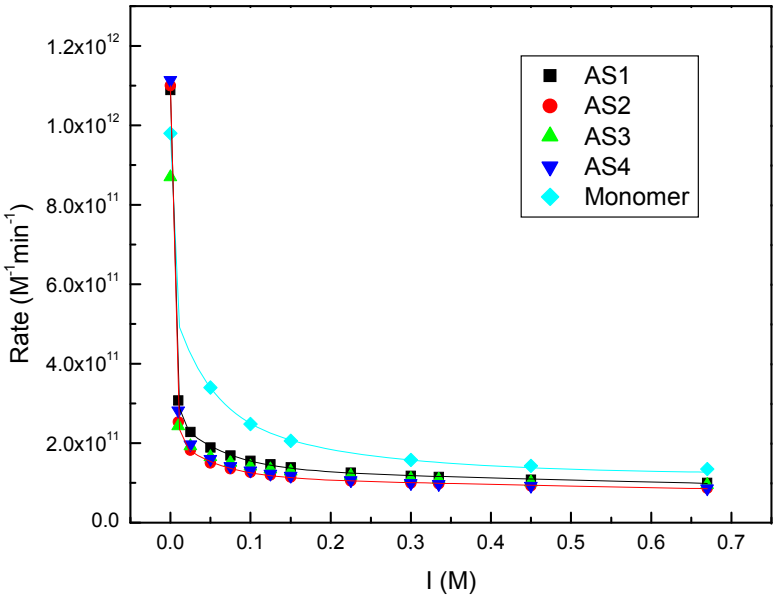

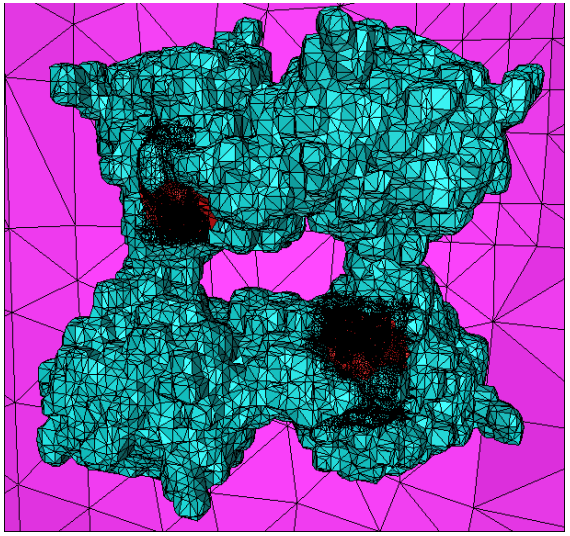

Intermediate b/w
1C2O and 1C2B

All Active Sites

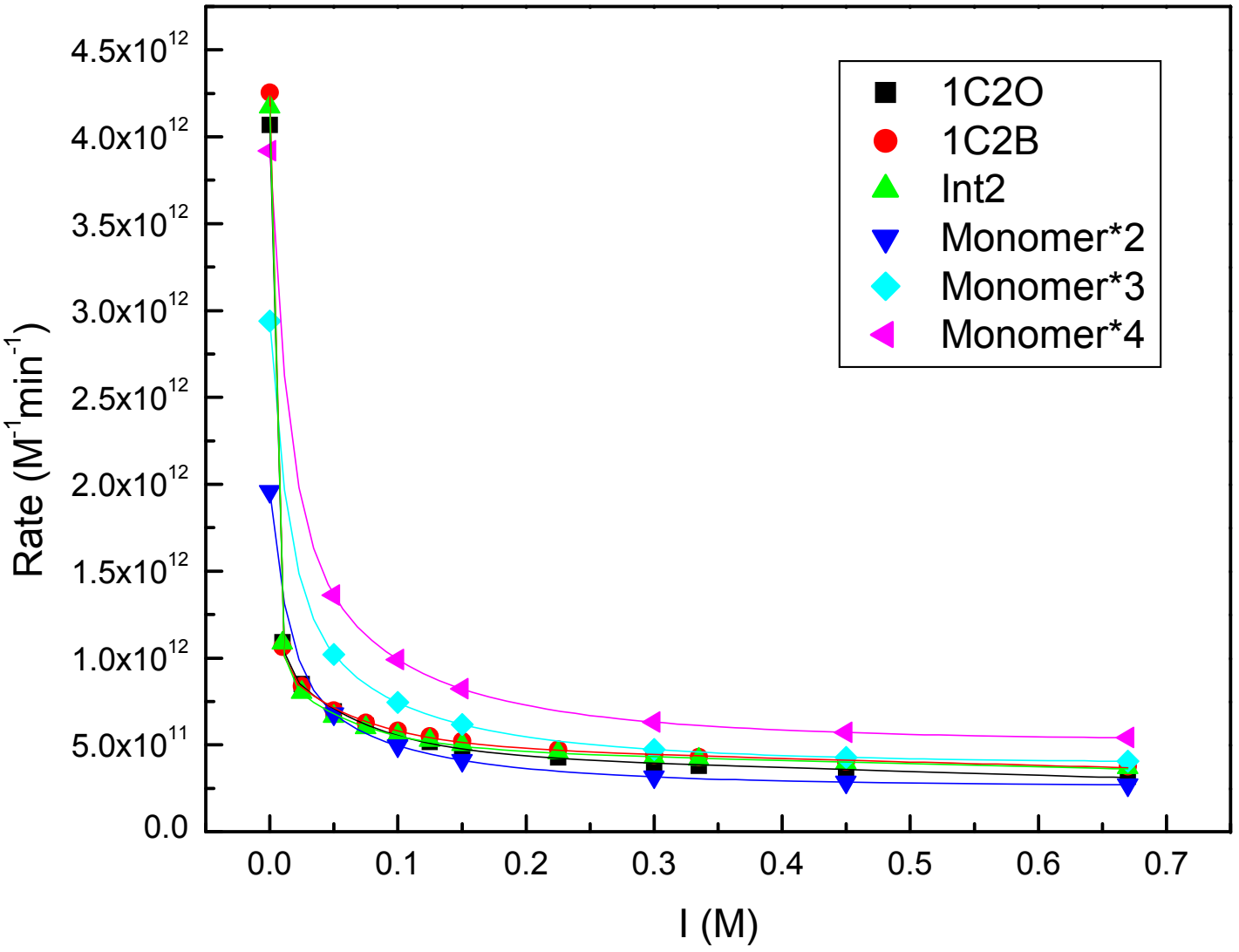

Time-dependent Formation

$$\frac{\partial p(\vec{r},t\,|\,\vec{r}_0,t_0)}{\partial t} = \nabla \cdot D e^{-\beta U(\vec{r})} \nabla e^{\beta U(\vec{r})}\, p(\vec{r},t\,|\,\vec{r}_0,t_0)$$

$$D'(\vec{r}) = D e^{-\beta U(\vec{r})} \qquad p'(\vec{r},t) = e^{\beta U(\vec{r})}\, p(\vec{r},t\,|\,\vec{r}_0,t_0)$$

$$\frac{\partial p(\vec{r},t\,|\,\vec{r}_0,t_0)}{\partial t} = \nabla \cdot D'(\vec{r}) \nabla p'(\vec{r},t)$$

$$-\nabla \cdot D'(\vec{r}) \nabla p'(\vec{r},t) + e^{-\beta U(\vec{r})} \frac{\partial p'(\vec{r},t)}{\partial t} = 0$$

→ symmetric

→ $p(\vec{r},t\,|\,\vec{r}_0,t_0) = e^{-\beta U(\vec{r})}\, p'(\vec{r},t)$

Analytical test

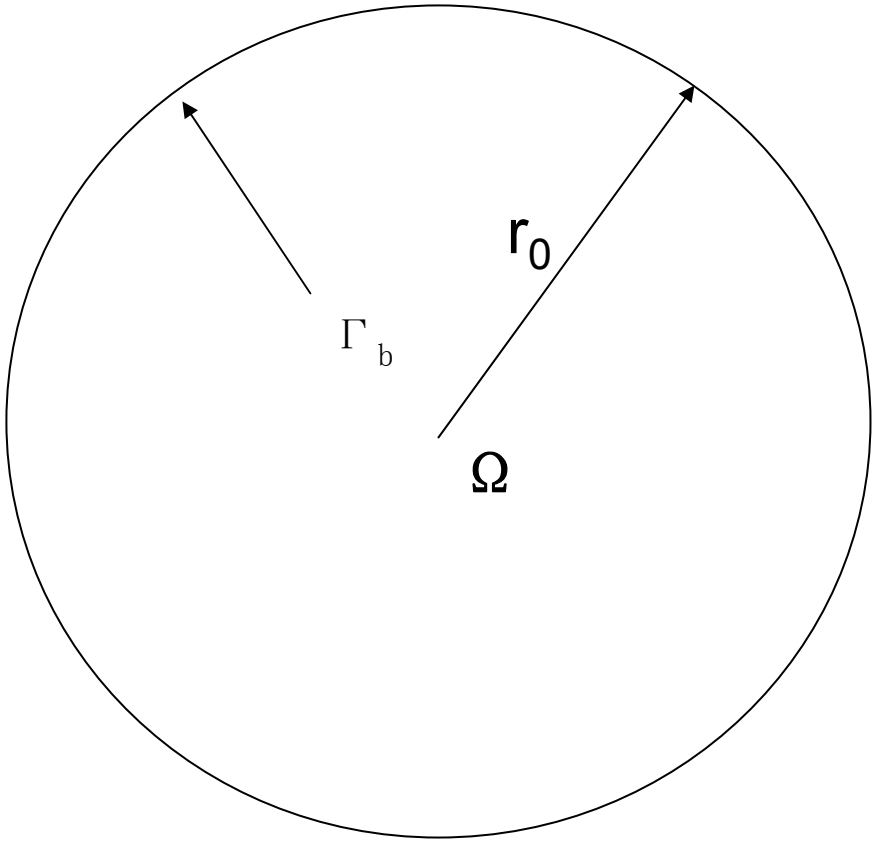

When the potential inside the sphere and the radius of the inner sphere are zero, the analytical solution can be easily written as below:

$$\begin{cases} \dfrac{\partial p(r;t)}{\partial t} - D\Delta_3 p(r;t) = 0 \\ p(r;0) = 0 \\ p(r_0;t) = p_{bulk} \end{cases}$$

$$p(r;t) = p_{bulk} + \frac{2p_{bulk}r_0}{\pi r}\sum_{n=1}^{\infty}\frac{(-1)^n}{n}\sin\frac{n\pi r}{r_0}\exp\left\{-D\left(\frac{n\pi}{r_0}\right)^2 t\right\}$$

Analytical test

- Vertex number: 109,478
- Simplex number: 629,760

- Vertex number: 857,610
- Simplex number: 5,038,080

- Inner radius: 10 A
- Outer radius: 50 A

- Time step: 5 ps

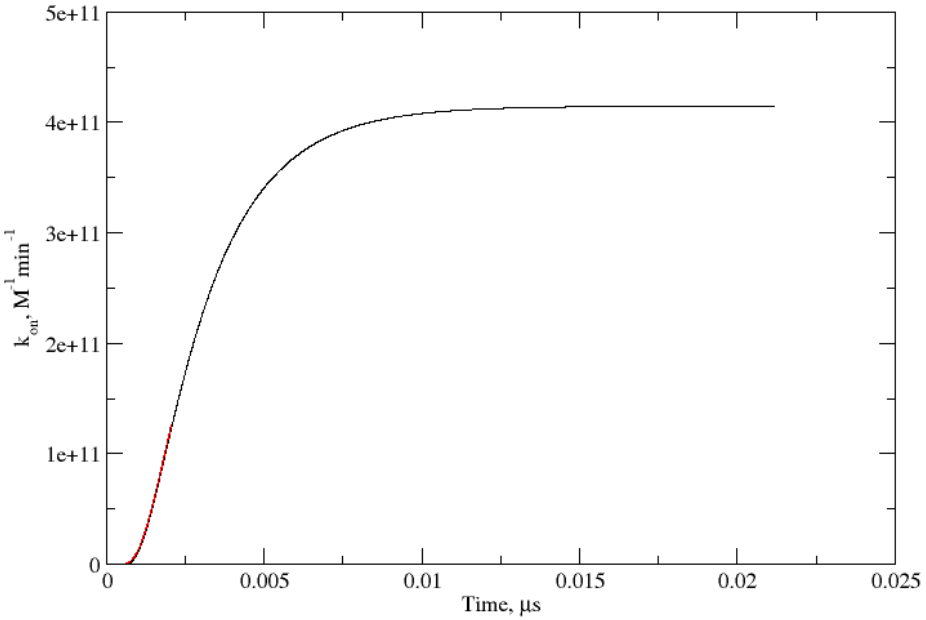

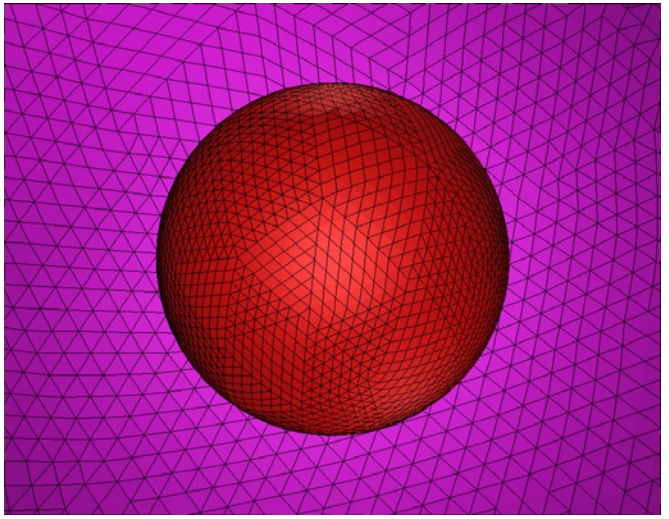

TDSE Results vs. SSSE Results

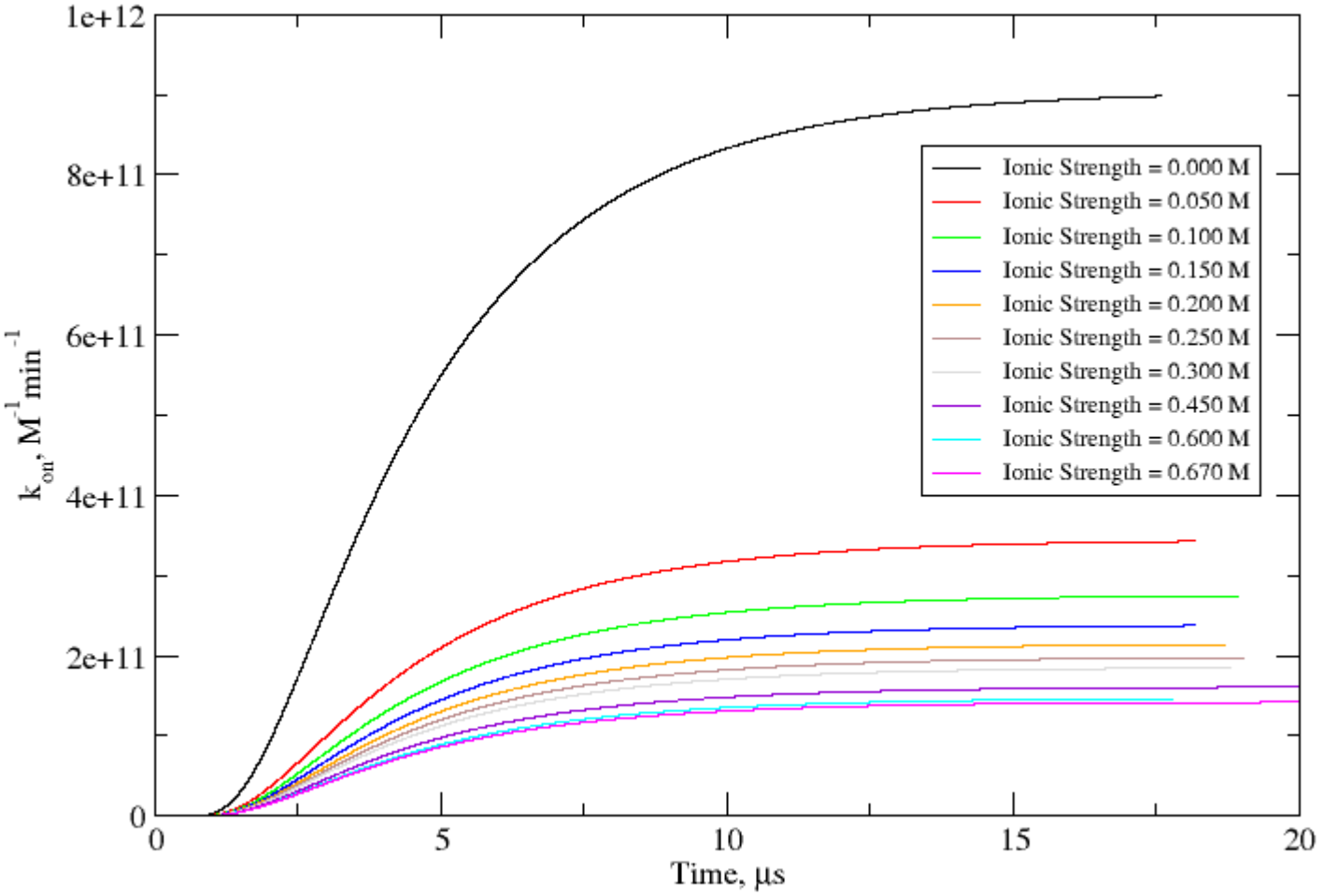

ionic strength (M)	0.000	0.025	0.100	0.300	0.600
SSSE results $k_{on}(10^{11}M^{-1}min^{-1})$	9.562	3.681	2.304	1.572	1.302
TDSE final results $k_{on}(10^{11}M^{-1}min^{-1})$	9.535	3.673	2.298	1.569	1.298

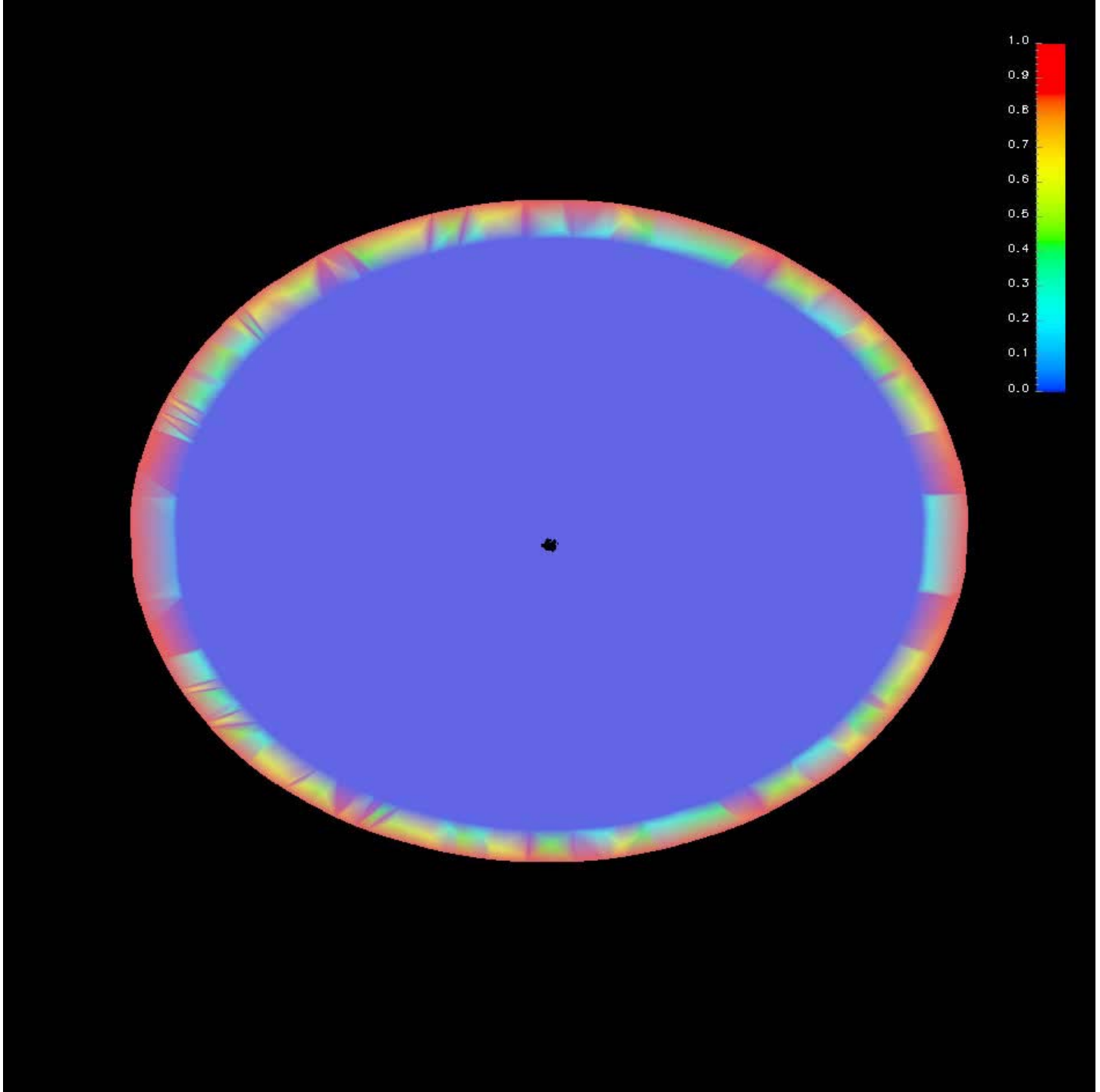
1.0
0.9
0.8
0.7
0.6
0.5
0.4
0.3
0.2
0.1
0.0

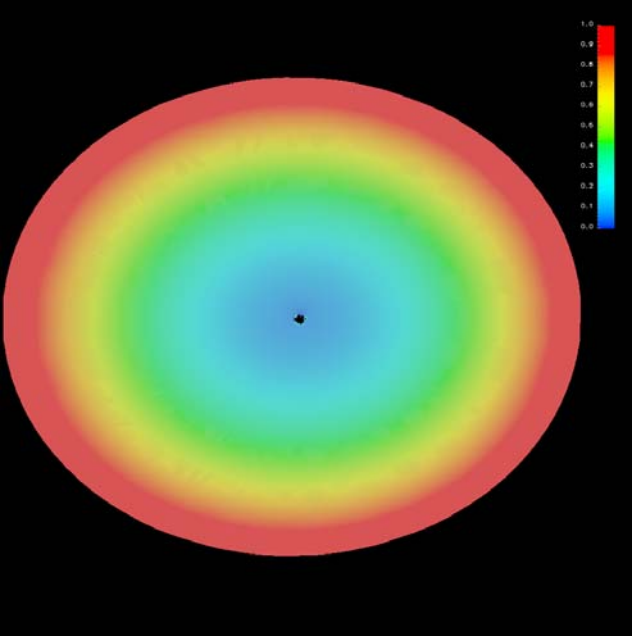

t = 0.05 μ s

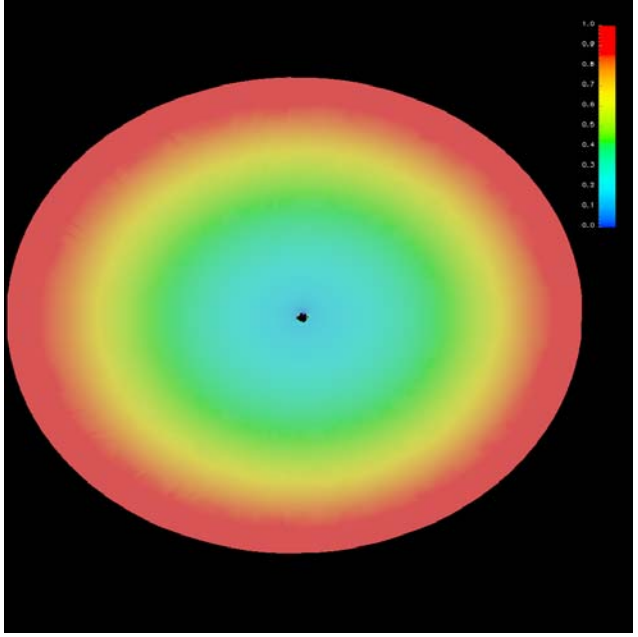

t = 0.50 μ s

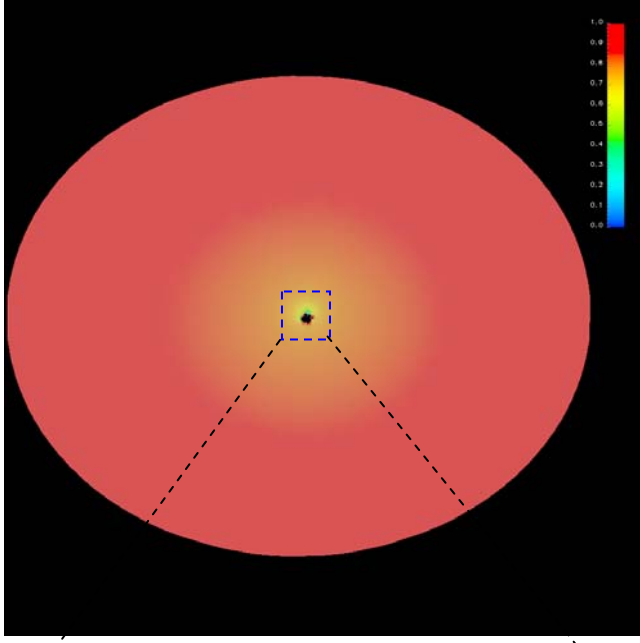

t = 5.00 μ s (global)

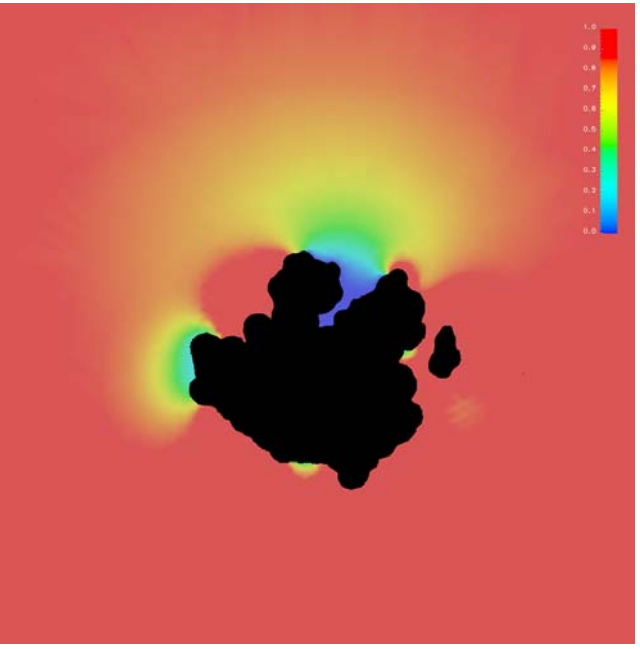

t = 15.00 μ s

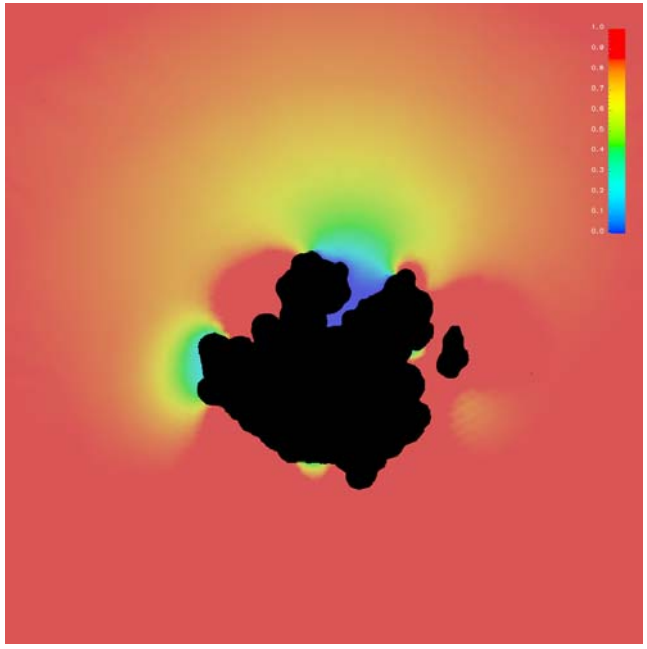

t = 10.00 μ s

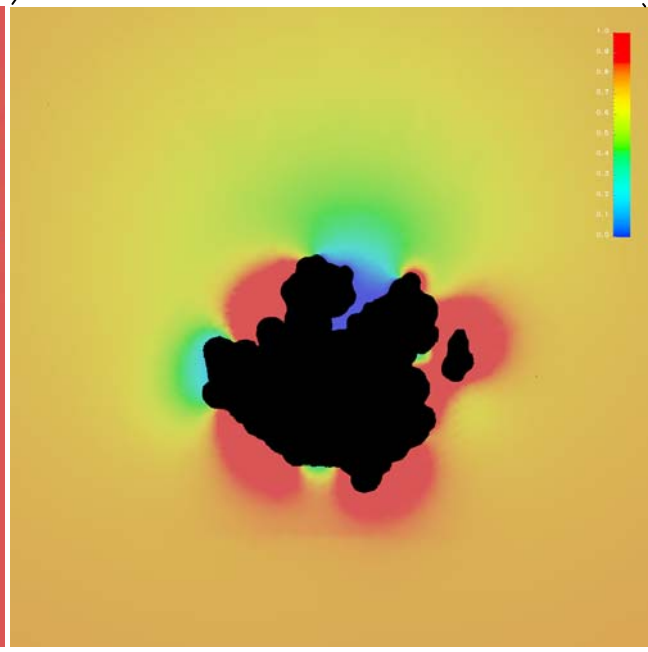

t = 5.00 μ s (close)

TDSE Results

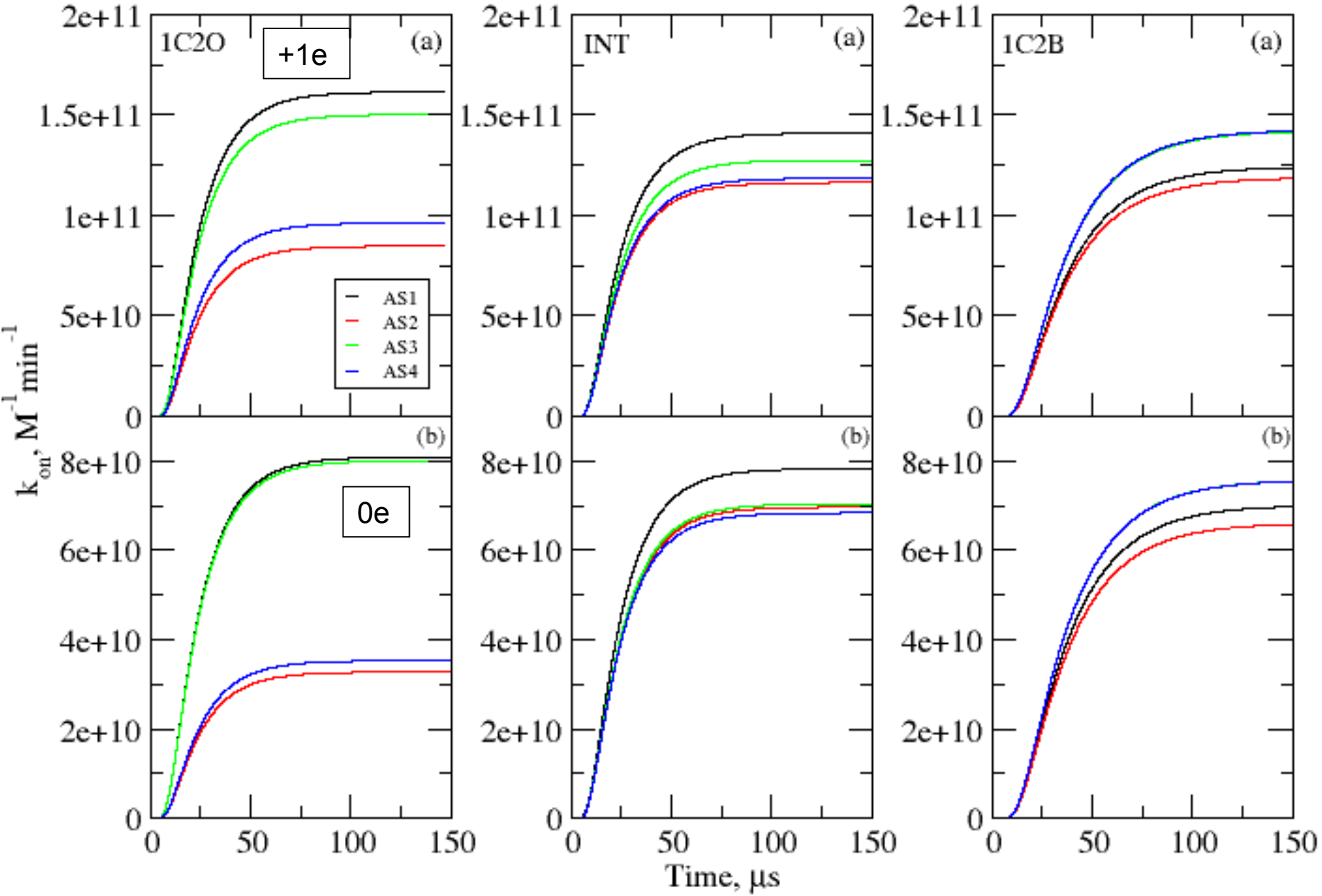

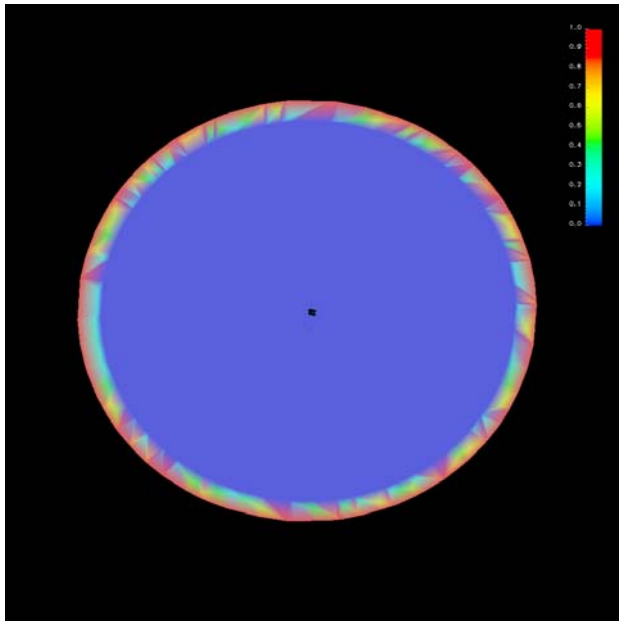

t = 0.000 μ s

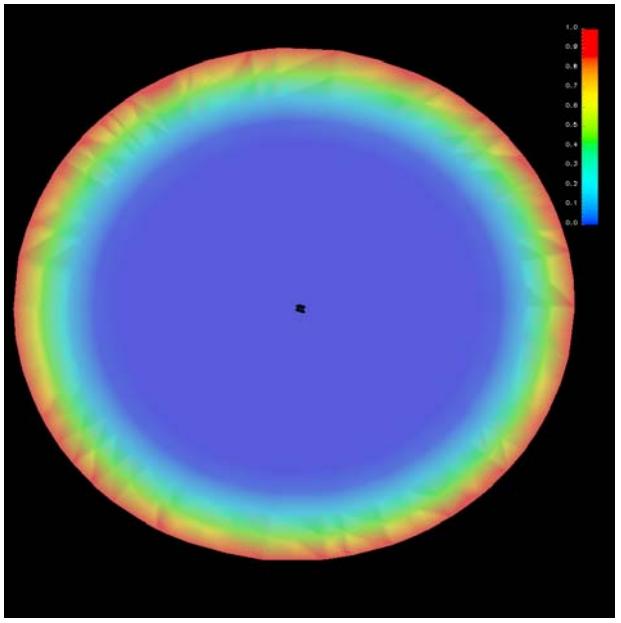

t = 1.000 μ s

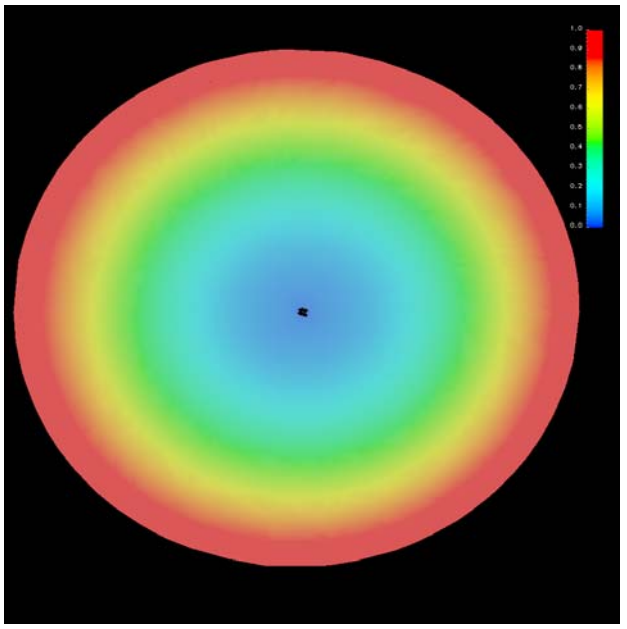

t = 10.00 μ s

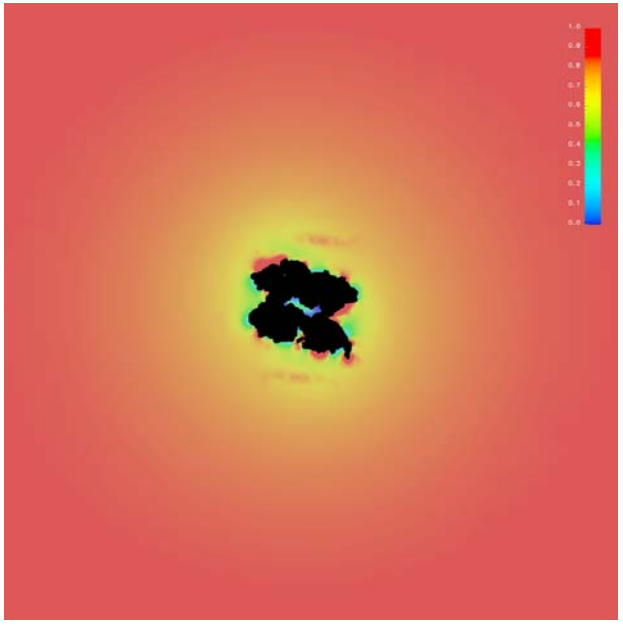

t = 50.00 μ s

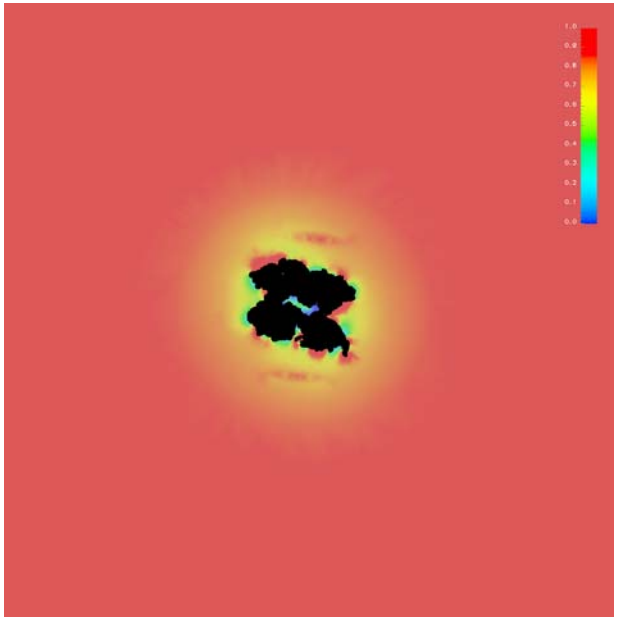

t = 100.0 μ s

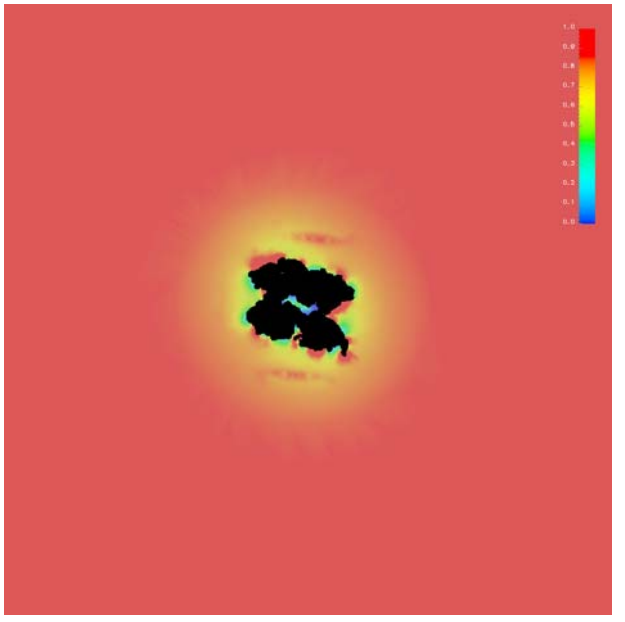

t = 150.0 μ s

Cellular level diffusion modeling

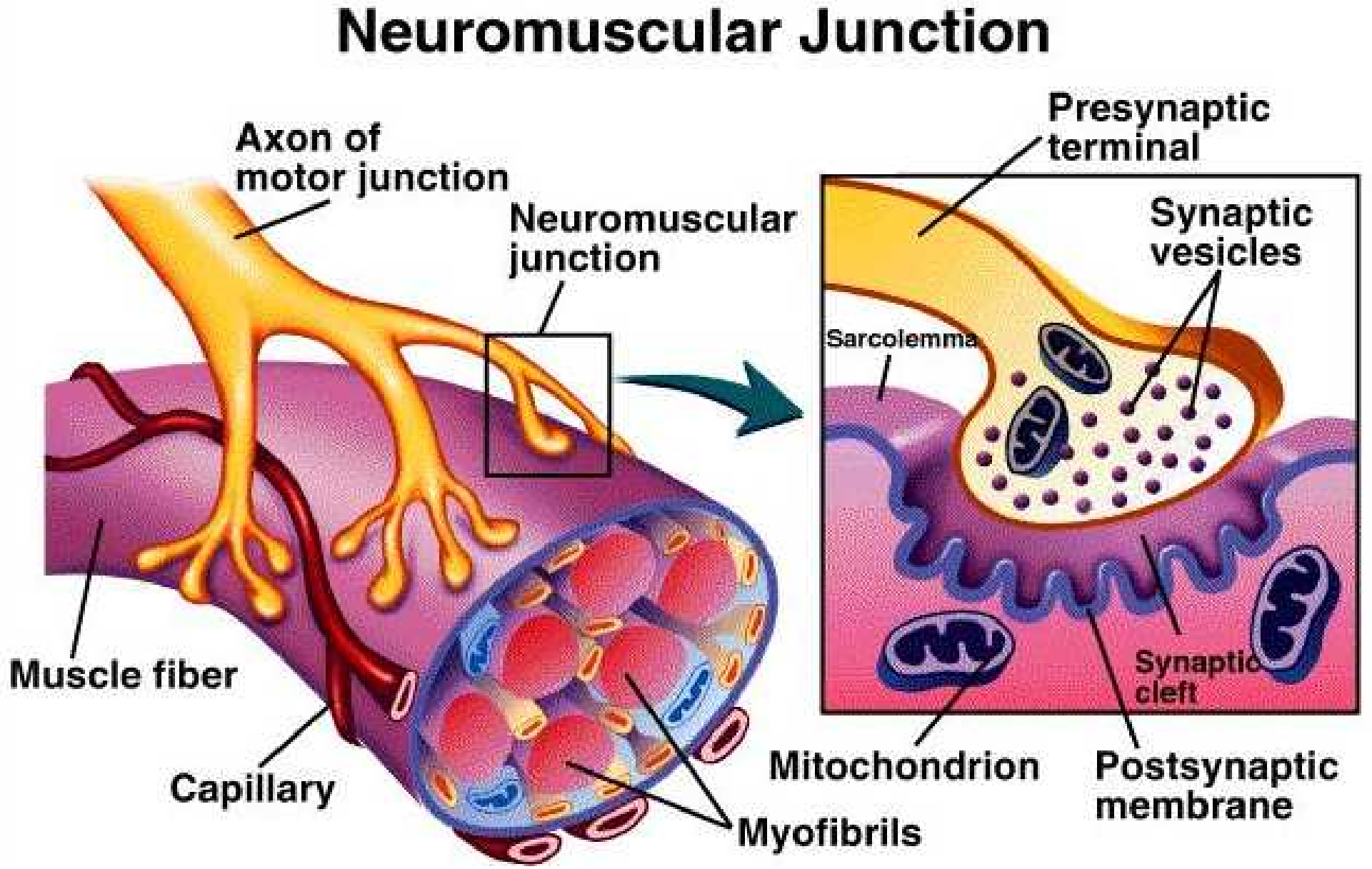

Neuromuscular Transmission

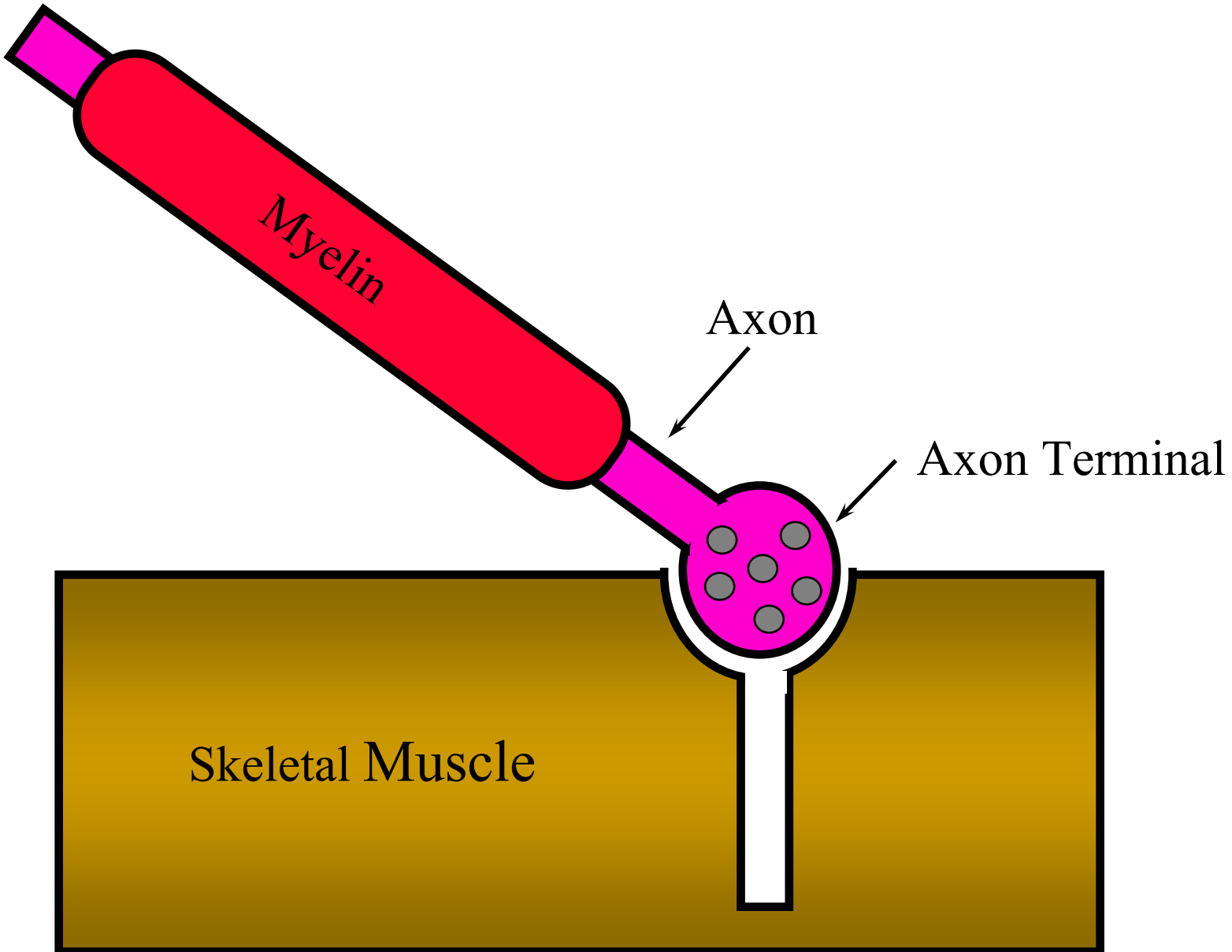

Neuromuscular Transmission: Step by Step

Depolarization of terminal opens Ca channels

Nerve action potential invades axon terminal

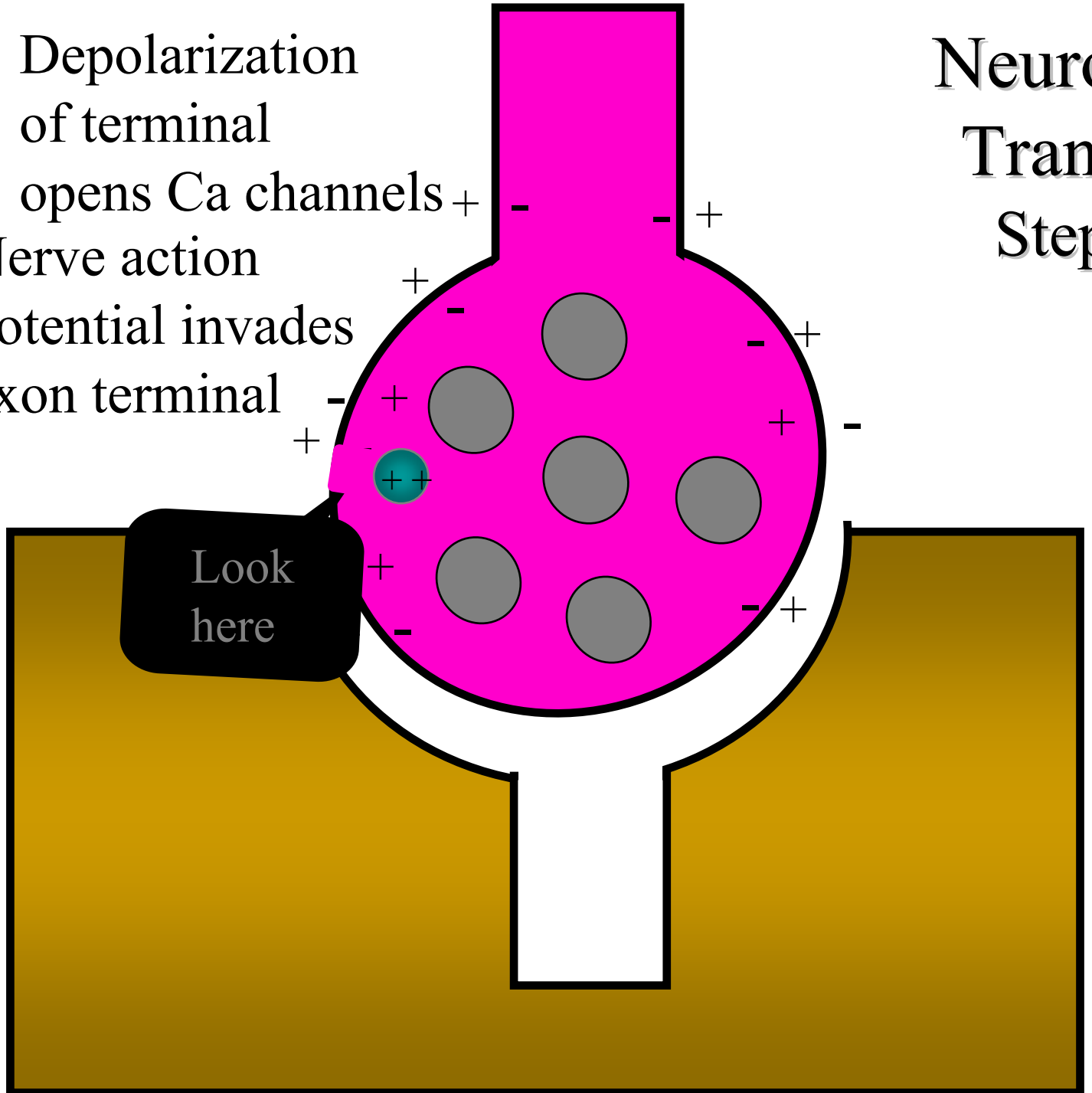

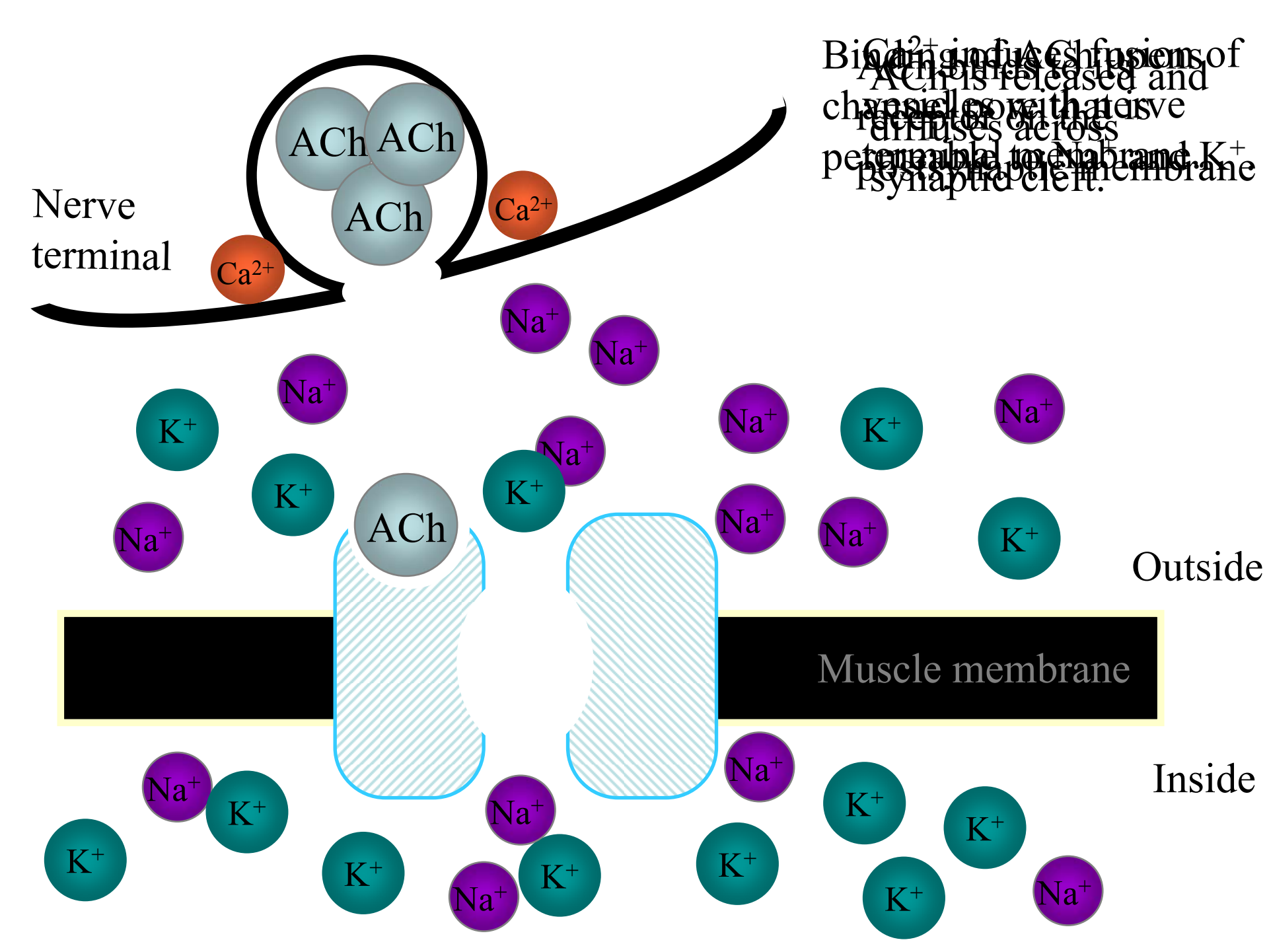
Nerve terminal
ACh
ACh
ACh
Ca2+
Ca2+
Na+
K+
Outside
Muscle membrane
Inside

Meanwhile ...

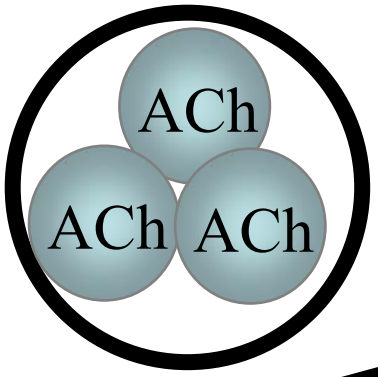

Nerve terminal

Choline is taken up into nerve terminal and acetate

Acetate

Outside

Muscle membrane

Inside

Structural Reality

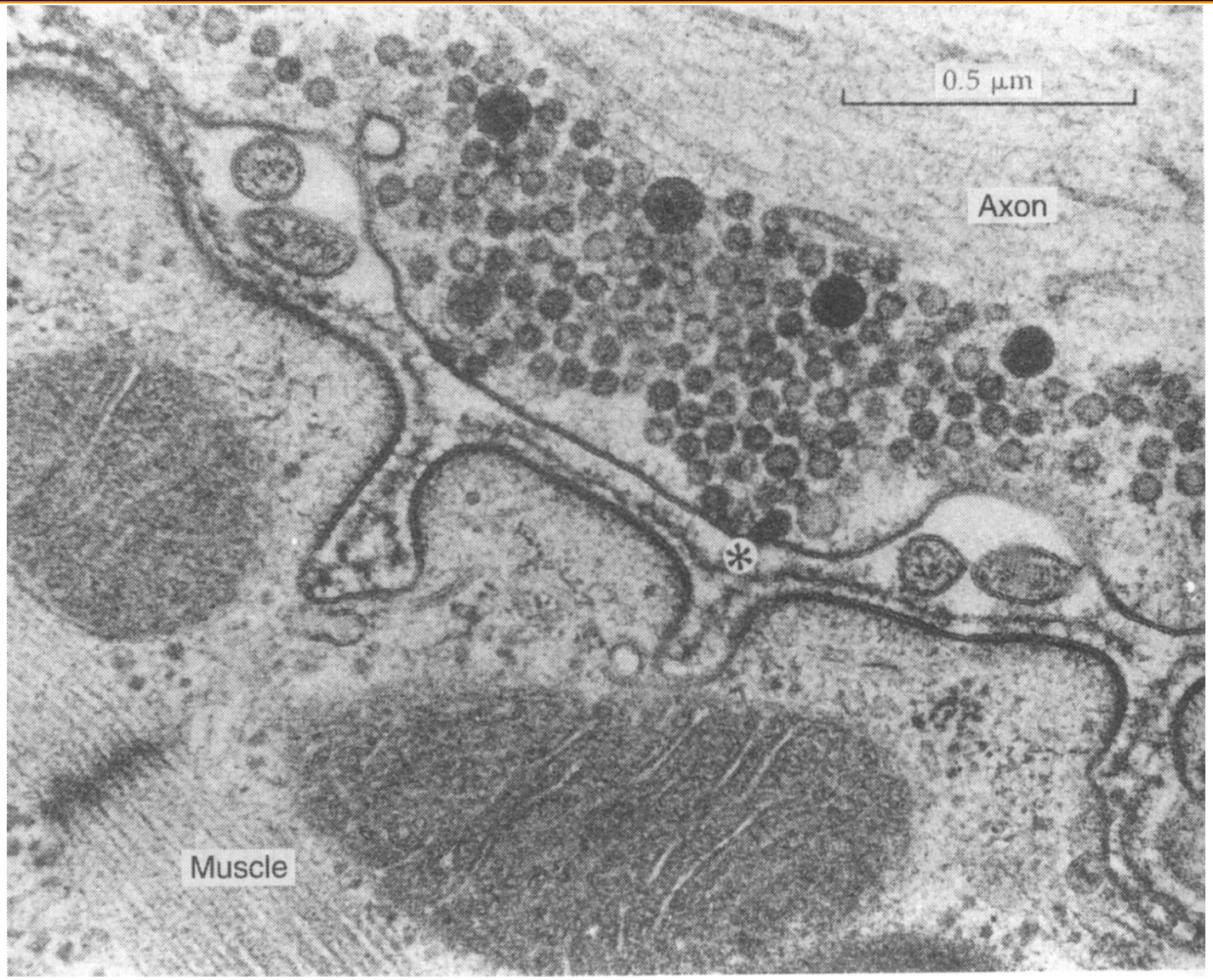

By John Heuser and Louise Evans
University of California, San Francisco

AChE Reaction Mechanism

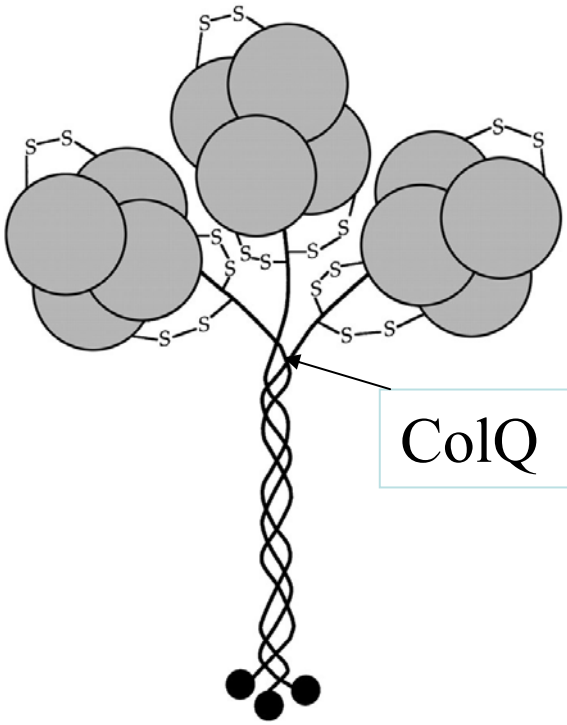

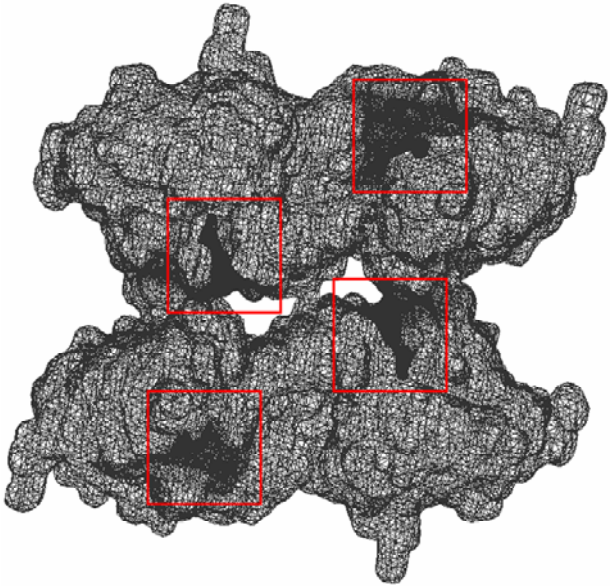

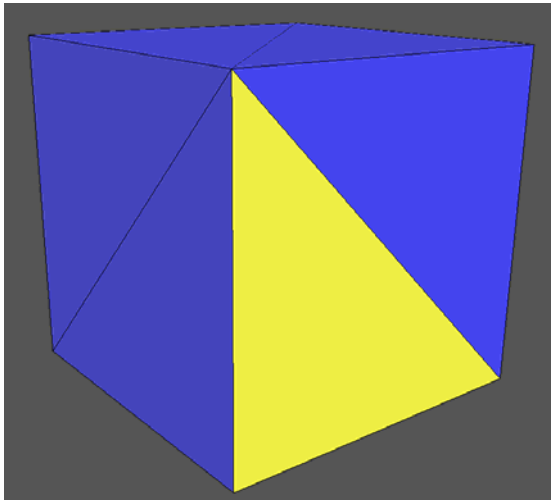

$$S + E \underset{k_s^-}{\overset{k_s^+}{\rightleftharpoons}} ES \xrightarrow{k_{cat}} E + P$$

θ_1

$$+ \qquad +$$

$$S \qquad S$$

$$k_{ss}^- \Big\| k_{ss}^+ \qquad k_{ss}^- \Big\| k_{ss}^+$$

$$S + SE \underset{k_s^-}{\overset{k_s^+}{\rightleftharpoons}} SES \xrightarrow{bk_{cat}} SE + P$$

θ_2 $\qquad$ θ_3

$\theta_1 = [ES]$

$\theta_2 = [SE]$

$\theta_3 = [SES]$

AChE Activity

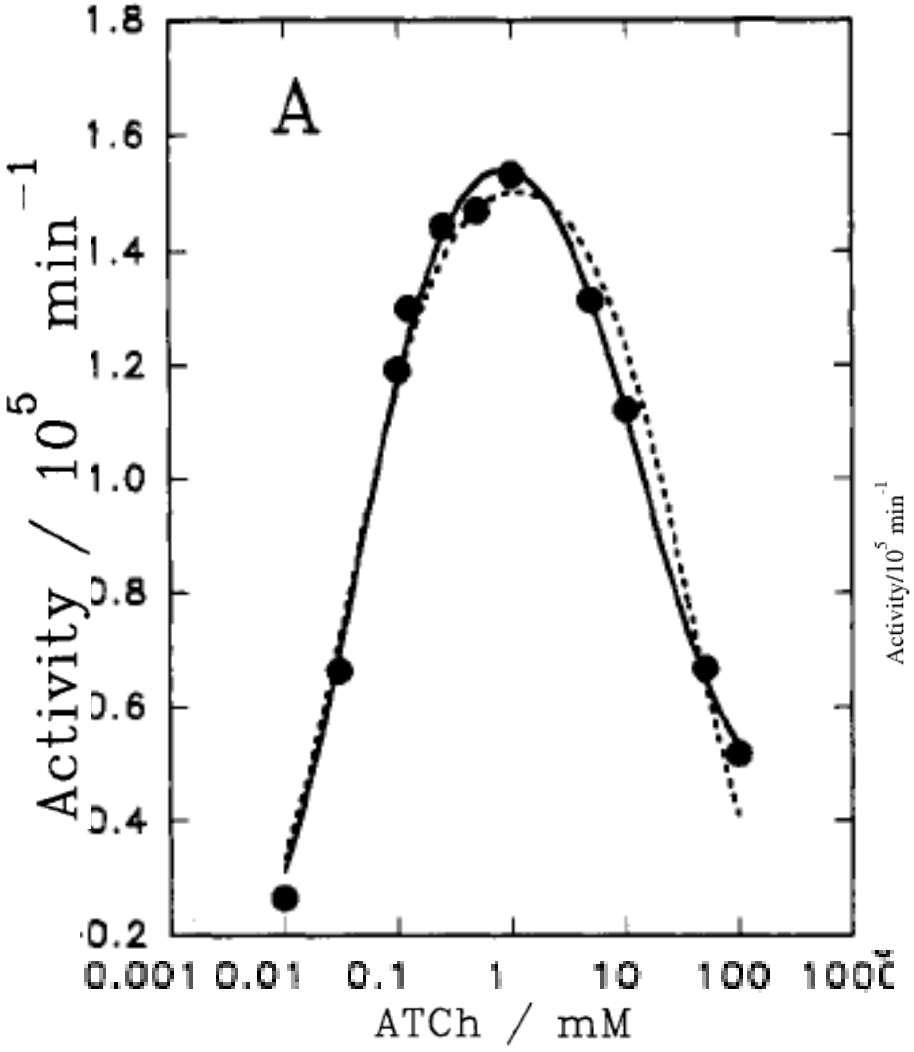

*Biochemistry, **1993;** 32(45)*

$$\upsilon(i) = [AChE]_0 k_{cat}(\theta_1 + b\theta_3)$$

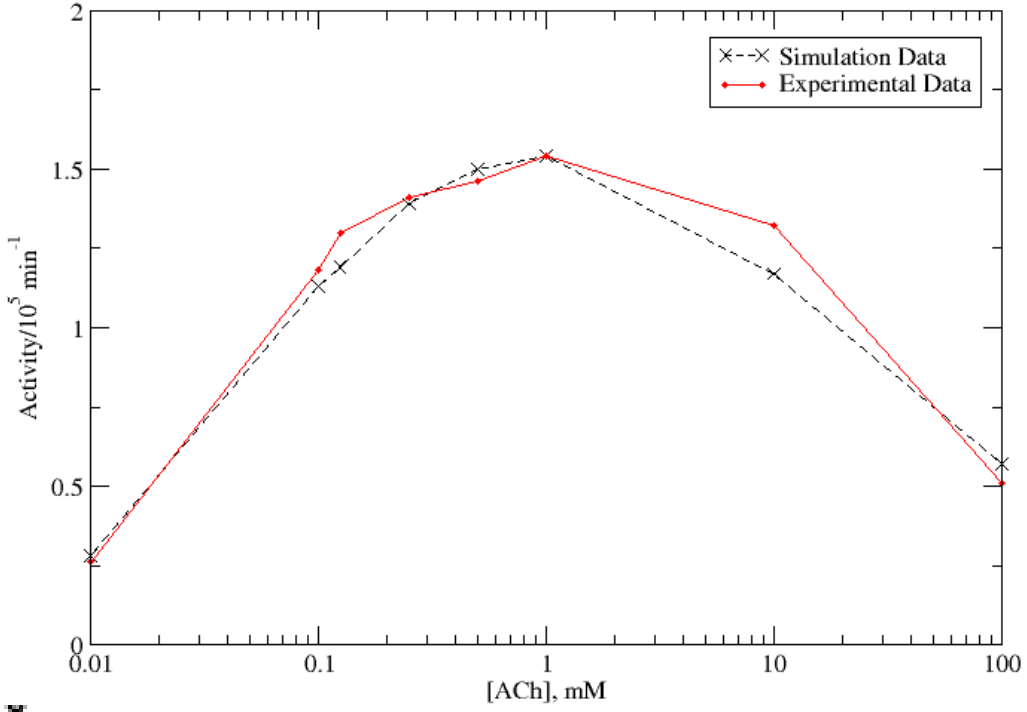

nAChR Reaction Model

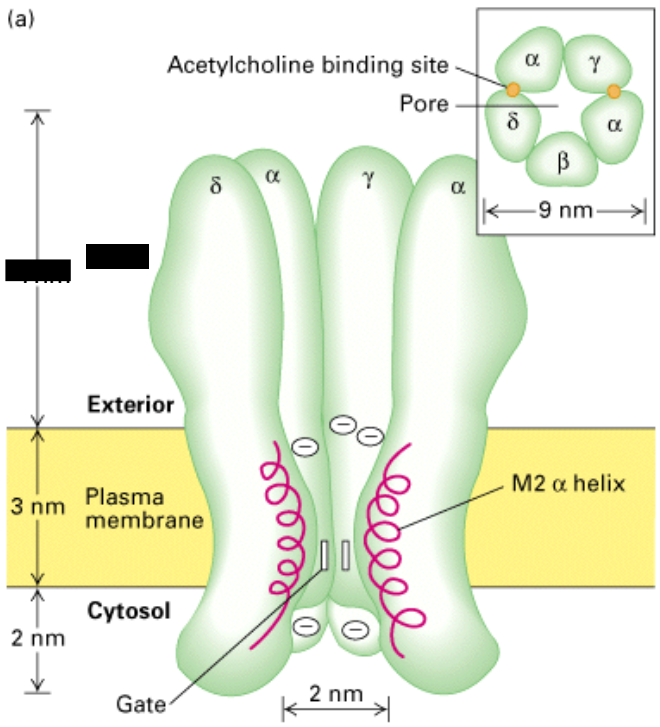

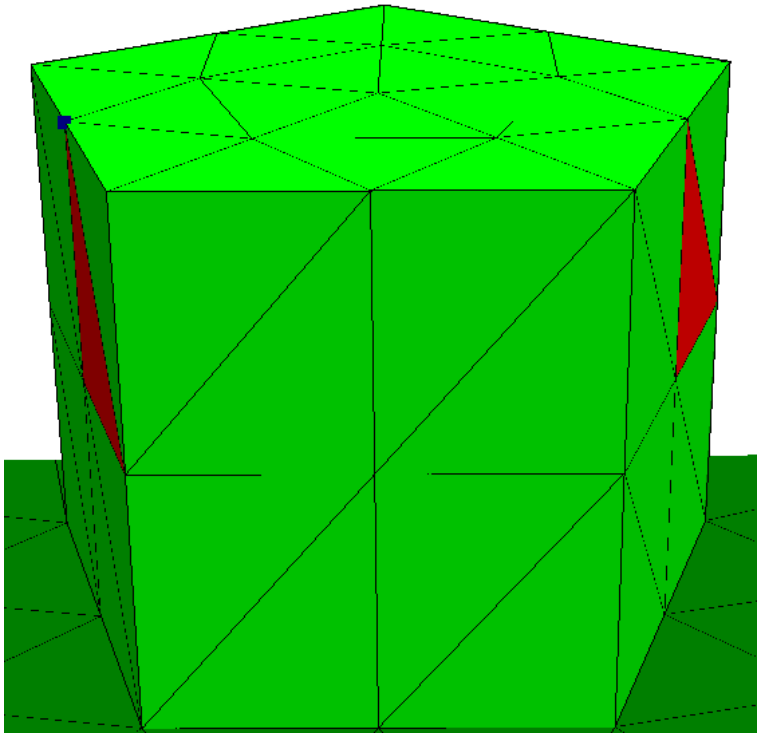

$$A + R^0 \rightleftharpoons AR^1 + A \rightleftharpoons AR^2 + A \rightleftharpoons C \overset{\alpha}{\rightleftharpoons}_{\beta} D^1 \overset{\alpha}{\rightleftharpoons}_{\beta} D^2 \overset{\alpha}{\rightleftharpoons}_{\beta} D^3 \overset{\alpha}{\rightleftharpoons}_{\beta} D^4 \overset{\alpha}{\rightleftharpoons}_{\beta} D^5 \overset{\alpha}{\rightleftharpoons}_{\beta} O$$

k_{+1}, k_{-1}, k_{+2}, k_{-2}, k_{+3}, k_{-3}, k_{+4}, k_{-4}

α_1, α_2, α_3, α_4, α_5, α_6

β_1, β_2, β_3, β_4, β_5, β_6

nAChR Conformational Statistics

$$I(t) = \int_{\partial\Omega_{nAChR}^{act}} \frac{N_{nAChR}}{S_{\partial\Omega_{nAChR}^{act}}} (k_{bind}^{+} p_{ACh}(r,t|r_0,t_0) - k_{bind}^{-}) dS$$

$$N(t') = \int_0^{t'} I(t) dt$$

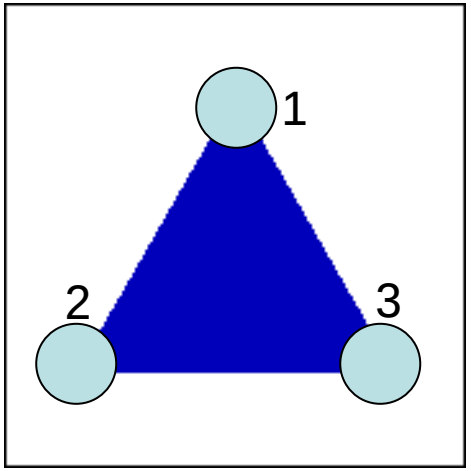

$N(t') \geqslant 2$, Diliganded

$1 \leqslant N(t') < 2$, Monoliganded

$0 \leqslant N(t') < 1$, Unliganded

$$p(O)^{I} = \frac{\int_{\partial\Omega_{nAChR}^{I}} \phi_8 dS}{\int_{\partial\Omega_{nAChR}^{I}} 1 dS}$$

$$p(O)^{II} = \frac{\int_{\partial\Omega_{nAChR}^{II}} \phi_8 dS}{\int_{\partial\Omega_{nAChR}^{II}} 1 dS}$$

$$p(O) = \frac{p(O)^{I} + p(O)^{II}}{2}$$

$$N(O) = N_{nAChR} p(O)$$

nAChR Activity

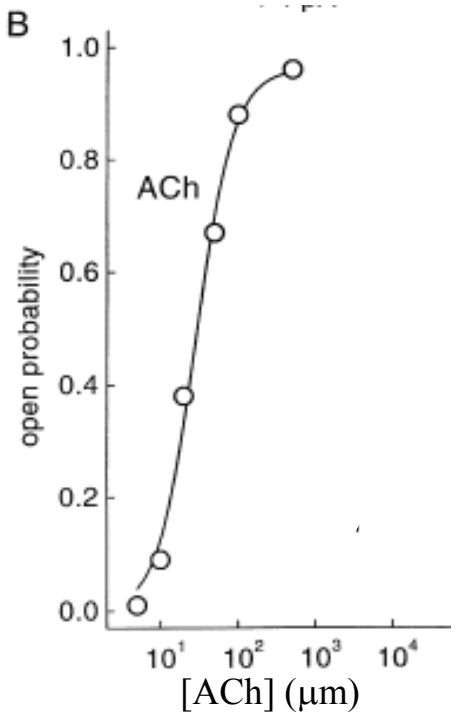

Br J Pharmacol 128: 1467-1476

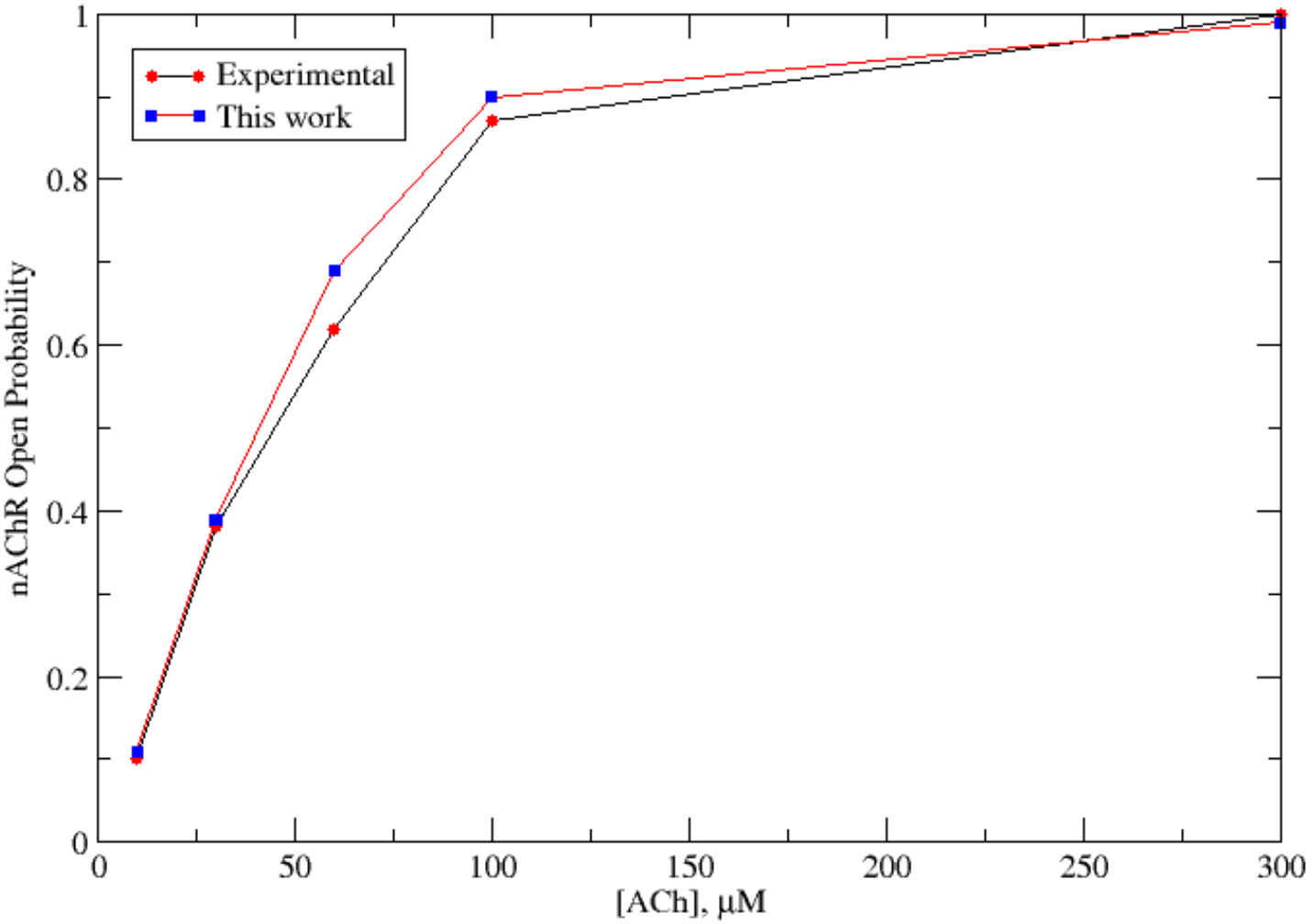

nAChR Open Probabilities

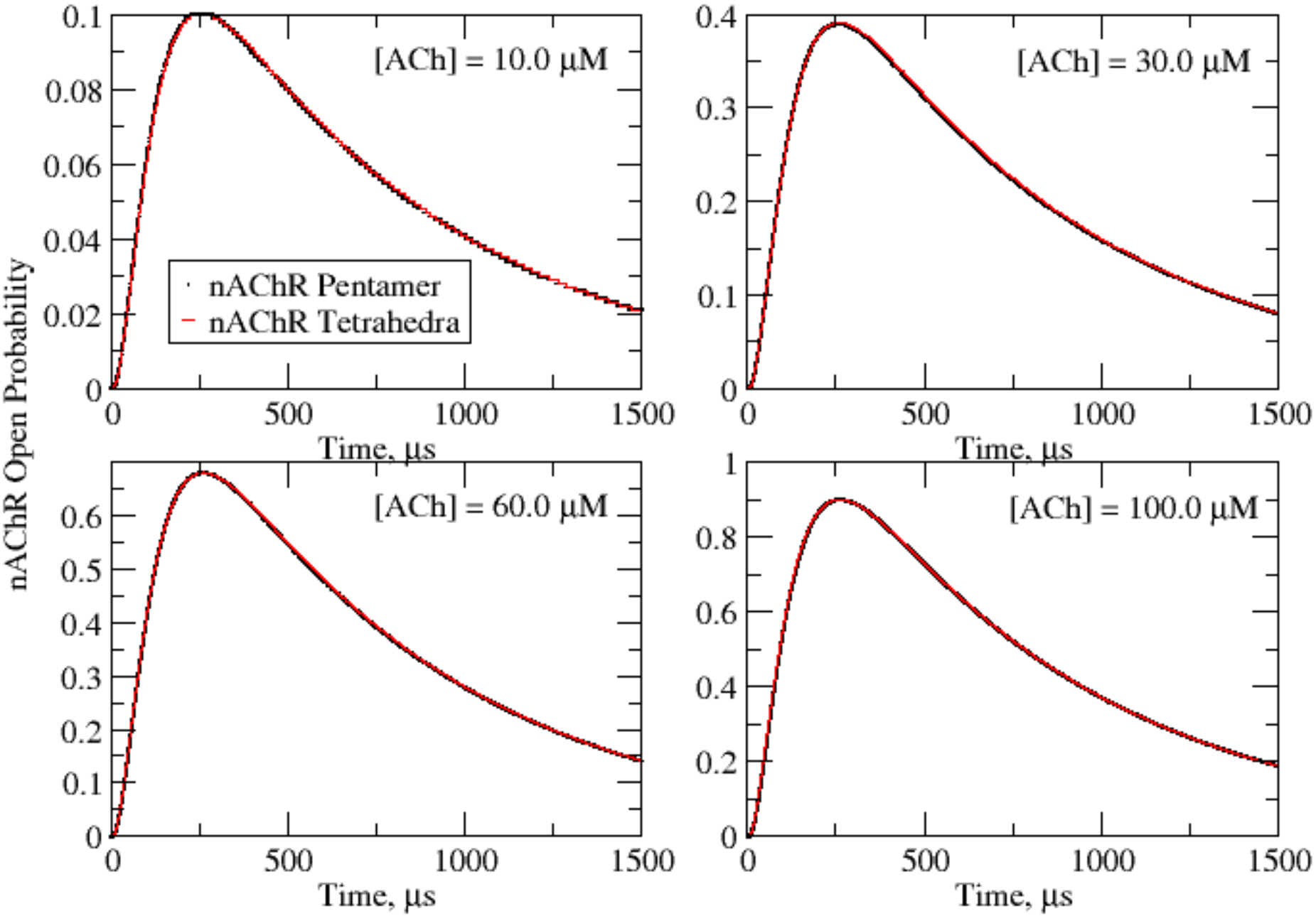

Assembly of Rectilinear NMJ

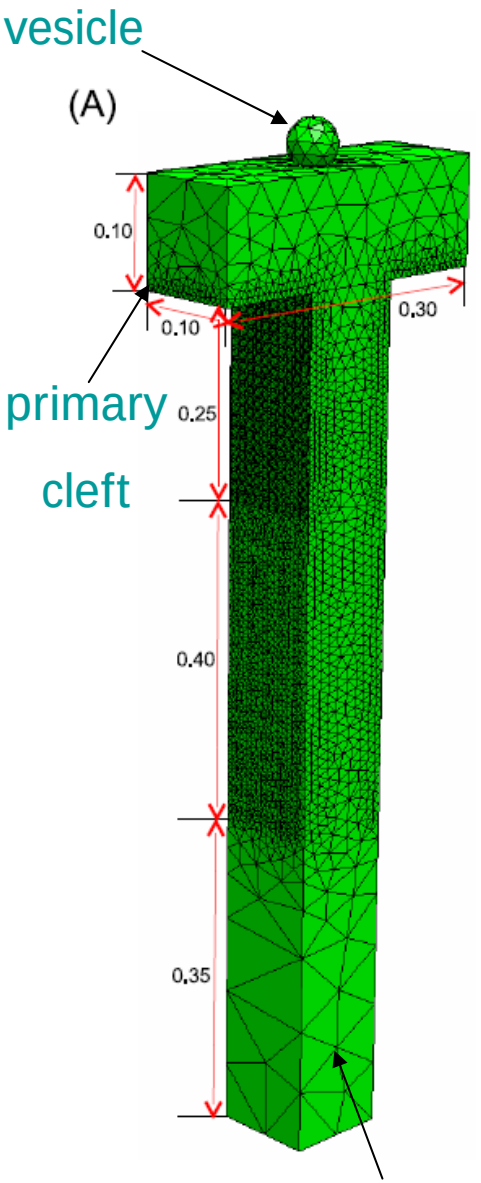

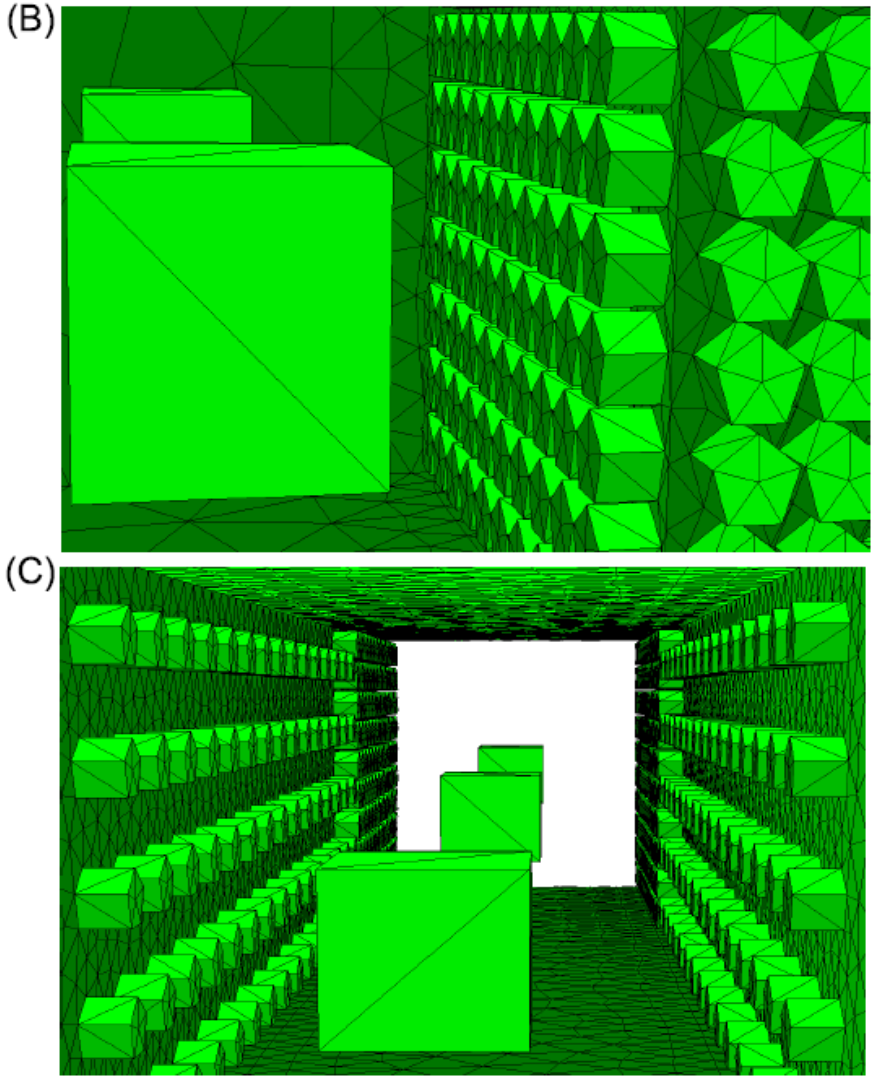

nAChR: 750

AChE: 8

ACh: 8,474

ACh Decay

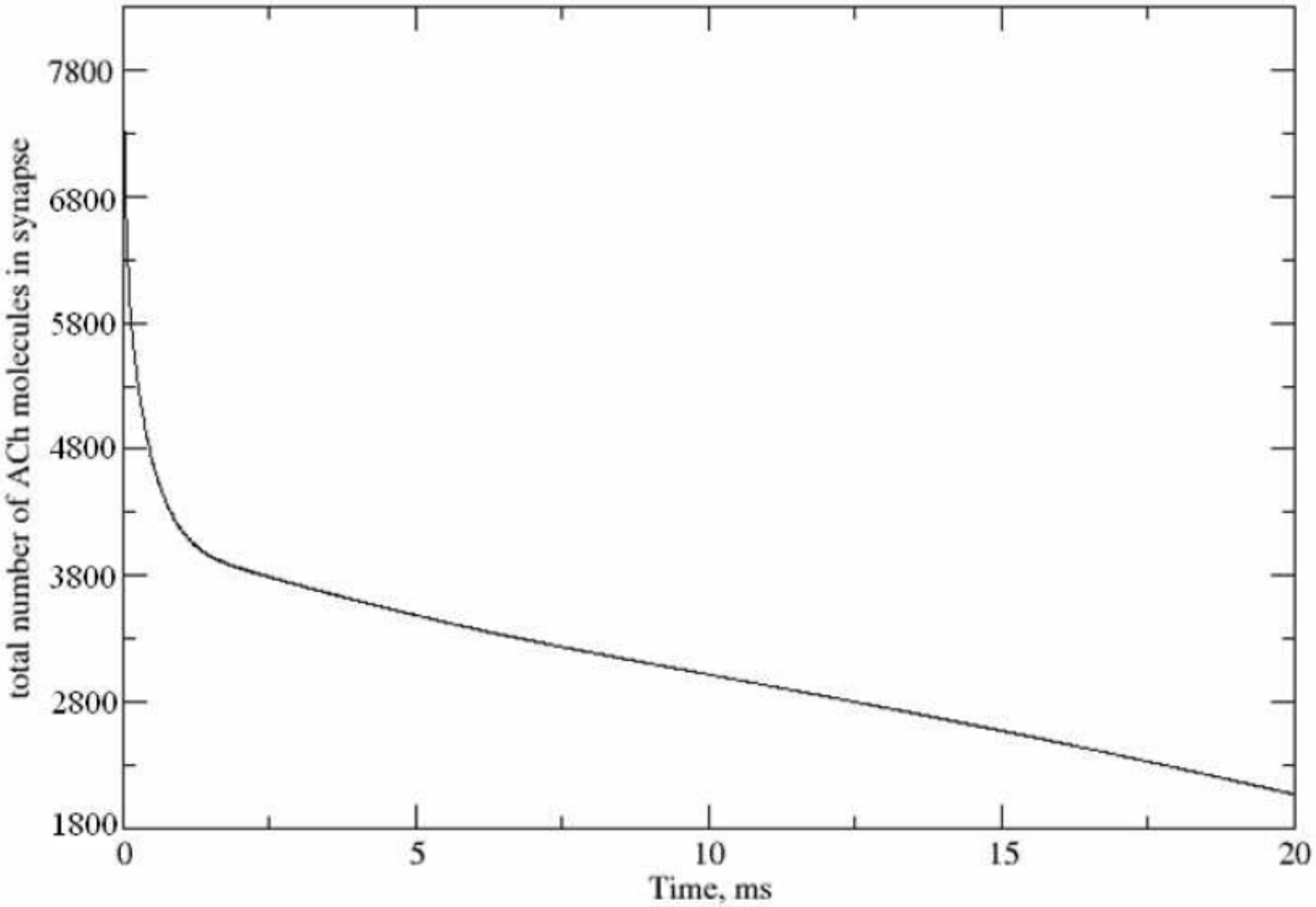
7800
6800
5800
4800
3800
2800
1800
total number of ACh molecules in synapse
0
5
10
15
20
Time, ms

AChE Intermediates

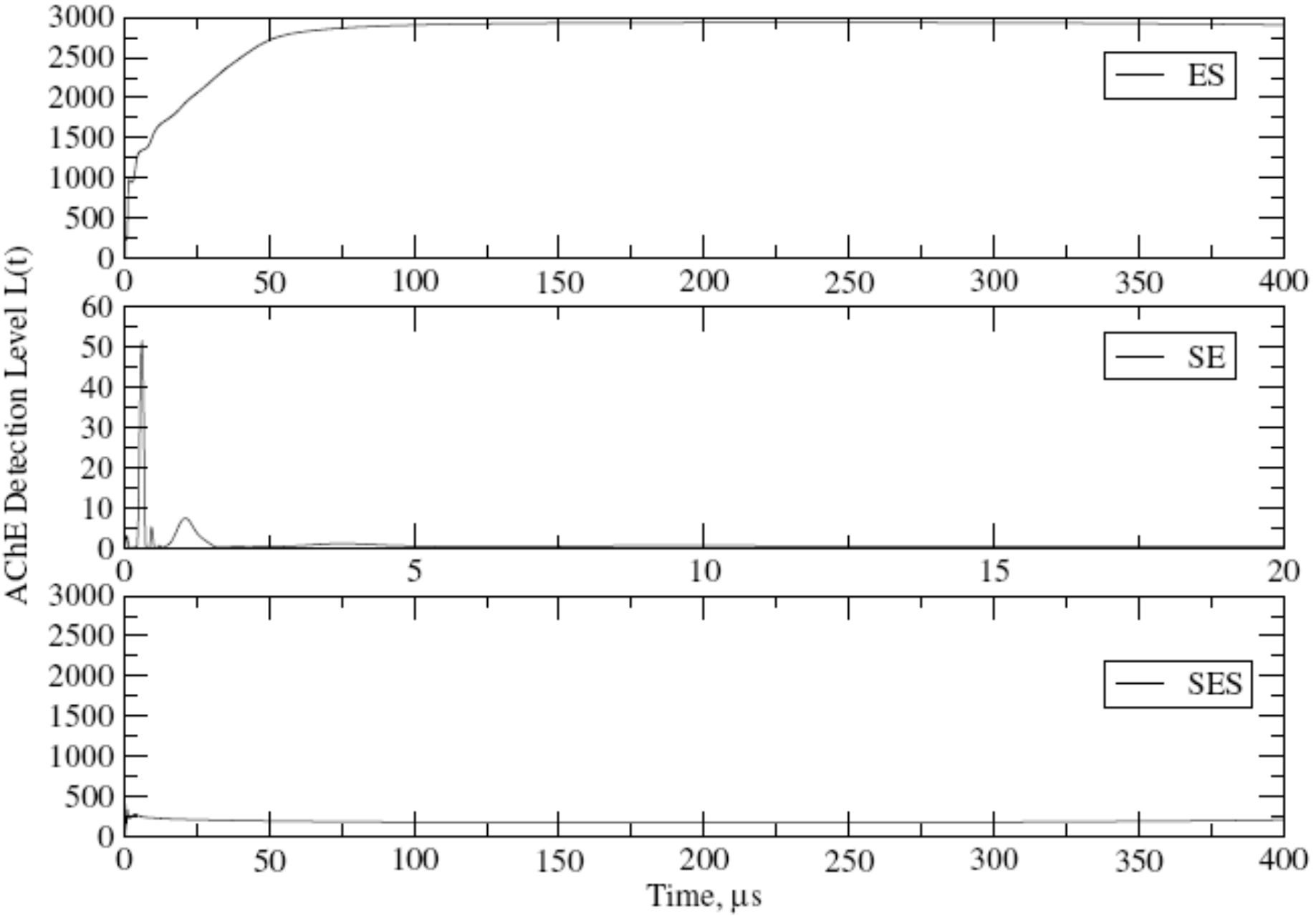

nAChR States

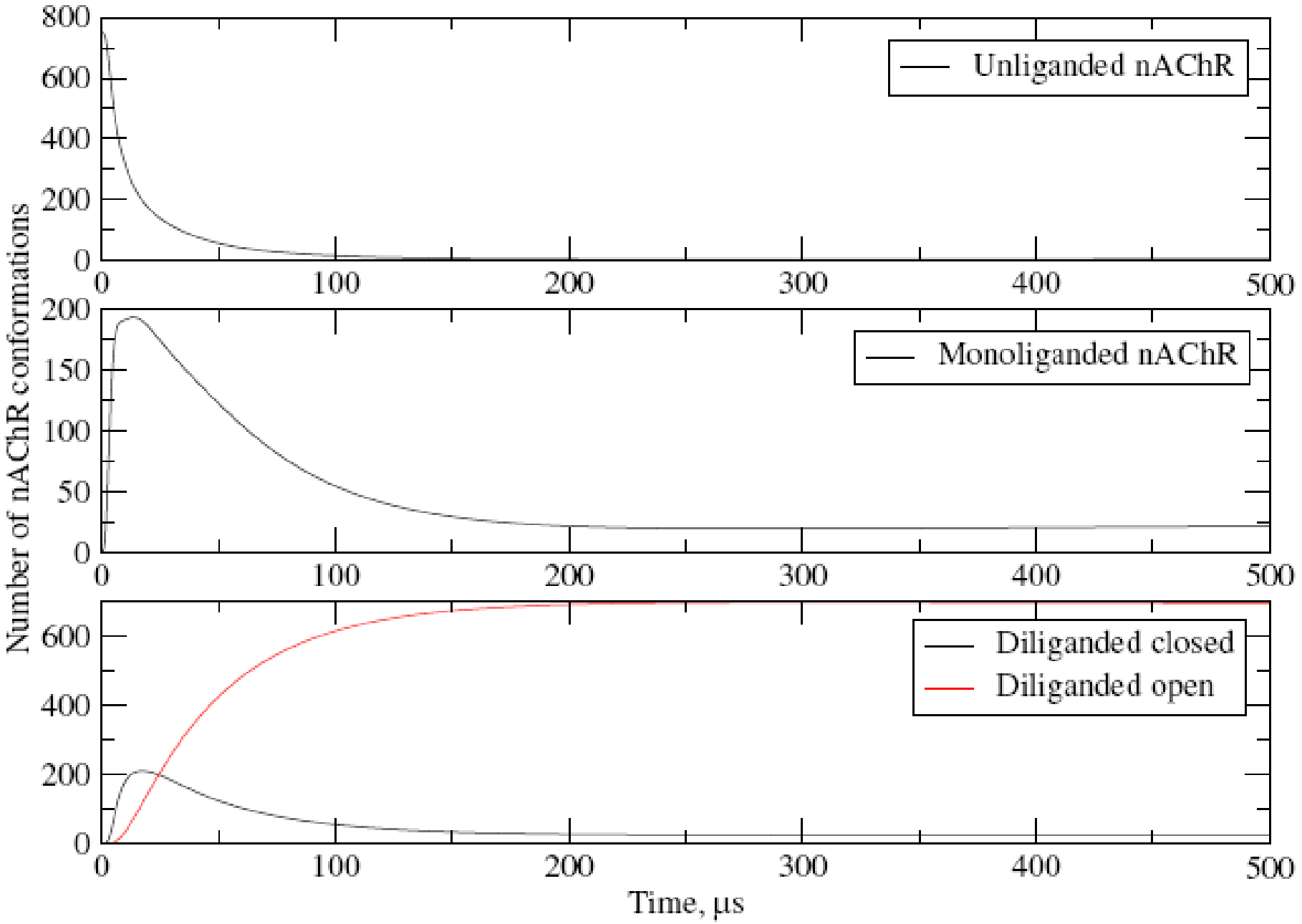

Open Channel Number vs. AChE Amount

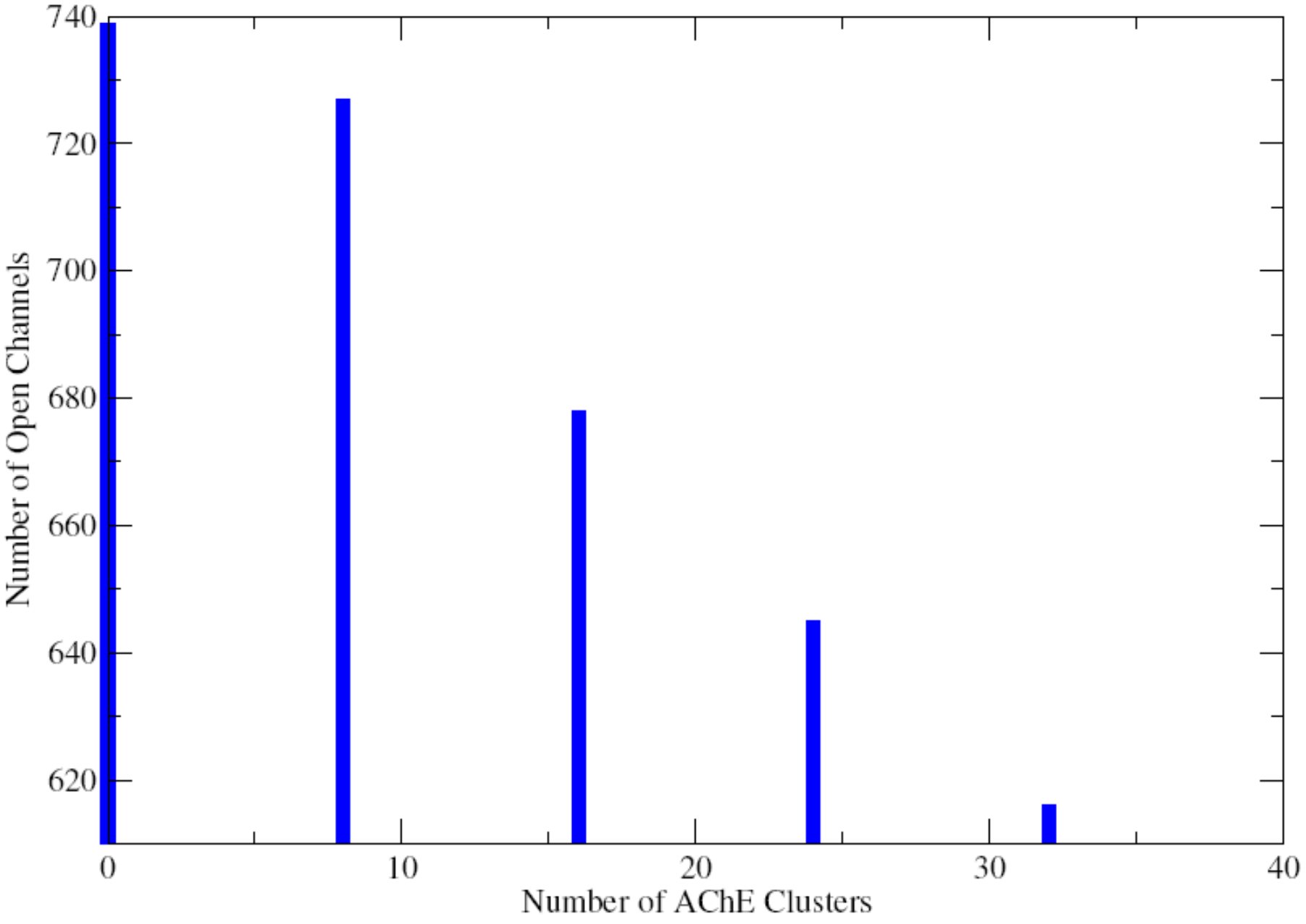

Larger NMJ Model

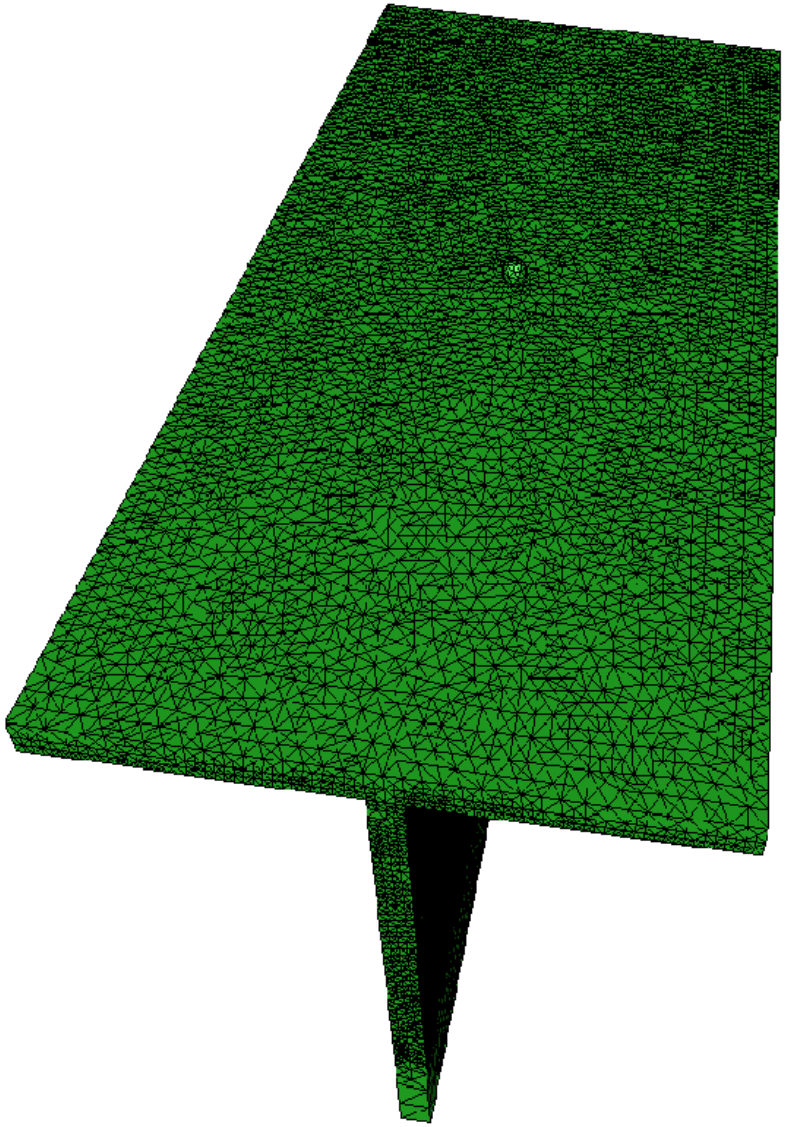

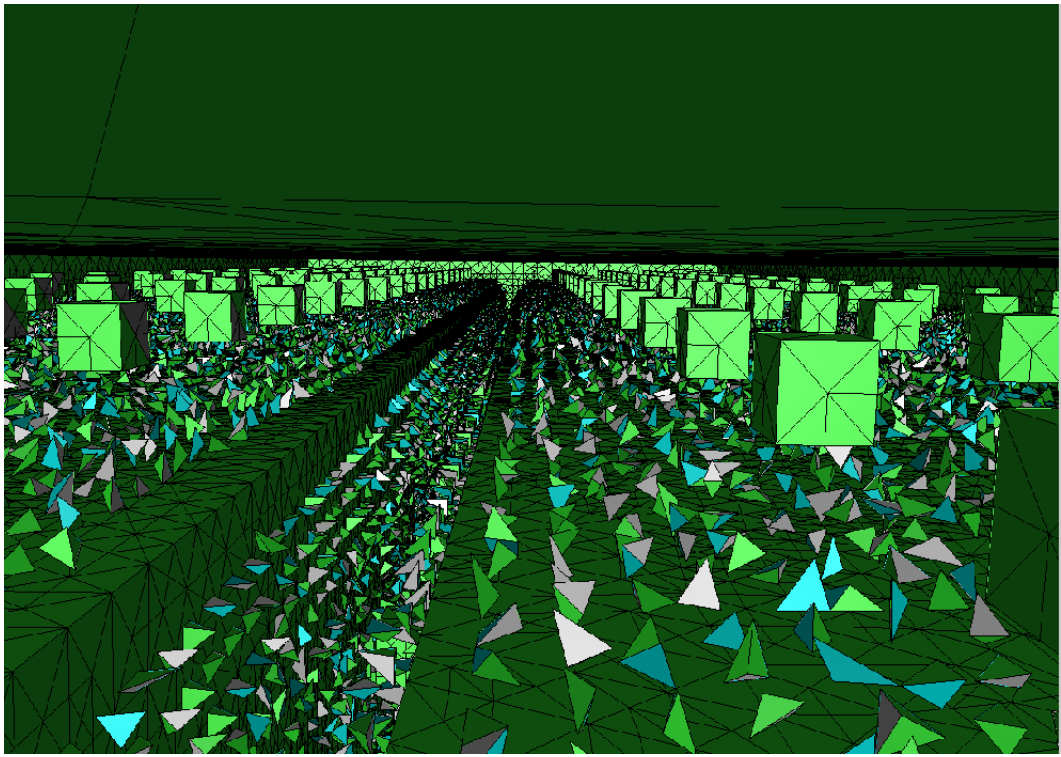

AChE Clusters: 323

nAChR: 29462

AChE Intermediates

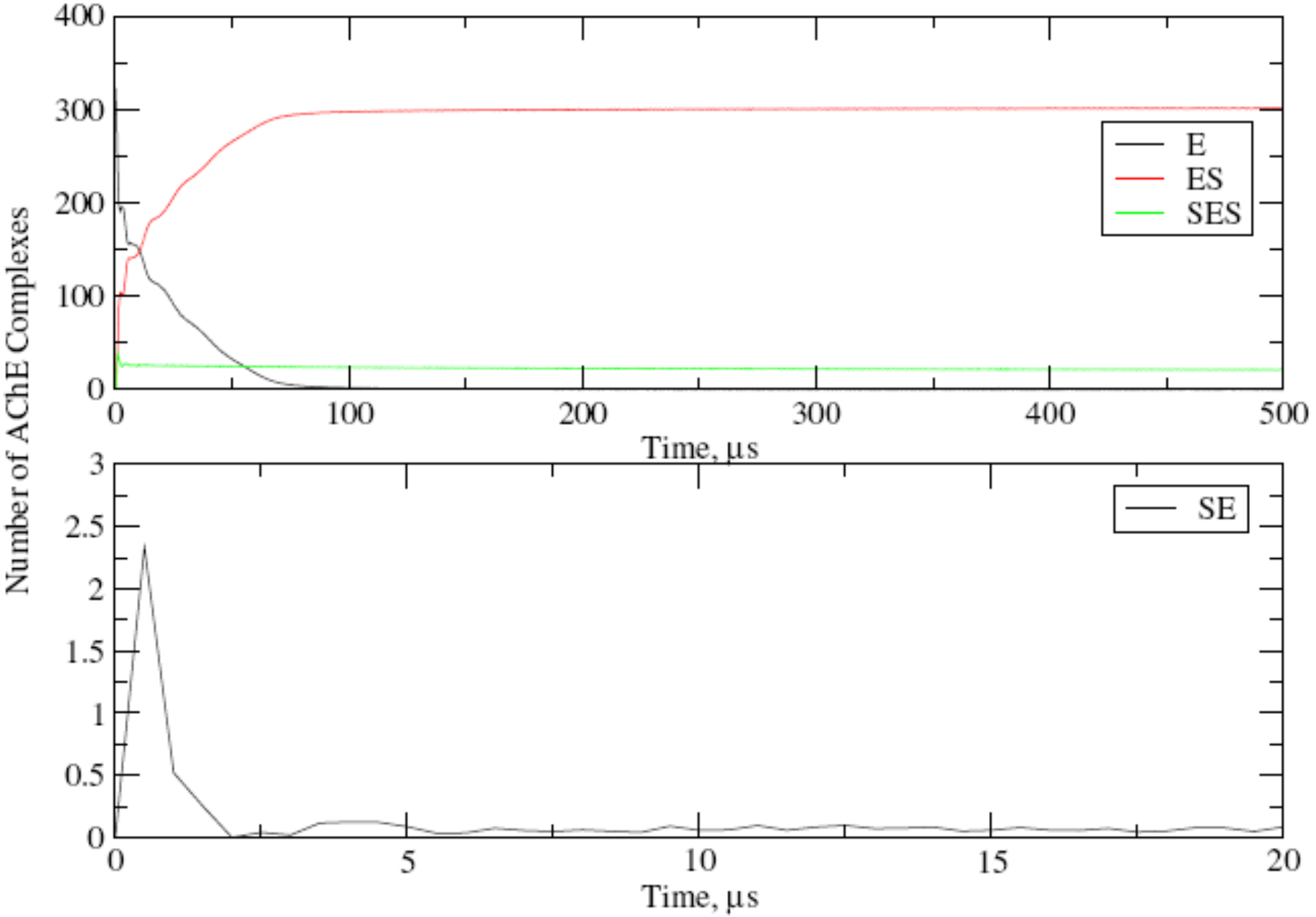

Open Channel Number

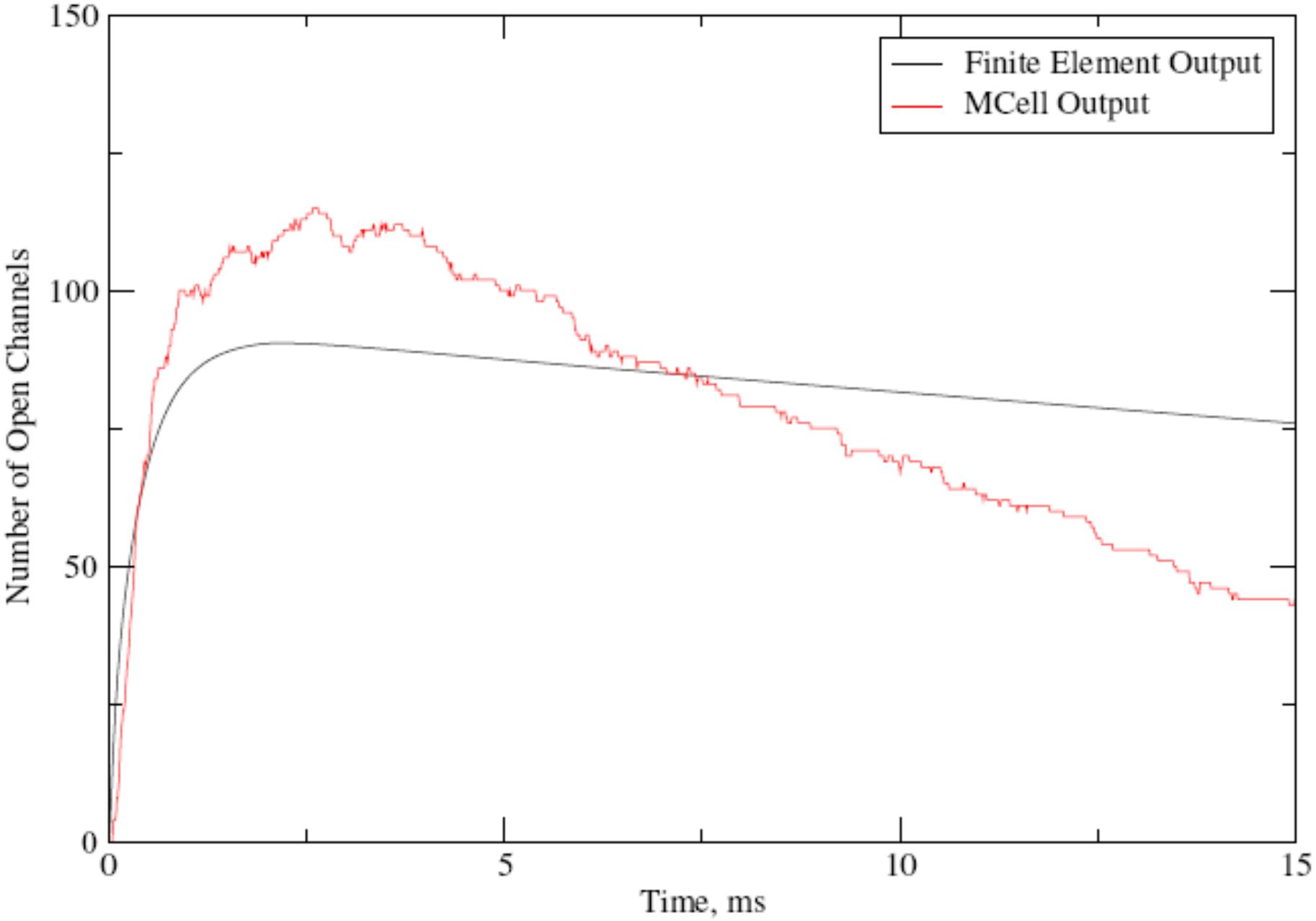

Neuromuscular Transmission

- The nAChR conformations are relatively insensitive to AChE densities or AChE inhibitor (More evidence in the future)
- Properties of neuromuscular junction designed to assure that every presynaptic action potential results in a postsynaptic one (i.e. 1:1 transmission)
- The NMJ is a site of considerable clinical importance

Future Direction

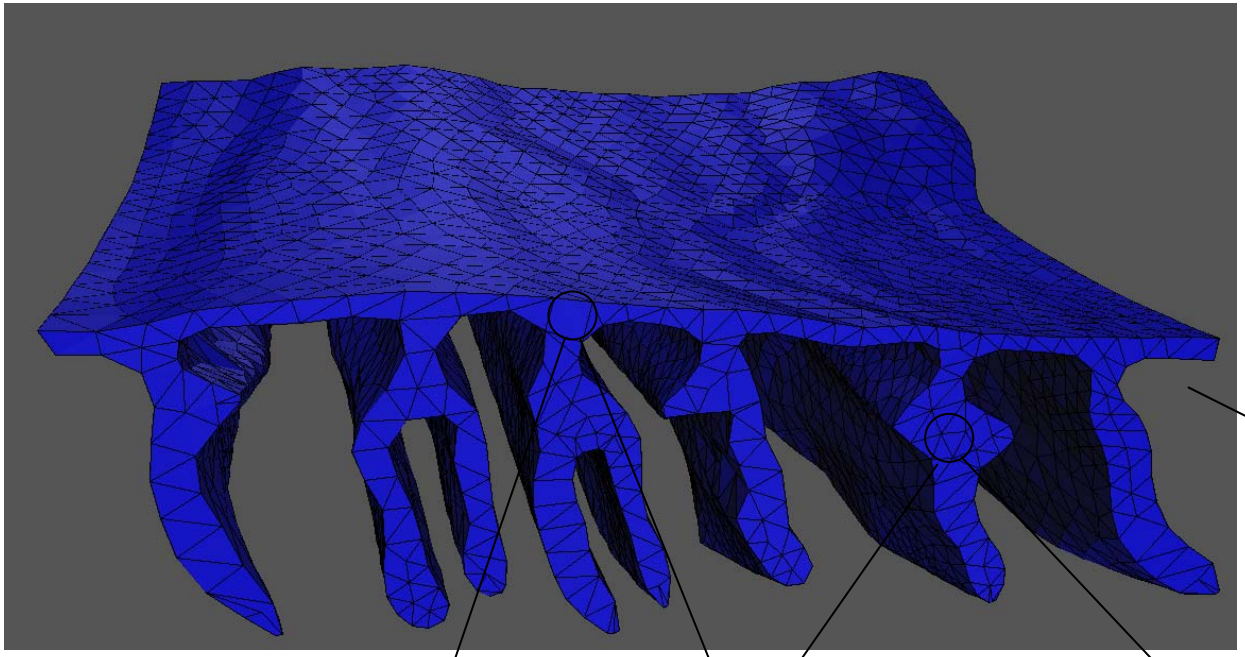

Substructure A

Substructure B_1

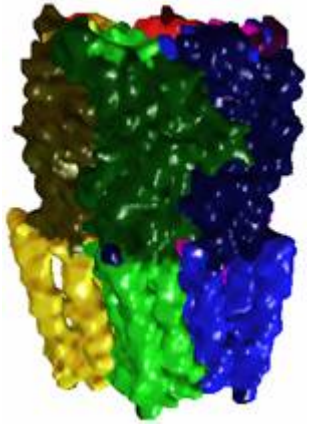

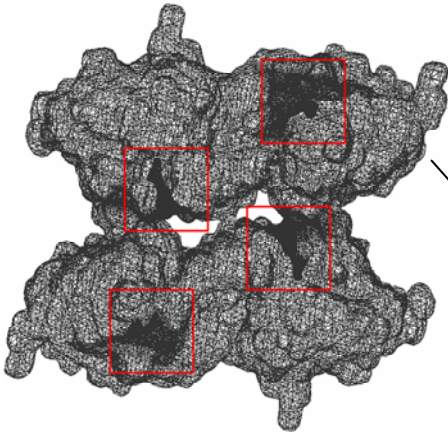

Substructure B_2

Poisson-Nernst-Planck Solver

$$\nabla \cdot (\varepsilon \nabla \phi(\vec{R})) + \kappa^2 sinh(\phi(\vec{R})) = \sum_i q_i \delta(\vec{R} - \vec{R}_i) + \sum_j q_j p_j(\vec{R};t) \quad (1)$$

$$\frac{\partial p_j(\vec{R};t)}{\partial t} = -\vec{\nabla} \cdot \vec{J}_j(\vec{R};t) \quad (2)$$

where the particle flux is defined as:

$$\begin{aligned} \vec{J}_j(\vec{R};t) &= D_j(\vec{R})[\vec{\nabla} p_j(\vec{R};t) + \beta \vec{\nabla} \phi(\vec{R}) p_j(\vec{R};t)] \\ &= D_j(\vec{R}) e^{-\beta q_j \phi(\vec{R})} \nabla e^{\beta q_j \phi(\vec{R})} p(\vec{R};t) \end{aligned} \quad (3)$$

Diffusion controlled rate constant: $k(t) = p_{j;bulk}^{-1} \int_{\Gamma_a} n(\vec{R}) \cdot \vec{j}(\vec{R};t) dS$

Local free energy density: $g(p_j(\vec{R};t)) = p_j(\vec{R};t)(\phi(\vec{R}) + \beta^{-1} ln \frac{p_j(\vec{R};t)}{p_j^{bulk}})$

Local entropy density: $s_j(\vec{R};t) = -k_B p_j(\vec{R};t) ln \frac{p_j(\vec{R};t)}{p_j^{bulk}}$

Poisson-Nernst-Planck Solver

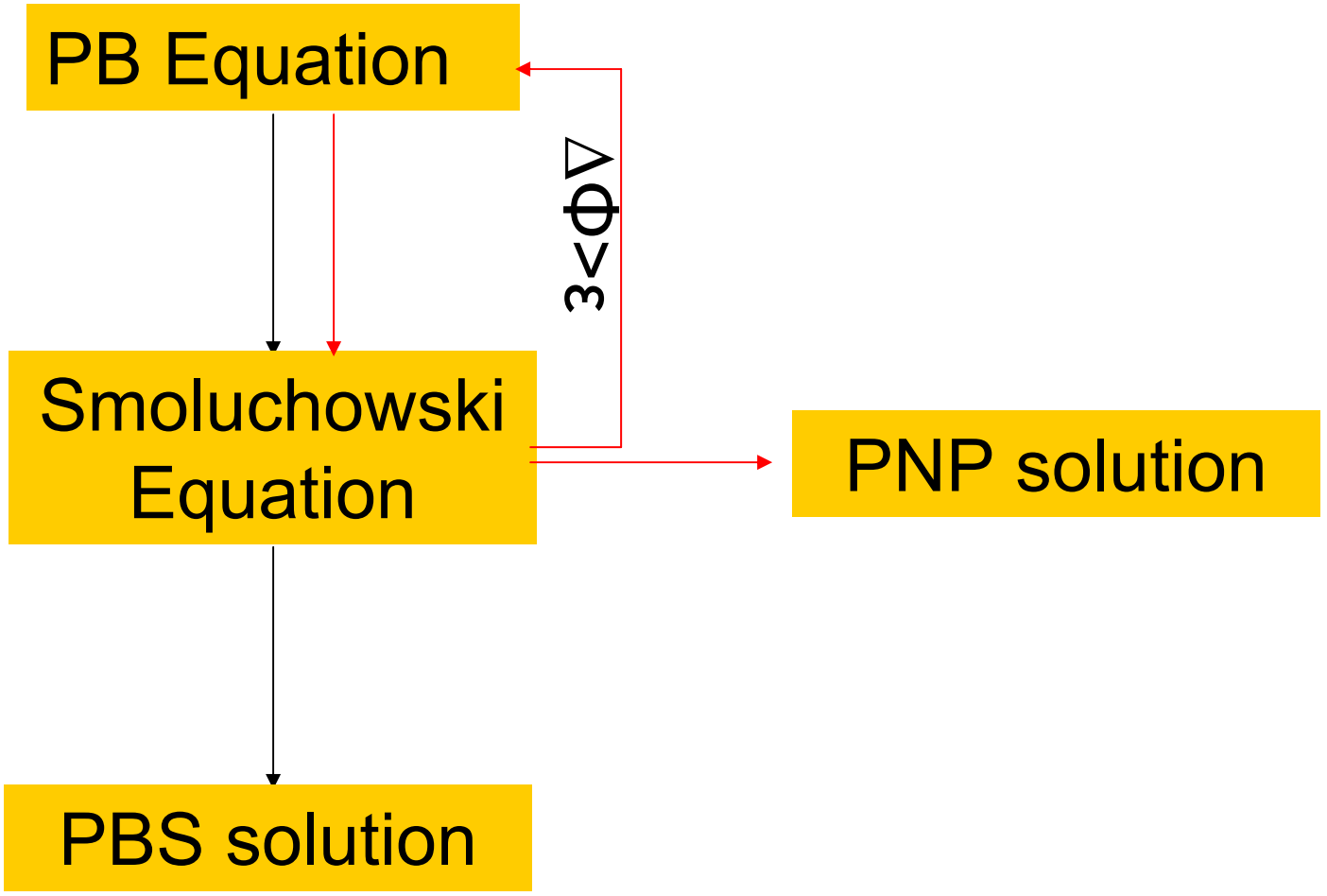

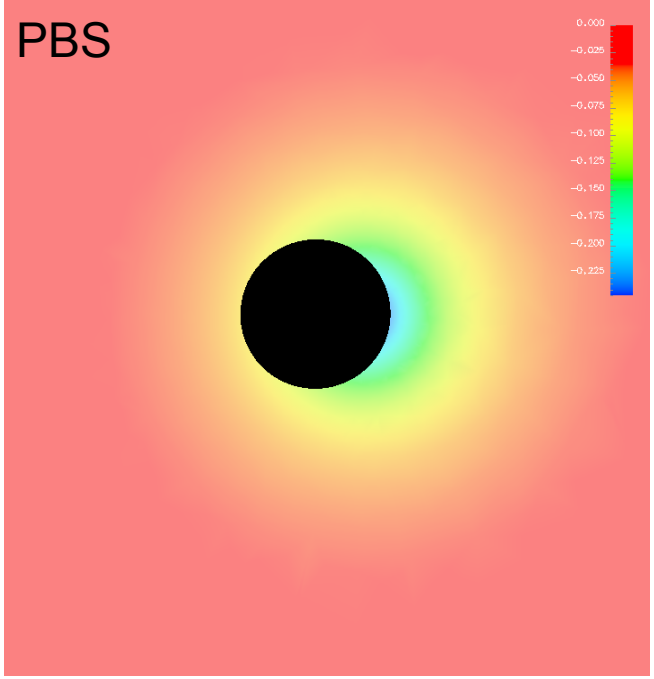

Free Energy

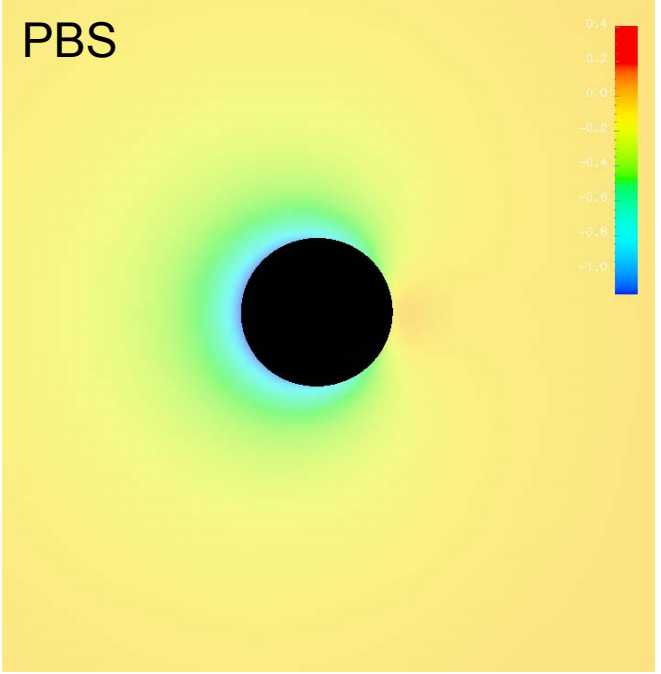

Entropy

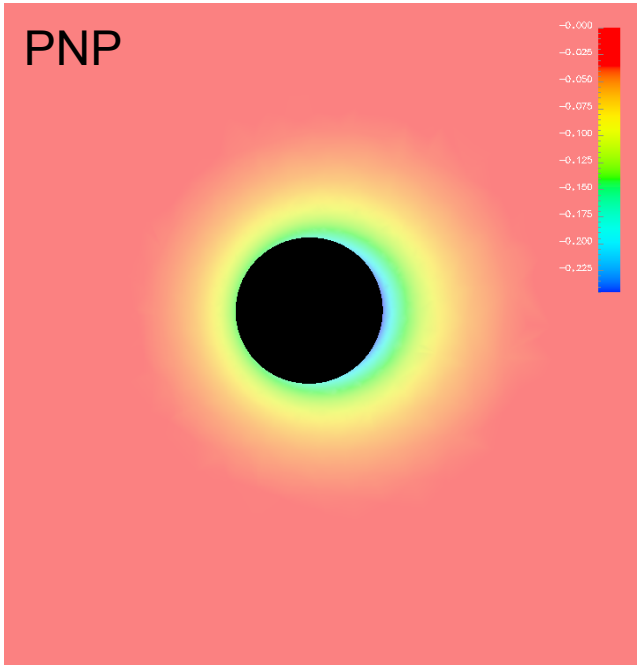

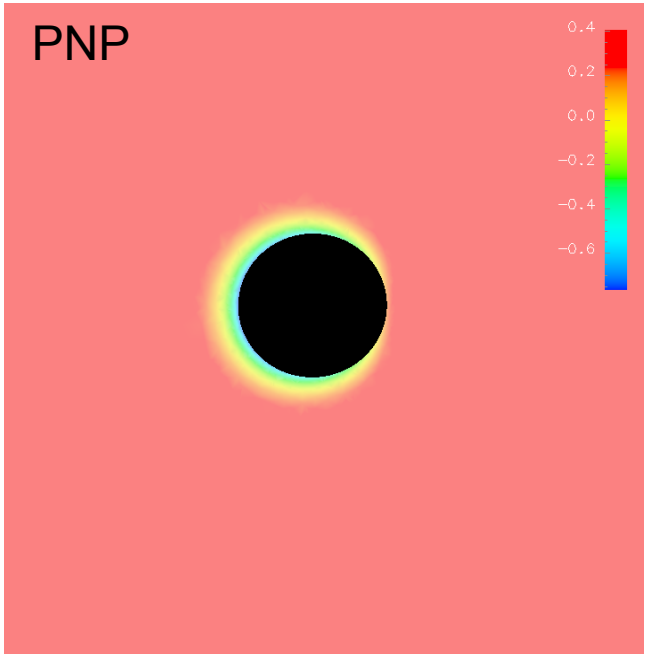

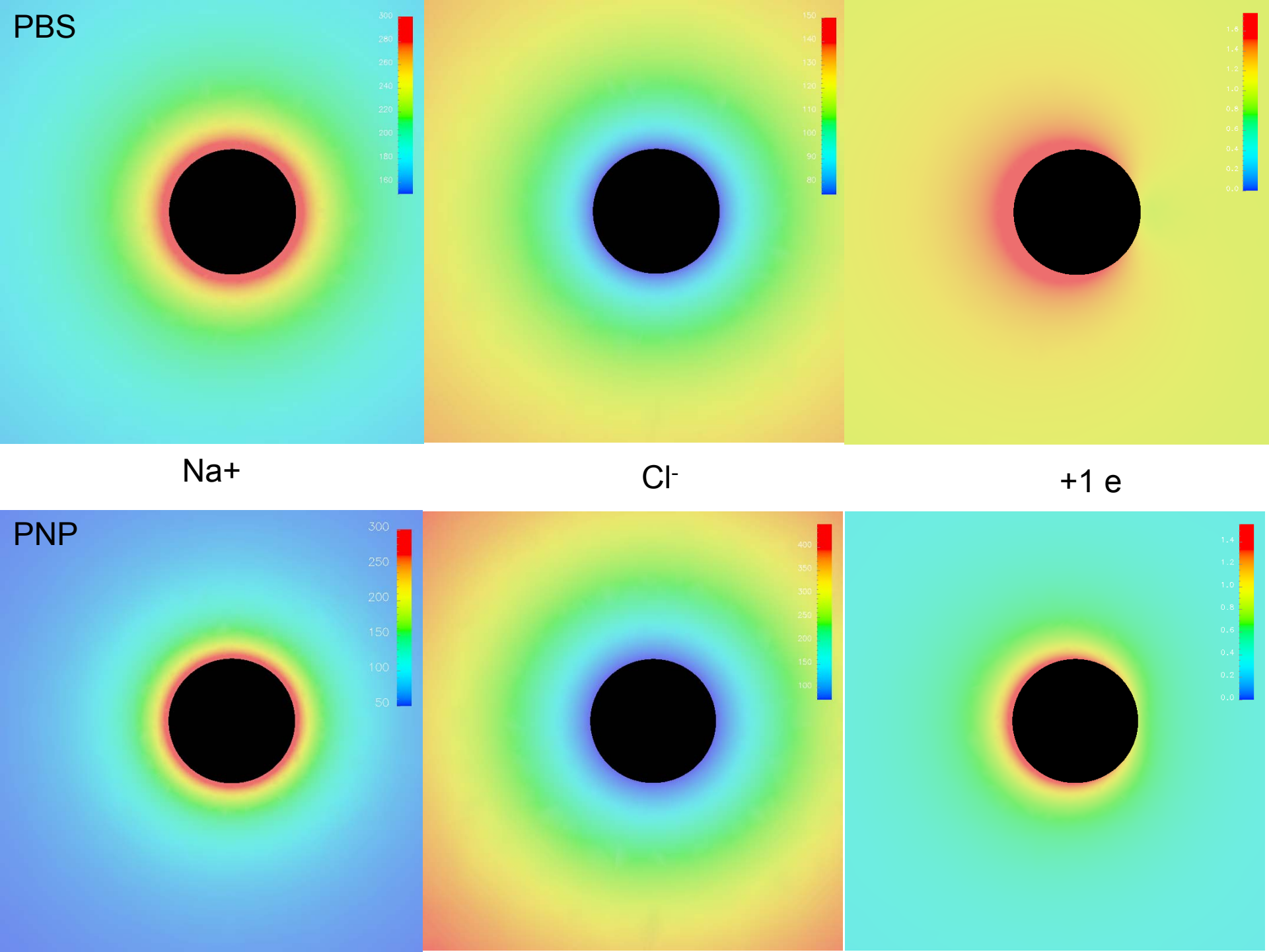
PBS
300
280
260
240
220
200
180
160
150
140
130
120
110
100
90
80
1.8
1.4
1.2
1.0
0.8
0.6
0.4
0.2
0.0
Na+
Cl-
+1 e
PNP
300
250
200
150
100
50
400
350
300
250
200
150
100
1.4
1.2
1.0
0.8
0.6
0.4
0.2
0.0

Drug diffusion in Avian Influenza Neuraminidase

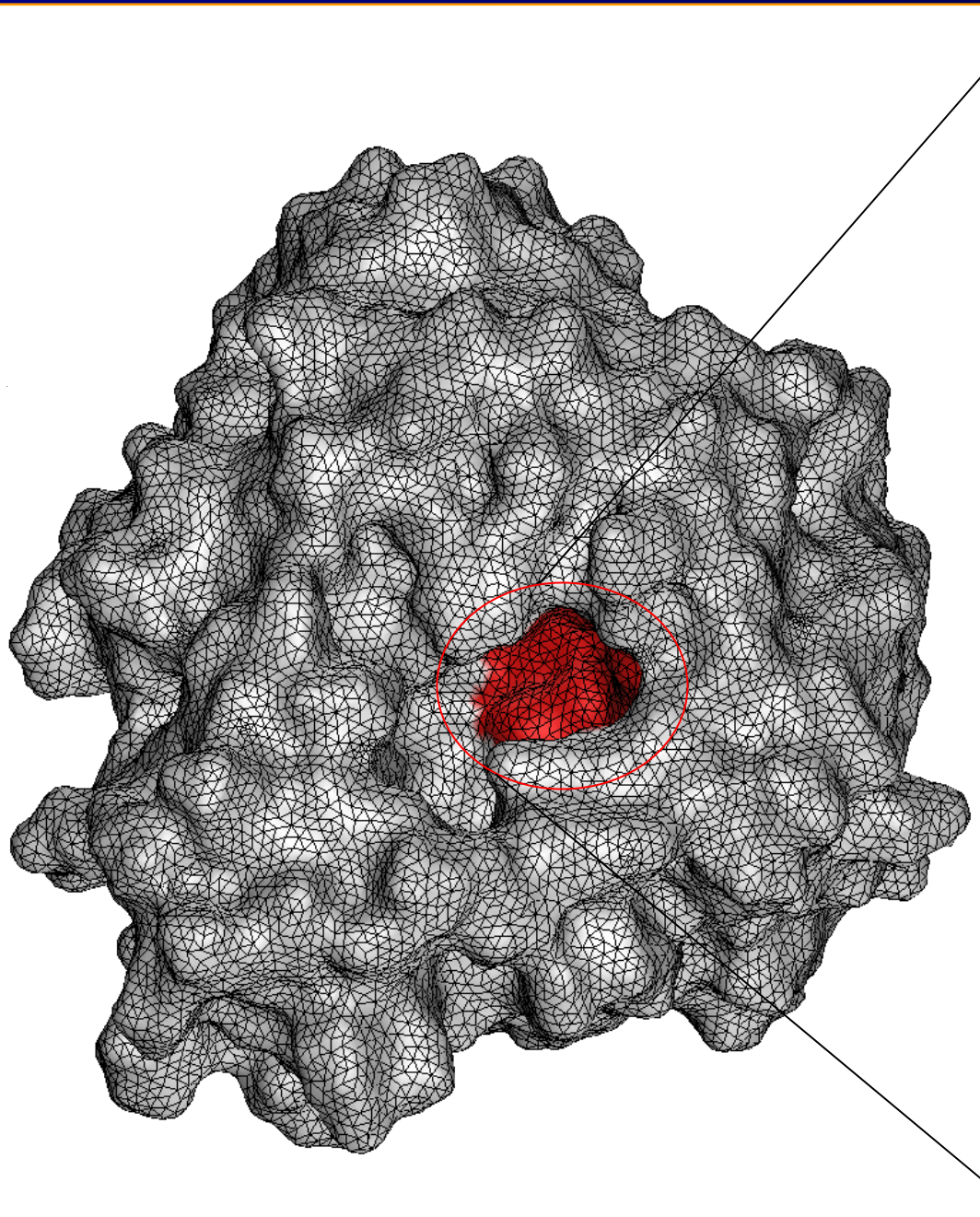

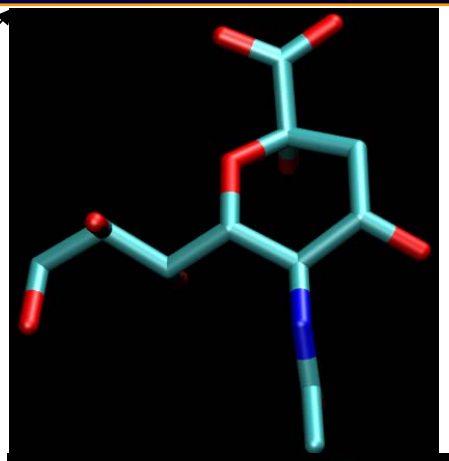

boat

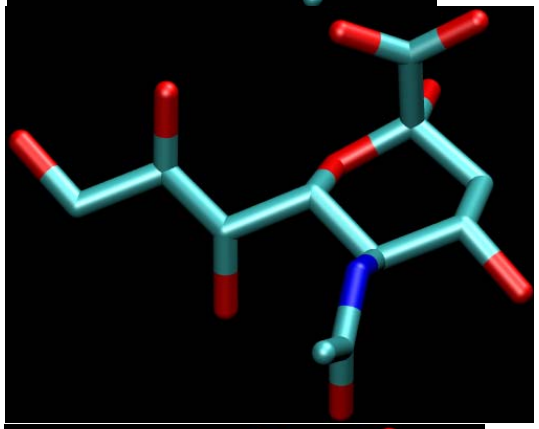

chair

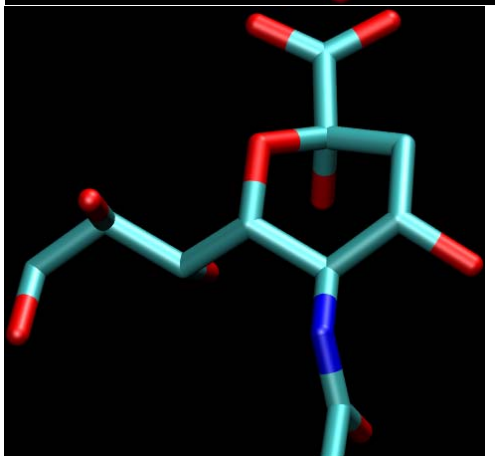

twist

Problems and new projects…

	rate(PBS)	rate(PNP)	experimental
wild-type open	18.1	14.6	2.52
wild-type closed	23.1	19.1	2.52
3CL0	11.9	8.17	0.24
3CKZ	12.4	7.32	0.35
3CL2	16.5	11.8	1.1

1.The reaction rate is the drug binding to the wild-type and mutated influenza virus neurominidase. The rate constant unit is $\mu M^{-1}s^{-1}$.

2.Continuum modeling predicts one order higher kinetic parameters than the experiment.

Numerical limitations and challenges

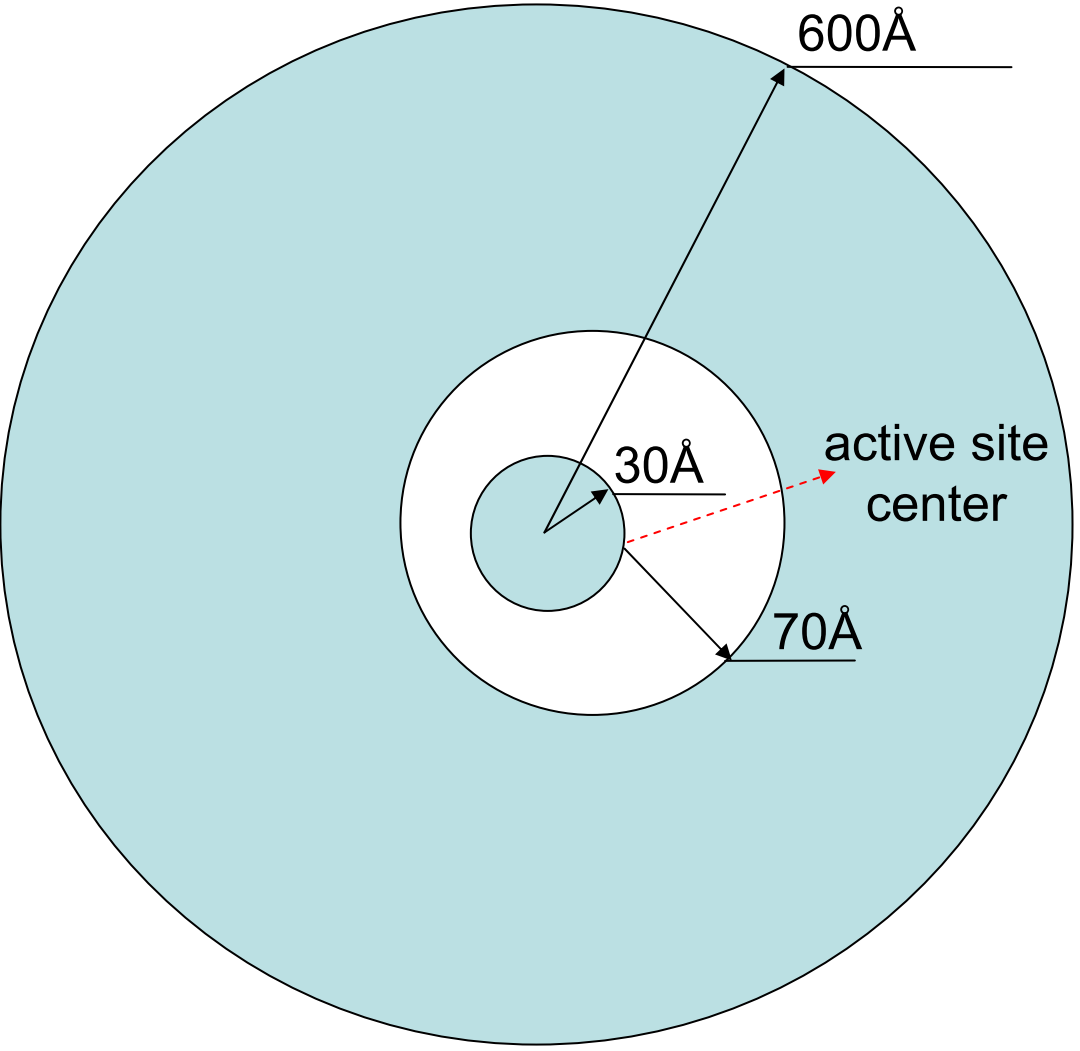

1. For a protein with 30 Å radius, Brownian dynamics region need at least 70 Å. The concentration of diffusion ions is approximately equal on the interface with 3% relative error.
2. The radius of the Brownian dynamics region is determined after the PBS or PNP steady state.
3. The "real" diffusion rate constant is

$$k = k_{cont}\,\beta$$

where k_{cont} is the rate constant predicted by continuum modeling and β is the reaction probability predicted by Brownian dynamics.

Additional reading materials

1. http://en.wikipedia.org/wiki/Diffusion
2. Berg, H C. *Random Walks in Biology*. Princeton: Princeton Univ. Press, 1993
3. advanced diffusion materials:

http://www.ks.uiuc.edu/Services/Class/PHYS498NSM/

4. Adaptive Multilevel Finite Element Solution of the Poisson-Boltzmann Equation I: Algorithms and Examples. *J. Comput. Chem.*, 21 (2000), pp. 1319-1342.
5. Finite Element Solution of the Steady-State Smoluchowski Equation for Rate Constant Calculations. *Biophysical Journal,* 86 (2004), pp. 2017-2029.
6. Continuum Diffusion Reaction Rate Calculations of Wild-Type and Mutant Mouse Acetylcholinesterase: Adaptive Finite Element Analysis. *Biophysical Journal,* 87 (2004), pp.1558-1566.
7. Tetrameric Mouse Acetylcholinesterase: Continuum Diffusion Rate Calculations by Solving the Steady-State Smoluchowski Equation Using Finite Element Methods. *Biophysical Journal,* 88 (2005), pp. 1659-1665.
8. Finite Element Analysis of the Time-Dependent Smoluchowski Equation for Acetylcholinesterase Reaction Rate Calculations. Biophys. J., 92(2007), pp. 3397-3406
9. Diffusional Channeling in the Sulfate Activating Complex: Combined Continuum Modeling and Coarse-grained Brownian Dynamics Studies. *Biophys. J.,* 95(2008), pp. 4659-4667